Comparative Analysis of Lightweight Robotic Wheeled and Tracked Vehicle

Christopher P. Johnson

Thesis submitted to the faculty of the Virginia Polytechnic Institute and State University in partial fulfillment of the requirements for the degree of

Master of Science
In
Mechanical Engineering

Corina Sandu, Committee Chair
Alexander Leonessa
Kevin B. Kochersberger

26 April 2012
Blacksburg, VA

Keywords: (keywords)

Lightweight robotic vehicle, terramechanics, mobility, energy efficiency

Comparative Analysis of Lightweight Robotic Wheeled and Tracked Vehicles

Christopher P. Johnson

ABSTRACT

This study focuses on conducting a benchmarking analysis for light wheeled and tracked robotic vehicles. Vehicle mobility has long been a key aspect of research for many organizations. According to the Department of Defense vehicle mobility is defined as, "the overall capacity to move from place to place while retaining its ability to perform its primary mission"[1]. Until recently this definition has been applied exclusively to large scale wheeled and tracked vehicles. With new development lightweight ground vehicles designed for military and space exploration applications, the meaning of vehicle mobility must be revised and the tools at our disposal for evaluating mobility must also be expanded. In this context a significant gap in research is present and the main goal of this thesis is to help fill the void in knowledge regarding small robotic vehicle mobility assessment. Another important aspect of any vehicle is energy efficiency. Thus, another aim of this study is to compare the energy needs for a wheeled versus tracked robot, while performing similar tasks.

The first stage of the research is a comprehensive review of the state-of-the-art in vehicle mobility assessment. From this review, a mobility assessment criterion for light robots will be developed. The second stage will be outfitting a light robotic vehicle with a sensor suite capable of capturing relevant mobility criteria. The third stage of this study will be an experimental investigation of the mobility capability of the vehicle. Finally the fourth stage will include quantitative and qualitative evaluation of the benchmarking study.

This thesis is dedicated to my parents, Kim and Ann Johnson, for instilling in me the value of education. Without their encouragement this thesis would not be possible.

ACKNOWLEDGEMENTS

Thank you to Dr. Corina Sandu, who has provided a guiding light throughout my time here at Virginia Tech. The advice that was given was always very much appreciated. It is no exaggeration to say that without your insight and words of wisdom I would not be graduating this May.

Thank you to Dr. Alexander Leonessa, for providing me with a vehicle to work with as well as giving me ample lab space to work throughout my thesis research.

To my fellow students in Randolph 9L, thank you for putting up with all my persistence questioning and for providing me with some perspective when I was too tired or frustrated to continue. You contribution to this thesis was a notable one.

TABLE OF CONTENTS

LIST OF FIGURES

LIST OF TABLES

List of Abbreviations

AVDL – Advanced Vehicle Dynamics Laboratory

BMT – Bekker's Mobility Theory

CI – Cone Index

DEM – Discrete Element Method

FCS – Future Combat Systems

FEM – Finite Element Method

GUI – Graphical User Interface

IED – Improvised Explosive Device

ISTVS – International Society for Terrain Vehicle Systems

MI – Mobility Index

MMM – Mobility Metrics Matrix

NRMM – NATO Reference Mobility Model

PWM – Pulse Width Modulation

RC – Radio Controlled

SUGV – Small Unmanned Ground Vehicle

VCI – Vehicle Cone Index

VAL – Vibration and Acoustics Laboratory

WES – U.S. Army Waterways Experiment Station

1. Introduction

Vehicle mobility has always been a subject of keen interest. If a vehicle does not have the required mobility characteristics for a given mission than this can have catastrophic consequences and may result in the vehicle becoming immobilized. In recent years there has been an intense focus on developing lightweight robotic vehicles to do a variety of tasks, from military reconnaissance to lunar exploration. The military has recently been heavily investing in small unmanned ground vehicles (SUGV) such as PackBot or the XM1216 and this trend shows no signs of stopping [2]. The Army's modernization program, Future Combat Systems (FCS) has stated that as much as 40% of the military fleet could be robotic [2]. On February 7th, 2011 the Chief of Staff of the Army directed that the FCS be re-designated as Army Brigade Combat Team Modernization Program [3]. Researchers have been developing was to characterize vehicle mobility since the late 1950's but the bulk of this research was aimed at large wheeled and tracked vehicles [4, 5]. With the increased use of small lightweight robotic vehicles the accepted conventions for large vehicles must be reexamined with a new focus on these small robotic vehicles.

This thesis focuses on analyzing the mobility and the energy efficiency of lightweight wheeled and tracked robotic vehicles. There has yet to be a comprehensive benchmarking analysis that explores the benefits of each configuration for a specific mission or operating environment. This study investigates vehicle parameters of interest and attempts to quantitatively and qualitatively compare each vehicle configuration under certain operating scenarios, and develop a systematic approach that can be employed to pick the vehicle that is best suited for a given set of operating conditions. This analysis will be conducting using the state-of-the-art methods in vehicle mobility and will attempt to apply standard vehicle conventions and equations to assess their applicability at the robotic vehicle scale. The analysis will be conducted on a variety of terrains and operating conditions and the vehicle will perform these test first in a wheeled

configuration and then in a tracked configuration. These separate vehicle configurations can be seen in Figure 1-1 and Figure 1-2.

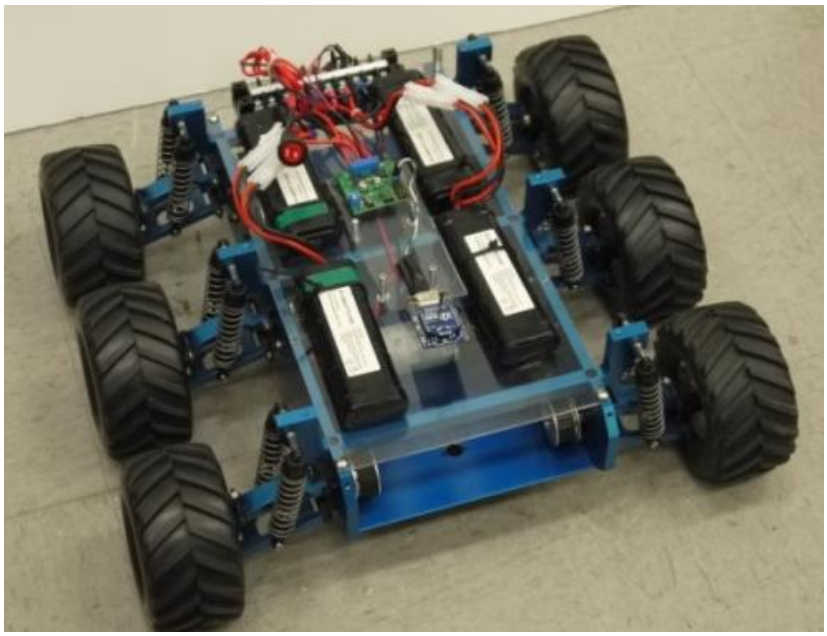

Figure 1-1: Test vehicle in wheeled configuration

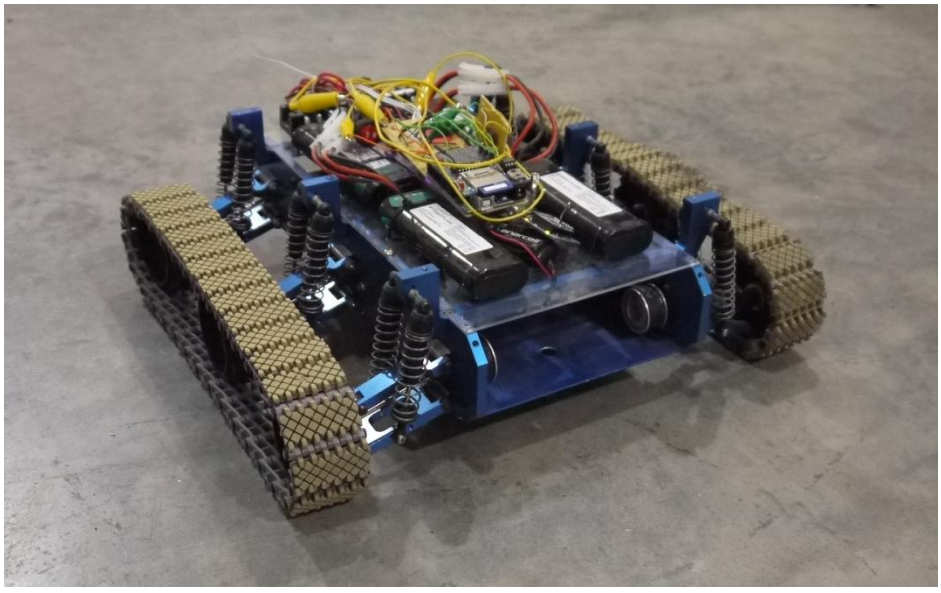

Figure 1-2: Test vehicle in tracked configuration

1.1 Motivation

There is no question that in the future SUGVs will continue to play an ever increasing role in tasks that are dangerous, monotonous, or not feasible to be performed with a manned vehicle. With this increase in usage it becomes apparent that a more fundamental understanding of vehicle mobility is needed. Having a better understanding of these vehicles mobility parameters we can design better vehicles for specific operating requirements, while also realistically estimating their energy needs. The currently accepted conventions for mobility have been developed for large, heavy vehicles and it has yet to be determined whether vehicles on the robotic scale can be described by these conventions. With this need in mind it is imperative that a better understanding of small robotic vehicle mobility be developed.

1.2 Project Objectives

The objectives of this thesis are as follows:

1) Examine and present the current state-of-the-art in vehicle mobility assessment with a special focus on research that has been conducted on vehicles in the class of SUGV.
2) Conduct a mobility assessment of a robotic vehicle in a wheeled and in a tracked configuration and study the benefits of each configuration in a variety of operating environments.
3) Present a quantitative and a qualitative evaluation of the benchmarking analysis in order to develop a systematic approach that can aid in the selection of a light robotic vehicle for a given mission and/or environment as well as for the improvement of the design of future robots.

1.3 *Research Approach*

The research presented in this study was started first by developing a set of mobility criteria that would enable the direct comparison of robotic vehicles in wheeled and tracked configurations. These criteria were then used to determine testing scenarios and environments. This detailed study included examining various vehicle parameters, such as drawbar pull, energy consumption, vehicle speed, etc, in numerous vehicle operating conditions. For example these operating conditions include; incline rigid surface, flat sandy silt loam, and numerous obstacle negotiation situations.

After a thorough review of published vehicle mobility research studies, several testing parameters were identified. These parameters were selected based on accepted methods, as identified from the literature, as well as current military standards. Models that described heavy vehicle mobility were also examined such as those presented by Bekker and then further adapted by Wong, to explore ways by which something similar can be employed for light vehicles. These mobility criteria were developed for this specific case study however, they should be general enough to be applied to any light robotic vehicles. Another goal of the review of prior studies was to learn from their conclusions and to better formulate our testing strategy. Vehicle parameters were also investigated to determine their relevant such as vehicle weight, power consumption, and specific mission requirements. From this initial work eighteen operating scenarios were selected. This research was used to facilitate the creation of a Mobility Metrics Matrix (MMM) that would be applicable to this case study and to lightweight robotic vehicles in general.

The experimental testing scenarios were defined and preliminary tests were conducted with the robotic vehicle in the wheeled configuration. These tests were very in-depth and examined several vehicle parameters including drawbar pull, slip, mobility index, pressure-sinkage relation, vehicle speed, power consumption, weight, and contact area. The vehicle was tested for eighteen different scenarios including: flat rigid surface, incline rigid surface, flat soft soil, inclined soft soil, rough random vegetated terrain, 1.5 inch obstacle negotiation, 1 inch obstacle negotiation, and finally a triangular cleat

obstacle negotiation. Once the testing for the robot in a wheeled configuration was complete the vehicle was re-configured to a tracked configuration and the same tests were then performed. After the testing was completed a quantitative and a qualitative analysis were conducted in order to help develop a set of guidelines that will be used in the selection of a vehicle for a given set of operating conditions and environments. The lessons learned could further be employed in future light robotic vehicles design.

1.4 Summary of Chapters

Chapter 2 presents a review of literature on subject matter relevant to this case study. This section provides a comprehensive background in terramechanics as related to light off-road vehicles, a highlight of research related to the selected key vehicle parameters, and a review of the state-of-the-art in vehicle mobility assessment.

Chapter 3 presents an in-depth review of this study's research methodology. In this section an overview of the MMM and its uses are discusses. This matrix was developed by a previous graduate student at Virginia Tech [6] and it identifies important measurable mobility criteria and how relevant they are for specific situations. The case study analyzed in this thesis is then presented.

Chapter 4 describes the design of the experiment that is conducted for this research. The experimental objectives are outlined and the parameters selected for the study are presented. This chapter also describes the scenarios developed for this study. The rationale for the selected parameters and scenarios are explored and presented in the context of the MMM. Finally this chapter concludes with a discussion of the experimental methods and settings used throughout this study.

Chapter 5 presents the results from the experimental study. The testing is described in detail and the parameter collection is discussed. The data from this study is displayed in a structured format. This section concludes with an analysis of the collected data.

Chapter 6 is the final chapter of the thesis and it includes the conclusions derived from the experimental study. These conclusions are presented and framed in terms of their impact on assessing the mobility and energy requirements for light vehicles. This chapter concludes with brief recommendations for future work.

2. Literature Review

A literature review has been conducted in order to gain an understanding on the current state-of-the-art in vehicle mobility assessment as it relates to small robotic vehicles. The literature review has been used as an aid to help develop the testing scenarios and to identify key vehicle parameters necessary to describe light vehicle mobility. This section contains equations relating key vehicle parameter as well as an in-depth examination of current vehicle mobility tests.

2.1 Background in Terramechanics as Related to Light Off-Road Vehicles

This section provides the background in terramechanics research that pertains to the light off-road vehicles category. Some brief background on terramechanics research is presented next. The field of research that explored vehicle terrain interactions and vehicle mobility was first focused upon in the 1950's with the publication of M.G. Bekker's paper on the theory of land locomotion [5] and Steeds paper on the mechanics of skid steering for tracked vehicles [4]. This field has been researched extensively since then but has almost exclusively been focused upon heavy weight vehicles such as tanks and passenger vehicles. J.Y. Wong advanced this field of research; his theories stem from the initial research done by Bekker, Steeds, and many others [7]. With the increased use of SUGVs it has become apparent that there is a gap in knowledge regarding light vehicle mobility. With a more advanced understand of small vehicle mobility better vehicles can be designed and a more knowledgeable selection can be made when choosing a particular vehicle for a given set of mission parameters. In the 1980s a study conducted by the Army was aimed at addressing which vehicle had the superior mobility, a wheeled versus tracked vehicle, but once again this study was focused on heavy military vehicles [8]. Until recently there was very little research being conducted in terramechanics of light off-road vehicles; a summary of the most relevant studies in this area is presented in this section.

SUGVs have seen increasing use over the past ten years but the vehicle performance of these small scale operating platforms have just recently started to be examined and studied. Currently all SUGVs need continuous human interaction in order to course correct and prevent the vehicle from becoming immobilized. Recently there has been some research performed that attempts to help model and characterize the terramechanics of such small vehicles to help increase mobility. These characterizations have been based on previous work in classical terramechanics dated back to initial work done by Bekker.

Characterizing vehicle-terrain interactions for a light robotic tracked vehicle is a fairly new area of research and has yet to fully mature. Many of the terrain characterization relations developed in the early 1960's have been applied to small tracked robotic vehicles with limited success. Early research done in the late 1950's by Bekker was mainly focused on vehicle mobility as well as the interactions between the vehicle and the terrain [5]. Bekker developed the Bevameter technique which subsequently leads to the development of the pressure-sinkage relation and his tractive effort-slip relation models. As Bekker was doing his initial work regarding tracked vehicles Steeds was studying the mechanics of skid-steering on firm ground [4]. Steeds worked to clarify the skid-steering mechanism and further this area of research by the consideration of longitudinal slip on the track of a tracked vehicle. In Steeds pioneering work and in many later works, Coulomb's law of friction is assumed to be valid for the shear stress developed between the tracks and the ground. Skid steering is essentially universally used for tracked vehicles consisting of a single unit. The robot chosen for this study relies on skid steering mechanisms for maneuverability.

In 1971 Weiss further extended the research on skid steering by including the lateral forces acting on the running gear [9]. Weiss used the lateral forces to help calculate vertical loads acting on each row of wheels. This research was directed at wheeled vehicles operating under skid steering. Crosheck used the foundation of research to theoretically study the skid-steering mechanism to the application of crawlers in 1975 [10]. In his analysis he considered both lateral and longitudinal track slip. Crosheck employed the pull-slip relation developed by Wismer and Luth to estimate the

coefficients of friction [11]. Crosheck never made any comparisons with test results. With Wong's *Theory of Ground Vehicles*, he presents equations to calculate the inner and outer track forces in a skid-steering situation. In this early work he assumes a constant value for the lateral coefficient of friction. Subsequent work would suggest that the coefficient of lateral friction is a function of the vehicle speed and turning radius [12]. This initial research laid the foundation for further work by, Kitano and Jyozaki, Ehlert, and others [13, 14]. A common assumption was made for the majority of this early work that the ground pressure was uniform but many studies have suggested that this is not the case [15, 16].

In 2001 Wong continued to build on the understanding of mechanism of skid-steering and publish a revised theory of skid-steering for tracked vehicles on firm ground. Wong's theory is an expansion of Steed's earlier work and analytically predicts track thrusts in addition to longitudinal and lateral moments experienced by the tracks. His general theory takes into account the shear stress- shear displacement relation at the track-ground interface. This differs from Steed's original work where he assumes that shear stress reaches an instantaneous maximum value. This assumption was made in Steed's model to accommodate for the assumption that this relation follows Coulomb's law of friction. Wong notes that studies have shown that the lateral coefficient of friction is perhaps a function of turning radius. However this relation must be characterized empirically and is a very time consuming process to determine. Wong notes that it is still uncertain if these empirical relations can be generally applied. For a general theory it is not necessary to introduce the term of lateral coefficient of friction and turning resistance should be a function of the soil parameters only [17].

In 2010 a simulator was created by Al-Milli that adapted Wong's model of skid-steering to a SUGV with a total mass of 2.5 kg [18]. An initial attempt was made using Wong's theory in which the coefficient of lateral resistance is considered constant. This initial simulation show that an increase in turning radius increase the difference in inner and outer track thrusts which has been proven to be unreasonable in real world applications [14]. Al-Milli revised the simulation to extend Wong's theory so that the model includes

factors for soil properties and vehicle dynamics behavior, i.e. turning radius and vehicle speed. Simulator results were compared with in house experimental results as well as those produced by Ehlert and show potential to accurately predict SUGV traversability. Results obtained showed a good match to the simulators predicted data but more work needs to be done to validate these results.

Recently there has been a push from the electrical engineering community to forgo modeling the dynamics of skid steering and rather treat the complex interaction between the soil and running gear as a control issue. There has been some success in this area with adaptive SUGV controls that course corrects for any inconsistencies in trajectory caused by poor skid steering models [19-21]. This area of research shows some promise but there is a lack experimental data to validate the findings. An exhaustive search was not done in this area of research as it was out of the scope of this thesis but it is important that the reader be aware of this field of study. Much of this early work on skid-steering and other terramechanics related properties has laid the foundation for the kinematic and dynamic modeling of tracked vehicles.

Dynamic and kinematic modeling is useful for prediction vehicle mobility characteristics and in most often derived from earlier work done in the field of terramechanics. Bekker developed relations that compute the inner and outer track thrusts required for a steady-state turning maneuver. This initial work by Bekker allowed Wong to develop an equation for minimum track design to achieve a steady-state turning maneuver based on a given set of soil conditions. Wong also developed a set of governing kinematic equations for a vehicle in a steady-state maneuver at low and high speeds [7]. Many models have been developed to describe the dynamics of heavy tracked vehicle and I will briefly discuss some of the most notable. In 1977 Kitano and Kuma developed a kinematic and dynamic model for tracked vehicles that included turning maneuvers considered non-stationary, or in other words not considered steady state, on soft terrain. The work done by Kitano and Kuma had no factors to related soil properties to tractive forces and might contribute to the fact that these relations are not widely used [16]. Building on the body of research in 1992 Murakami et al, proposed a mathematical model that was aimed at

predicting the spatial motion of a tracked vehicle on non-level terrain. This model had its basis on soil plasticity theories [22]. While these models were originally developed for heavy vehicles in recent years these models have been applied and adapted for use with small unmanned ground vehicles.

The usages of these dynamic models have changed when adapted to apply to light unmanned ground vehicles. Researchers have attempted to adapt these models in order to facilitate parameters estimation. These parameters are most often vehicle slip or soil properties. One of the earliest attempts to apply previous models to an unmanned vehicle was done in 1997 by Le [23]. Le retrofitted a 1.5 ton tracked vehicle with a suite of sensors and controls to be autonomous. Le used the dynamic model outlined by Schiller in 1992 [24]. Schiller's dynamic model was based on previous work done by Wong, Kar, and others. Le's work concluded that it was possible to use previous dynamic models for autonomous vehicles in order to estimate parameters such as slip. Le also noted that it might be possible to estimate trajectory and tractive effort with further development. While this test vehicle wasn't in the range of the SUGVs of today, it provided the groundwork for others to follow.

In 2004 Song attempted to apply earlier work done in modeling by Bekker and Wong to estimate slip for SUGVs [25]. Songs method applied extensive numerical techniques, such as the Extended Kalman Filter to obtain more accurate slip estimations. Song was able to obtain three slip parameters. Song also combined his slip estimations with a soil model and estimated soil parameters. In 2006 Song further this work by using a Sliding Mode Observer technique and was able to achieve more accurate results [26]. Remote parameter estimation is very attractive for applications such as planetary expedition and there have been numerous attempts to use classical models and equations to estimate soil parameters such as cohesion and internal angle of friction. The most notable research has been performed by Iagnemma [27, 28]. Other attempts at estimating vehicle and terrain parameters have been performed by Dar, Ray, Ojeda, and others [29-32]. While much of the research performed shows promise in various applications from mine exploration to

planetary rovers, there has been limited experimental validation and it has yet to be seen how applicable these parameters estimation techniques are.

2.2 Research Highlights on Key Vehicle Parameters

In order to assess the mobility of a vehicle there are a few key vehicle parameters that provide great insight into the vehicles off-road performance. These off-road mobility assessment parameters include the vehicle sinkage, drawbar pull, slip, pressure distribution, Mobility Index (MI), etc. Many of these parameters have been calculated using analytical expression or empirical relations first formulated in the late 1950's [5, 7, 33, 34]. These vehicle parameter relations were developed for heavy vehicles and may not adequately compute these parameters for small, light vehicles.

Since the 1950's when the initial research regarding vehicle mobility and terramechanics was performed, there have been many pressure-sinkage models proposed. The most commonly used pressure model was developed by Bekker in the 1950's. Bekker's pressure sinkage-model was derived from earlier work performed by Bernstein-Goriatchkin [5, 15]. Bekker used their model for deriving both his sinkage and compaction resistance equations. The Bernstein-Goriatchkin model is given as,

$$P = kz^n \qquad 2.1$$

where P is the pressure, k is the sinkage modulus, z is the sinkage, and n is the sinkage exponent. Bekker's model builds on this earlier work by separating the sinkage modulus, k, into two distinct parameters. These new parameters that were introduced are k_c, k_ϕ which respectively represent the modulus of soil deformation for cohesive and frictional components of the soil. Bekker also introduced a new parameter b, which represents the width of the plate used to apply the pressure to the soil. Bekker's pressure-sinkage is expressed as:

$$p = \left(\frac{k_c}{b} + k_\phi\right) z^n. \qquad 2.2$$

in which, b is the smaller dimension of the contact patch, usually the width of a rectangular contact area or the radius of a circular contact area. In this relation k_c, k_ϕ and n are empirical pressure-sinkage parameters that must be obtained and can be readily found in a soil properties text. The variables k_c, k_ϕ represent the modulus of soil deformation for cohesive and frictional components of the soil respectively and n represents the exponent of soil deformation. Depending on the terrain properties the new modulus parameters could go to zero. For example for a highly cohesive soil such as clay, the frictional modulus will most likely be negligible. It is also important to note that equation 2.1 is essentially an empirical relation and the various parameters must be determined for each soil type.

In 1965 Reece proposed a new equation to model the pressure-sinkage relation [35]. He noted that the relation between the plate width, b, and the modulus of soil cohesion, k_c, was overly simplistic in the Bekker model and could be improved upon. Reece's proposed equation goes as follows,

$$p = \left(ck_c' + \gamma_s b k_\phi'\right)\left(\frac{z}{b}\right)^n \qquad 2.3$$

where n, k_c', and k_ϕ' are pressure-sinkage parameters, c is soil cohesion, and γ_s is the weight density of the terrain. In this relation the values of k_c' and k_ϕ' are dimensionless whereas in Eq. 2.2 k_c and k_ϕ have dimensions that are dependent on n. While Reece has stated that his relation only varies in the effect of width it is sufficient to warrant a radical improvement in the pressure-sinkage relation. It must be noted that this relation is only applicable to homogeneous terrain. These relationships have been thoroughly researched and are generally accepted as being an accurate representation for heavy weight vehicles. More recently, in 2007, Ishigami proposed an improved version of Reece's equation [36]. Ishigami's model took into account the semi-elliptical stress distribution beneath the

wheel arc length. Ishigami developed these relations while working with planetary exploration rovers. His proposed model is,

$$p(\theta) = \left(ck'_c + \gamma_s b k'_\phi\right)\left(\frac{z}{b}\right)^n (\cos\theta - \cos\theta_s)^n \qquad 2.4$$

where θ is an arbitrary wheel angle and θ_s is the wheel static contact angle. This relation makes a distinction between the stress distribution beneath a loaded plate and the stress distribution beneath a wheel section. One assumption all these relations make is that the pressure-sinkage relation is independent of wheel diameter and curvature. This is how these relationships were able to be developed because the author's assumes that the flat plate approximation was valid.

Recently there have been some studies conducted that suggest these relations might not be valid for smaller, lighter vehicles [15, 37]. These new studies suggest that use of Bekker theory for vehicles with wheels that are either less than 50 cm in diameter or experience less than 45 N in normal load can lead to inaccurate results. This would definitely pose a huge challenge because the major or SUGVs would fall into this category. It is hypothesized that this inaccuracy is a result of the sharp curvature of the contact patch that small diameter wheels display. These studies indicate that the Bekker theory would only be appropriate for vehicles in which the sinkage to wheel diameter ratio is such that the contact patch is approximately flat. Bekker himself had stated that for wheels less than 20 inches in diameter the sinkage relation became less accurate as the wheel diameter decreased [33]. In 2011 Meirion-Griffith proposed a modified relation that takes into account the vehicles wheel diameter and was developed specifically with SUGVs in mind. The proposed relation goes as follows,

$$p = \hat{k} z^{\hat{n}} D^{\hat{m}} \qquad 2.5$$

Where D is the wheel diameter and m is the diameter exponent. This proposed relation is based on the Bernstein-Goriatchkin model for which k, n, and m are fitting constants. As you can see this relation is highly empirical and while the author did do some validate

work it has yet to be seen how well this relation describes pressure-sinkage. It is clear however that further work needs to be done to determine the applicability of existing pressure-sinkage models for small, lightweight ground vehicles operating in off-road.

Vehicle slip models are not readily available for light, small vehicles and in order to investigate this vehicle parameter researchers are adopting models developed for heavy vehicles [18, 30, 31]. A vehicle's longitudinal slip for a pneumatic tire as defined in the *SAE Handbook Supplement, Vehicle Dynamics Terminology* [38], is the ratio of the longitudinal slip velocity to the spin velocity of a straight free-rolling tire expressed as a percentage. The longitudinal slip velocity is defined as the difference between the spin velocity of the driven tire and the spin velocity of the straight free-rolling tire. If this relation is defined as suggested by the SAE then the longitudinal slip, i', goes as,

$$i' = \left(\frac{r\omega}{V} - 1\right) \times 100\% = \left(\frac{r}{r_e} - 1\right) \times 100\% \qquad 2.6$$

in which V is the linear speed of the tire center, r is the free-rolling tire radius, ω is the angular speed of the tire, and r_e is the effective rolling radius of the tire. When a torque is applied to the tire a tractive force is developed that is proportional to the applied torque under steady-state conditions. It is therefore understood that slip is a function of tractive effort. According to the available experimental data wheel slip is initial linear because of the elastic deformation of the tire tread and peaks between approximately 15 to 20% slip [7]. A theory that can accurately predict the relation for a pneumatic tire between the longitudinal slip and tractive effort has yet to be validated but there has been numerous proposed theories [7]. The slip relation for a tracked vehicle is characterized slightly differently based on the obvious differences in running gear. The slip of a tracked vehicle is defined as,

$$i = \left(1 - \frac{V}{r\omega}\right) \times 100\% = \left(1 - \frac{V}{V_t}\right) \times 100\% = \left(\frac{V_j}{V_t}\right) \times 100\% \quad 2.7$$

Where V is the forward speed of the track, r is the radius of the pitch circle of the sprocket, V_t is the theoretical speed, and V_j is the speed of the slip of the track with respect to the ground. Early work by Bekker using his Bevameter technique attempted to characterize the slip relation by adapting the Coulomb-Michlethwaite equation to the following form,

$$\tau = (c + p\tan\varphi)\left(1 - e^{-\frac{j}{K}}\right) \qquad 2.8$$

Where K is the slip coefficient, c is soil cohesion, φ is soil friction, and j is the amount of soil deformation which produces stress τ. It is important to note that c, φ, and K are coefficients that are determined by curve fitting empirical data [5, 33, 34]. These relationships were further extended by Wong [7] in order to predict the motion resistance of the track as well as the tractive effort and slip.

The maximum tractive effort of a track is determined by the shear strength of the terrain that the vehicle is operating on and the area of contact,

$$\begin{aligned} F_{max} &= A\tau_{max} \\ &= A(c + p\tan\phi) \\ &= Ac + W\tan\phi \end{aligned} \qquad 2.9$$

where A is the contact area, W is the normal load. This relation highlights the accepted notion that the dimensions of the track are very critical and the larger the contact area the higher thrust a vehicle can develop. In order to incorporate vehicle slip in the thrust relation Wong examined the development of shear displacement beneath a track. Wong [7] proposed that tractive effort and slip are related as,

$$F = (Ac + W\tan\phi)\left[1 - \frac{K}{il}\left(1 - e^{-\frac{il}{K}}\right)\right] \qquad 2.10$$

where the parameters involved are the same as the ones in the previously defined equations. It is important to note that this relation has been developed under the assumption that the track exhibits a uniform normal pressure distribution which in real world applications is seldom uniform. Wills attempted to correct this problem and proposed a new relation to account for a non-uniform normal pressure distribution [39]. In the review of literature conducted for this study, though, the model developed by Wills is seldom used. While many models for slip have been proposed these are the few that are most commonly used. It has still yet to be seen if these models developed for heavy vehicles can be applied to lightweight SUGVs but the research community is starting to investigate this by applying these models to their SUGV research.

The drawbar performance of off-road vehicles has been researched and characterized since the late 1960's. This performance characteristic is especially important for vehicles that are designed with traction as the main feature in mind, such as an agricultural vehicle. The drawbar performance represents the vehicles ability to push or pull various loads. The definition for drawbar pull according to the International Society for Terrain Vehicle Systems (ISTVS) is, "the force available for external work in a direction parallel to the horizontal surface over which the vehicle is moving" [40]. The drawbar pull test was first developed by the U.S. Army Waterways Experiment Station (WES) with the express purpose to develop a technique that would aid the Army in tire selection. This early work with the drawbar pull produced mixed results as this parameter was new and not fully understood.

By the mid 1970's this performance metric saw more use and a better understanding through research that was developed. Today there have been a few studies attempting to characterize drawbar pull testing procedures but the trend is still for researchers to develop their own testing procedures.

The drawbar pull is equal to the difference between the tractive effort developed by the running gear and the resultant vehicle resistant. This relation can be expressed as,

$$F_d = F - \sum R \qquad 2.11$$

where F_d is the drawbar force, F is the tractive effort, and $\sum R$ is the sum of the resistant forces [7]. The development of thrust from the tractive effort often results in slip. This leads to the consideration that drawbar pull and vehicle speed are a function of slip. The most common sources of resistance are due to internal resistance of the running gear, resistance due to vehicle-terrain interactions, ground obstacle resistance, and aerodynamic resistance.

While there have been extensive research on these vehicle parameters for heavy vehicles, it has yet to be seen how accurately these established relations apply to SUGVs. As mentioned in the previous section the majority of research has been focused on solving challenges as related to SUGVs with adaptive and novel control schemes. The research focusing on the Mobility Index will be discussed in the next section.

2.3 Review of the State-of-the-Art in Mobility Assessment

Mobility assessment for vehicles operating in off-road conditions has traditionally been determined by three main methods which have been developed with heavy weight vehicles in mind.

The first method is the Bekker's Mobility Theory (BMT), which is an analytical tool that has been developed using Bekker's equations for vehicle soil interactions [5, 7, 33, 34, 41]. The BMT model was established to give a first past general evaluation of a vehicles mobility. It is a simple static one-degree of freedom (1-DOF) model that assumes the soil in homogenous and the loading effects are linear. This model while analytical has seven empirically defined soil strength properties that must be determined.

The second method, the Cone Index (CI), is a measure of terrain characteristics which are obtained using a device called a cone penetrometer [7, 42]. The value of the CI is then

empirically correlated to vehicle performance on a go/no go basis using a series of relationships called the vehicle cone index (VCI). The cone index also formed the basis for the future development of the NATO Reference Mobility Model (NRMM).

The final type of method for characterizing off-road vehicle performance is employing the use of the finite element method (FEM) and discrete element method (DEM). These methods attempt to describe vehicle mobility and vehicle soil interactions by the idealization of the tire and soil as an assembly of a finite number of elements. These computational methods have seen considerable advances in accuracy and efficiency and are continually being used for more applications [7]. These methods has seen limited use in the study of mobility of robotic scale vehicles and are beyond the scope of this literature review.

In addition to these three traditionally used methods there have been some novel methods recently developed that aim at specifically describing mobility for small, lightweight vehicles. These methods will be examined at the end of this section. The first two traditional methods will also be discussed in detail in the following paragraphs.

Bekker's Mobility Theory is an analytical tool developed for evaluation vehicle off-road mobility and was developed to create a way to directly compared vehicle mobility performance of different vehicle platforms [41]. The BMT is a simple, linear, static 1-DOF model that has been created using Bekker's equations of vehicle soil interactions that have been established since the late 1950's with the publication of Bekker's *Theory of Land Locomotion; the Mechanics of Vehicle Mobility*. Bekker's relations for vehicle terrain interactions are semi-empirical and characterize the vehicles pressure-sinkage relation, the slip-shear relation, resistance to motion, and the drawbar pull that the vehicle experiences during operation on a variety of terrain conditions.

These relationships originally derived by Bekker made use of a novel technique known as the Bevameter technique. This technique measures the response of a given terrain to loading scenarios that were relevant to vehicle mobility studies. This technique comprises

of two basic tests in which the terrain is tested in a penetration mode to characterize pressure-sinkage as well as a shear mode to characterize the slip-shear relation [7, 33, 34]. Bekker designed an apparatus, a Bevameter, to conduct these tests and an example of this device can be seen in Figure 2-1.

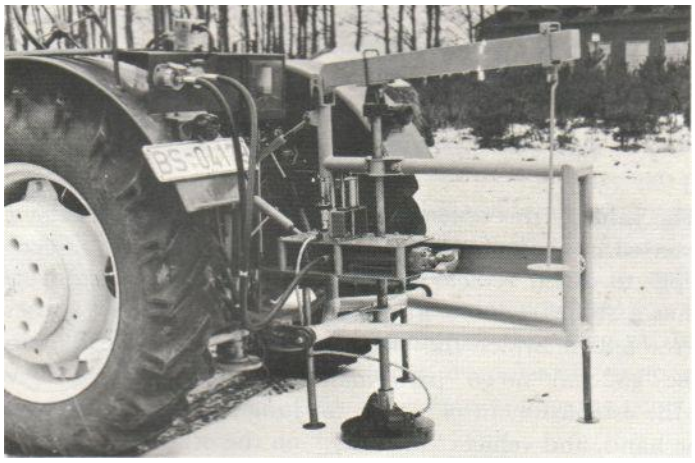

Figure 2-1: A vehicle-mounted Bevameter [33]

The penetration tests uses a plate with the same approximate area as the contact area of the vehicle you would like to test for. This test is used to predict the normal pressure distribution on the vehicle-terrain interface as well as the vehicle sinkage. This plate is driven into the ground at a constant rate of increasing normal load. Once the applied pressure and the resulting sinkage of the plate are recording the experimenter can then characterize the pressure-sinkage relation of the vehicle being tested. The shear test uses a shear ring or plate to simulate the shearing action of the vehicles running gear. An example of a shear ring can be seen in figure 2-2. In most instances a shear ring is preferred to a shear plate [7]. This shear ring is driven into the ground and rotated at a constant applied torque. The torque applied and the resulting angular displacement of the ring are measured and recorded. This will allow the experimenter to characterize the shear stress- shear displacement relation. After these tests are conducted the experimenter will have all the necessary information to predict the shear stress distribution at the vehicle terrain interface as well as the tractive effort-slip relationship of the vehicle that

you are testing for. These empirical relationship developed by Bekker were developed for large, heavy wheeled and tracked vehicles and it has been noted that using these relationships for vehicles lightweight robotic vehicles may lead to inaccuracies in certain instances [15]. The equations used in the BMT were empirically developed by Bekker in the late 1950's and early 1960's and have been employed many times in subsequent years by various researchers.

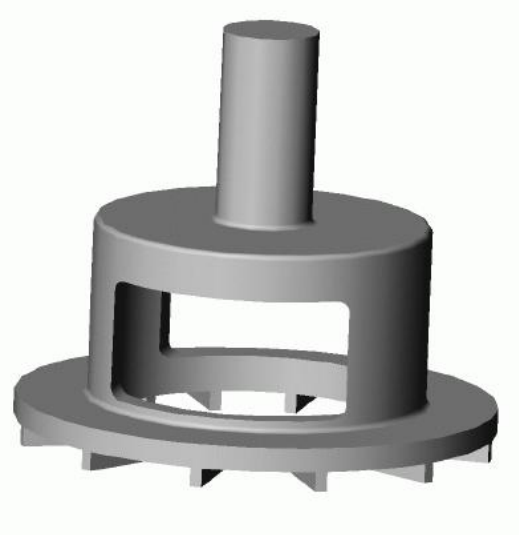

Figure 2-2: An annular shear plate used in Bevameters [43]

The BMT characterizes the pressure-sinkage relationship of the vehicle using an equation proposed by Bekker. This equation relates normal pressure, p, exerted by the vehicle to vehicle sinkage depth, z. This relation takes the form of the equation in 2.2. This equation proposed by Bekker is intended to be used for vehicles operating on terrain that can be considered homogeneous and makes the assumption that the pressure-sinkage relation is independent of the wheel diameter and or curvature. Bekker assumes that the contact area is approximately flat because the intent for this relation is to be applied to vehicles with large diameter wheels. Bekker himself notes in *Introduction to Terrain-Vehicle Systems*, that as the wheels because smaller than 20 inches in diameter the predictions for sinkage became less and less accurate [33]. Recently there has been some research performed that suggest Bekker's relation give inaccurate results for wheels less than approximately 50

cm in diameter or that experience less than 45 N in normal load [15, 37]. This range of indices that have been suggested to be inaccurate represents a significant portion of current SUGVs and presents a significant challenge that must be addressed. There have been many pressure-sinkage models proposed since Bekker developed his in 1956 but the BMT continues to use the equation above [5].

The BMT characterizes the slip-shear relation using many of the conventions developed by Bekker in which the relation between certain soil properties and shear strength are used to prediction the vehicles cross country mobility. When a torque is applied to the running gear a shearing action is initiated. The tracks grousers move relative to the soil and the maximum shear force is not developed instantaneously. The grousers compact the soil beneath the vehicle before it can reach its maximum mechanical shearing stress [41]. This implies that the vehicle experiences some amount of slip before the vehicle can achieve maximum traction. There are many factors that affect the shear stress. Shear stress is defined as the ratio between the vehicle's tractive force and the area of the running gear normal to the terrain surface. The vehicle experiences opposition to the developing tractive force from the soil resistance as the grouser slips during shear. Another factor to consider is that the vehicle's normal force contributes to soil compaction beneath the grousers and affects the soil resistance experiences by the grousers. To summarize the track forces push against the soil and generate a soil resistance. This soil resistance is a function of the physical soil properties. The slip-shear relation developed in a vehicles contact patch is proposed in the BMT as

$$\tau = A_1 e^{(-K_2+\sqrt{(K_2^2-1)})K_1 S} + A_2 e^{(-K_2+\sqrt{(K_2^2-1)})K_1 S} \qquad 2.12$$

in which K_1 and K_2 are coefficients of slippage, τ is the soil stress, S is the soil deformation. The variables A_1 and A_2 are constants that must be solved for. After solving for A_1 and A_2 a general equation for the shear can be developed

$$\tau = \frac{(c + p\tan\emptyset)}{y_{max}} \left[e^{(-K_2+\sqrt{(K_2^2-1)})K_1 S} + e^{(-K_2+\sqrt{(K_2^2-1)})K_1 S} \right] \qquad 2.13$$

in which c is the cohesion of the soil, ϕ is the angle of friction, and y_{max} is the largest possible value of the bracket expression in the equation. This is how the BMT describes the slip-shear relationship. This relation can be manipulated to arrive at expression for the vehicle performance measures tractive effort. The BMT gives an expression for tractive effort as

$$H_i = \left(\frac{b(c + ptan\phi}{K_1 \cdot i \cdot y_{max}}\right)\left(\frac{-1 + e^{\left(-K_2 + \sqrt{K_2^2 - 1}\right)K_1 id}}{-K_2 + \sqrt{K_2^2 - 1}} + \frac{1 - e^{\left(-K_2 - \sqrt{K_2^2 - 1}\right)K_1 id}}{-K_2 - \sqrt{K_2^2 - 1}}\right). \quad 2.14$$

This characterization by the BMT of the slip-shear and the derived tractive effort equations can lead to great insights in the vehicles cross-country mobility and can help determine the vehicles overall performance.

The final two vehicle parameters that are characterized by the BMT are the vehicles resistance to motion due to terrain compaction and the drawbar pull. As the vehicle generates thrust not all of it is converted to forward motion, some of it is lost to the resistance cause by soil compaction and bulldozing. This resistance is described by Bekker with the following expression

$$R_c = \left(\frac{1}{(n+1)(k_c + bk_\emptyset)}\right)\left[\frac{W}{l}\right]^{\frac{n+1}{n}}. \quad 2.15$$

The drawbar pull is then defined as the difference between the total tractive efforts minus the resistive forces. The drawbar pull is the vehicles ability to push or pull a load; quite simply it is the force available at the vehicles drawbar. The drawbar pull is defined by the BMT as

$$F_d = H - R_c \qquad 2.16$$

The BMT is one of the available tools used to evaluate a vehicles off-road mobility. It was developed as a simple 1-DOF system model to quickly evaluate the vehicles performance. This method was derived from Bekker's theory of terramechanics for heavy weight vehicles and has yet to be validated for use with lightweight vehicles. This method also requires that he assumptions made in Bekker's work are correct and if this method is applied to scenarios outside these assumptions this method might not be valid.

In 2006 an attempt was made by Lever to design and built a SUGV that was scaled according to the mobility theory developed by Bekker [44, 45]. The robot that was developed was design for travel over snow and was appropriately named SnoBot. The reference vehicle that SnoBot was designed and scaled after was a ST-4B or Snow-Trac. A comparison of the test vehicle's scaling can be seen in figure 2-3 and 2-4.

Figure 2-3: ST-4B [46]

Figure 2-4: SnoBot [45]

The ST-4B vehicle is designed for travel over snow and is a 1400-kg manned vehicle. During these tests measurements were taken including snow characteristics, vehicle sinkage, motion resistance, and drawbar pull. These measurements were used to characterize the vehicles mobility in deep-snow. A few discrepancies arose when using Bekker theory for the scaling of SnoBot. The robotic vehicles sinkage exceeded the ground clearance and immobilized the vehicle. This was corrected and through a doubling of the ground clearance. The ground pressure was also decreased by widening the vehicle's tracks. It was noted by Lever that large discrepancies were observed in the measured and predicted snow-compaction resistance and sinkage on different test days. This was attributed to a difficultly in capturing the actual behavior of the snow pack using simple Bekker theory. Lever comments that overall the Bekker theory provides useful guidelines for scaling but should be tailored to individual operating environments.

The second tool for assessing vehicle mobility is the Cone Index. This empirical method was originally developed during WW II by the WES and later formed the basis for the development of the NATO Reference Mobility Model (NRMM). In this method an empirical equation is first used to calculate the mobility index (MI) of a given vehicle [47]. This value for MI is then used to calculate a parameter call the vehicle cone index (VCI). The VCI is value that represents the minimum soil strength a given terrain must have in order for the vehicle to make a specific number of passes. In other words it

reflects the degree of floatation and traction achievable for a given platform on a given soil [48]. The vehicles cross-country mobility is then determined by comparing the VCI and the CI or the rating cone index RCI. In most cases the RCI is used to describe fine-grained soils and the CI is for coarse-grain soils [7]. A general rule of thumb for comparing the VCI versus the RCI is that for a vehicle is be able to negotiate the terrain in question the VCI should be 10 to 20 points lower than the RCI [48] . This would mean that the soil would have the strength to support the vehicle as it negotiates the off-road terrain.

A cone penetrometer, seen in Figure 2-3, is used in these empirical methods to determine terrain characteristics. The cone is driven into the terrain and a measure of the soil properties is taken. The cone penetrometer gives a measure called the cone index (CI) and this measure is generally considered unit less but it does have the unit of force per unit cone bases area [7]. The CI is a measure of the soil's resistance to the penetration of a right-circular cone and is usually driven into the terrain at a rate of 1.2 in/sec [42]. The cone penetrometer was originally developed by the WES in drawbar pull studies. There were inconsistencies between drawbar pull tests and a way to characterize the soil was needed.

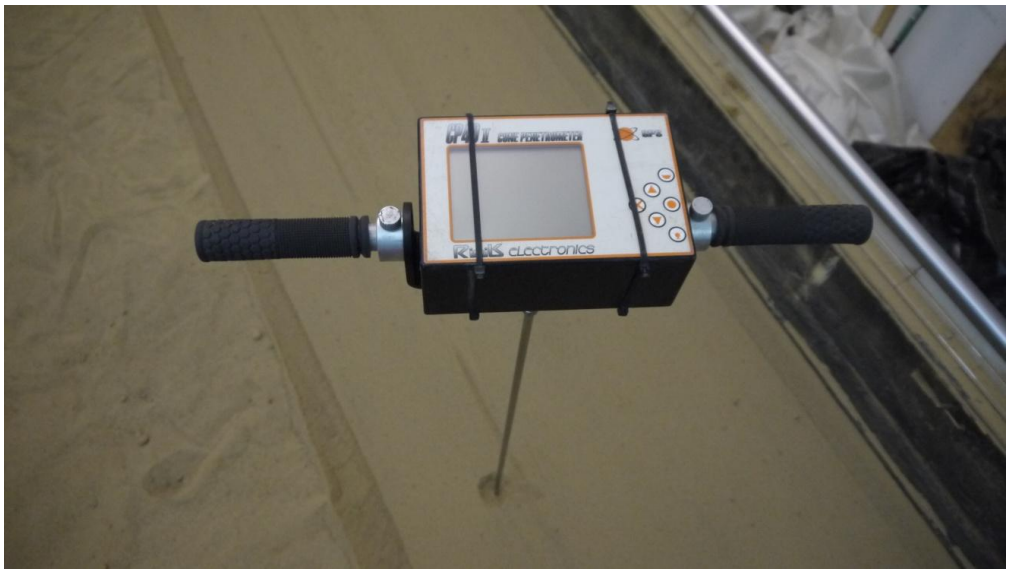

Figure 2-5: A Cone Penetrometer from Rimik Electronics

The vehicle's MI is an empirical relation developed by WES for predicting tracked or wheeled vehicle performance [47]. This empirical relation was developed for heavy weight vehicles and may not be appropriate for SUGV application. The mobility index for tacked vehicles is calculated as

$$MI = \left(\frac{Contact\ Pressure\ Factor \times Weight\ Factor}{Track\ Factor \times Grouser\ Factor} + Bogie\ Factor - Clearance\ Factor\right) \times Engine\ Factor \times Transmission\ Factor \quad 2.17$$

where

$$Contact\ Pressure\ Factor = \frac{gross\ weight, lb}{area\ of\ tracks\ in\ contact\ with\ ground, in^2.}$$

$$Weight\ Factor = \begin{cases} less\ than\ 50{,}000\ lb\ (222.4\ kN) = 1.0 \\ 50{,}000 - 69{,}999\ lb\ (224.4 - 311.4\ kN) = 1.2 \\ 70{,}000 - 99{,}999\ lb\ (311.4 - 444.8\ kN) = 1.4 \\ 100{,}000\ lb\ (444.8\ kN) or\ greater = 1.8 \end{cases}$$

$$Track\ Factor = \frac{track\ width\ in.}{100}$$

$$Grouse\ Factor = \begin{cases} Grousers\ less\ than\ 1.5\ in\ (3.8\ cm) high = 1.0 \\ Grousers\ less\ than\ 1.5\ in\ (3.8\ cm) high = 1.1 \end{cases}$$

$$Bogie\ Factor = \frac{Gross\ Weight, lb, divided\ by\ 10}{\left(\begin{matrix} total\ number\ of\ bogies\ on\ tracks \\ in\ contact\ with\ ground \end{matrix}\right) \times (area\ of\ one\ track\ shoe, in^2.}$$

$$Clearance\ Factor = \frac{clearance, in}{10}$$

$$Engine\ Factor = \begin{cases} \geq 10\dfrac{hp}{ton} of\ vehicle\ weight = 1.0 \\ < 10\dfrac{hp}{ton} of\ vehicle\ weight = 1.05 \end{cases}$$

$$Transmission\ Factor = \begin{cases} automatic = 1.0 \\ manual = 1.05 \end{cases}$$

Based on the calculated MI, the VCI can be calculated for a given vehicle making one or fifty passes. While equation 2.7 describes the MI for a tracked vehicle a similar expression has been developed by wheeled vehicles. The following equation gives the VCI for a tracked vehicle operating in fine-grained soils,

$$VCI_1 = 7.0 + 0.2MI - \left(\frac{39.2}{MI + 5.6}\right) \qquad 2.18$$

$$VCI_{50} = 19.27 + 0.43MI - \left(\frac{125.79}{MI + 7.08}\right) \qquad 2.19$$

Once these values are calculated then other vehicle parameters can be empirically determined such as max drawbar pull, motion resistance, etc. The excess of the RCI over the VCI can be used to empirically determine the vehicles drawbar pull performance. The drawbar pull is proposed as being the difference between the vehicles tractive effort and the internal resistance of the running gear. This relation has been developed for heavy weight vehicles and it has yet to be seen these relations are applicable to SUGVs. These vehicle parameters can be determined as functions of the VCI and CI. The CI is related to the values of k_c, k_ϕ and n through the following empirical relation proposed by Bekker,

$$CI = 1.625\left\{\frac{k_c}{(n+1)}[(z+1.5)^{n+1} - z^{n+1}] + 0.517k_\phi\left[\frac{(z+1.5)^{n+2}}{(n+1)(n+2)} + \frac{z^{n+2}}{n+2} - \frac{(z+1.5)z^{n+1}}{n+1}\right]\right\} \qquad 2.20$$

where the values of k_c, k_ϕ and n can be solved for given you have three values for CI [33]. While the CI has been used for many years as a method to predict vehicle mobility, this application has been question by some.

The interaction between the vehicles running gear and the soil are very complex and some question whether the CI can accurately predict vehicle performance. Research performed by Godbole suggests that the CI is not an parameter that should be used to describe or predict vehicle mobility [49]. He claimed that this is because the CI is a poor measure of the soil strength. These findings were made by comparing results made from previous work dating by to original research performed by the WES. These claimed were supported by researched performed by Dwyer [50], In which traction tests were conducted using the CI as well as a soil shear meter to measure soil parameters. Predictions that were made using the CI showed a poor correlation to measured data in the work performed by Dwyer. While the CI is commonly used these studies call into question using the CI as a way to characterize a vehicle's mobility. The development of the CI eventually laid the foundation for the formation of the NATO Reference Mobility Model.

The NATO Reference Mobility Model is a software tool that was developed in the 1970's and was designed to analyze and examine the potential mobility characteristics of a specific vehicle over a large tract of terrain. The NRMM is one of the only software packages that is specifically design to evaluate a vehicle in a battlefield environment and is the most widely used [51]. The initial work on the Cone Index method provided the ground work for this mobility assessment tool. The NRMM uses the CI value as well as many other inputs such as obstacle crossing, vehicle dynamics, and brush pushover ability [48, 51]. The NRMM mobility assessment tool also includes subjective inputs such as driver vision level and driver ability which might not be applicable to SUGVs being teleoperated or autonomous. For a SUGV the driver ability level could be replaced by an input based on instrument sensitivity or sensor degradation [51]. The NRMM software makes a qualitative assessment based on all the given inputs and then typically

outputs a percent go or no-go response as well as a V90 speed. The percent no-go represents the portion of the terrain that is impassable by the vehicle. The V90 speed is the cumulative speed over the worst 90% of the terrain tract [48, 51]. The NRMM has been developed for heavy vehicles, specifically vehicles in the range of 1 to 70 tons. Recently there have been some attempts to apply these classic methods to small lightweight vehicles as well as to develop novel methods more suitable for vehicles in this class. In 2005 there was an attempt to apply the NRMM mobility tool to the SUGV, PackBot.

PackBot is a SUGV produced by iRobot and is used by the Army for various missions. Some of these missions include surveillance, reconnaissance, and examining improvised explosive devices (IED) remotely [51]. This allows the soldiers to complete their given missions without being directly exposed to potentially dangerous situations. The PackBot is approximately 45 pounds with a minimum ground clearance of 2 inches. This is well outside the constraints that this program was originally developed for. When attempting to use the NRMM with a vehicle this small the issue of terrain resolution arises. Earlier versions of the NRMM software did not even predict obstacles less than four inches high [51]. The authors also noted that because of the unique geometry of the PackBot, mainly due to the flippers, many unique challenges were presented in attempting to define all the input parameters. In figure 2-4 you can see the unique geometry of the PackBot. The conclusion of this work was that NRMM was able to show a potential "concise snapshot" of the SUGV mobility given that the terrain inputs were scaled accordingly. The main reasons for a no-go determination were vegetation and obstacle override problems. The reduced override however, is compensated by the PackBot's greatly increased maneuverability in part due to its small size. Through this study it has been shown that the NRMM has potential for use as a mobility evaluation tool for small robotic vehicles. While it has potential this method has a few obstacles such as the lack of mapped terrain at a suitable fidelity and appropriate inputs to match robotic vehicles unique geometry challenges.

Figure 2-6: The SUGV PackBot [52]

A new method that has recently been developed is the Mobility Metrics Matrix (MMM). The MMM is a assessment tool that attempts to compare the mobility performance of different vehicle platforms for a given set of mission requirements and operating terrains [6]. This mobility assessment method attempts to identify important measurable mobility performance criteria and is largely based on previous theory developed by Bekker. The MMM directly compares different vehicle platforms and assigns a important to specific vehicle parameters based on the mission characteristics. This method results in a mission-specific rank for each vehicle platform based on its performance for the given parameters. This method allows the users to customize each assessment based on the user's needs and mission parameters. The MMM method was developed in 2007 and has yet to see extensive validation.

Methods for mobility assessment have largely remained the same since their development decades ago. These methods are for the most part empirical and were originally developed for vehicles that were in the range for 1 to 70 tons. There recently been studies aimed at determining these methods applicability to smaller unmanned vehicles but there has yet to be any definitive method developed specifically for lightweight vehicles. In 2007 the MMM method was developed for lightweight vehicles but this is the only new development. The current methods are largely based on theory developed by Bekker in

the 1960’s and recent studies have indicated that these methods might not be suitable for small, lightweight vehicles [6, 15, 45].

3. Research Methodology

This chapter contains an overview of the research methodology used for this case study. First the proposed research approach is examined and identified. Following this is a description of the Mobility Metrics Matrix. The MMM's origin, use, and adaptability are all considered. The chapter concludes with an in depth overview of the vehicle used in this case study including; vehicle metrics, hardware, and software.

3.1 Proposed Research Approach

The research aimed at being conducted in this case study is proposed to be performed in four distinct phases. The first proposed research phase is a literature review phase. In this first phase the state-of-the-art in mobility assessment is examined and a test criterion is developed. During this phase the vehicle is also outfitted with a suite of sensors capable of capturing the necessary vehicle mobility parameters. The second phase of the case study is to conduct vehicle testing with the vehicle in a wheeled configuration. In this testing phase the vehicle will be put through a series of experiments aimed at highlighting the vehicles mobility performance. The specific tests to be conducted will be determined in the first proposed phase and derived from literature review. The third phase will be performing the same series of mobility tests but with the vehicle in a tracked configuration. This change of running gear is to examine any mobility distinctions between the two configurations. The final phase of the proposed case study is to analyze the collected data and compare the data to the established vehicle mobility relations to see if any conclusions can be drawn.

The first phase of the comparative analysis involved a complete review of the current state-of-the-art in vehicle mobility assessment. Testing procedures and parameters of interest will be derived from this initial literature review. This review is presented in chapter 1 of the thesis. Traditional terramechanics conventions and relations will be examined with a key focus on their method of development and intended application. As

discussed in chapter 2 many of these relations were developed for heavy vehicles and have not been thoroughly research for their applicability to light unmanned vehicles. With this review possible operating environments and scenarios will be identified. These scenarios will be selected after careful consideration of what would be the most beneficial operating environments to examine. Major users of small unmanned vehicles include the US Army as well as NASA. Operating environments that would be most beneficial to these groups will be given special consideration. The final step of the first phase is to determine a sensor suite that can be used to capture the desired vehicle mobility parameters while the vehicle is operating in the identified scenarios. In order to maintain a feasible scope the vehicle parameters will be limited to an appropriate number. Because a feasible scope must be maintain these performance parameters will be determined through a careful and complete review of the literature. This first research phase will conclude with the installation of the sensor suite onboard the test vehicle.

The second portion of the case study will be the testing of the vehicles mobility while the vehicle is in a wheeled configuration. The test vehicle will be run through a series of mobility tests as identified by phase one of the case study. These tests will be aimed at highlight the mobility characteristics of the vehicle. During this phase the relevant data pertaining to the mobility performance characteristics will be collected and stored for use in phase four the case study. The second phase will conclude when all necessary testing has been done with the vehicle in its wheeled configuration.

The third phase will begin with the vehicles conversion to a tracked configuration. This change in running gear will be done in a manner so that all necessary dimensions will be preserved. These dimensions include effect sprocket/wheel diameters, ground clearance, etc. This will allow for the comparison to highlight any mobility performance differences that can be attributed to the change in running gear alone. This aspect of the case study is essential because without preserving the vehicles dimension then a difference in mobility performance could be attributed to difference vehicle geometries and would not facilitate a direct comparison. The vehicle while in the tracked configuration will be run through the same operating scenarios and the testing will follow the same procedures. The third

phase of the case study will conclude when all the necessary tests have been performed with the vehicle in the tracked configuration.

The qualitative and quantitative analysis of the collect mobility performance data will be the focus of the fourth phase of the proposed research approach. In this phase the collected data sets for the wheeled and tracked vehicles will be qualitatively and quantitatively analyzed and compared. The aim of this phase is to determine if any distinct conclusions can be drawn regarding the differences in mobility performance between the wheeled and tracked vehicle configuration. This collected data will also be compared to the established mobility relations to determine their applicability to small unmanned ground vehicles. The scalability aspects of the mobility relations established by Bekker and Wong have seen limited research and are an area of study that needs to be explored. Finally by using various techniques, including the Mobility Metrics Matrix, the data will be analyzed to determine if any conventions can be formed as to determining the best vehicle configuration for a specific set of mission criteria and operating environment. This proposed research approach is aimed at being thorough and encompassing the state-of-the-art of mobility assessment.

3.2 Mobility Metrics Matrix

The Mobility Metric Matrix (MMM) is an assessment tool that was first developed by Worley in 2007. This assessment tool is used to identify the most important measurable mobility performance criteria for a given set of mission criteria [6, 53]. The MMM is a tool that allows a direct comparison of vehicles with different running gear configurations or mobility platforms. One basic assumption that is made is that all the vehicles in the comparison pool can meet the minimum mission requirements. This means that if there is a specific ground clearance required than all the possible vehicles will meet this basic mission need. The vehicles are directly compared using an indexing function that allows an intuitive and quick comparison. This tool is very flexible and can be adapted for each mission. This allows the various metrics to be added or removed based on the users' preferences. Worley developed a template that provides the MMM user with a great

starting point from which the specific metrics can be adapted. This template can be seen in figure 3-1.

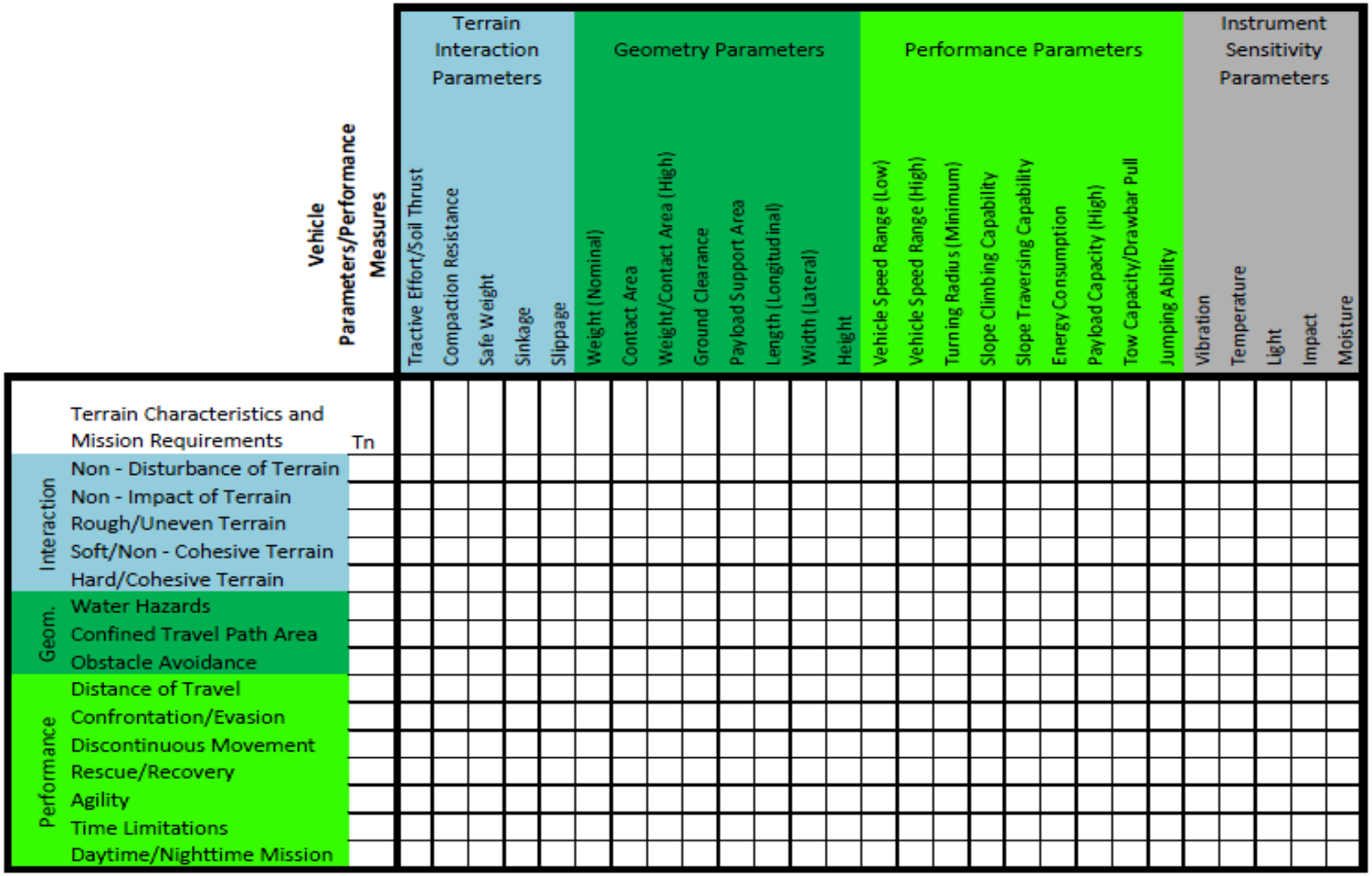

Figure 3-1: Mobility Metrics Matrix template adapted from Worley

The MMM was developed based on a common business tool call the House of Quality (HOQ). The HOQ is a long standing tool that is commonly used in business practice and product development to match customer needs with specific product features [54]. The HOQ lists the customer needs in the rows and the product specification in the columns. The main body of the matrix is then used to note the correlation between these two areas. This technique was adapted by Worley and employed in her MMM. The MMM uses the main HOQ matrix and is used to catalogue the relation between mission criteria and vehicle parameters and performance characteristics. The template developed considers the vehicle-terrain interaction, vehicle geometry, vehicle performance, and the vehicles instrument sensitivity. The vehicle-terrain interaction is the consideration of the classical terramechanics parameters such as compaction resistance, sinkage, etc. A new area of consideration that must be examined with unmanned vehicles is the instrument sensitivity. The available instrumentation and sensitivity of these instruments can have a great impact on the vehicles mobility. All these parameters and specifications can be adapted to the specific mission needs and presents a very useful evaluation tool.

The MMM has a distinct area for each type of vehicle parameter group. The vehicle parameters have been organized into the following groups; vehicle-terrain parameters, vehicle geometry parameters, vehicle performance parameters, vehicle instrument sensitivity parameters. The corresponding terrain characteristics and mission criteria have been organized in the same manner. As you can see on the template these correlating characteristics are easy to identify because all the groups have been color coded.

The first group of vehicle parameters is the vehicle-terrain interaction parameters. This group is based on the classical terramechanics relations developed by Bekker and then furthered by Wong [5, 7, 33, 34]. These empirical relations characterize various vehicle-terrain interaction parameters such as slip, sinkage, etc. The soil characteristics play a vital role in determining many of these characteristics and the empirical relationships take into account these soil properties. Many of these soil properties that were used by Wong and Bekker were obtained from Whitlow's initial soil mechanics research [55]. An example of these parameter groupings can be seen in figure 3-2.

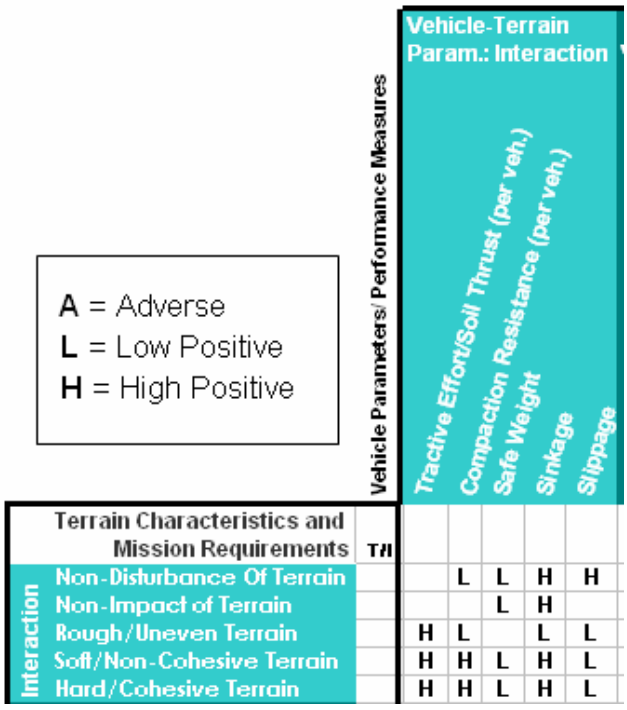

Figure 3-2: Vehicle-Terrain parameters with corresponding terrain characteristics [6]

The vehicle geometry parameters consist of measures of soil characteristics as well as operational area characteristics. These limiting factors could include size and obstacle limits. This section is used to describe the operating terrain and can be adapted to each mission specific terrain characteristics. The vehicle geometry parameters include basic vehicle dimensions such as weight, ground clearance, contact area, etc. These vehicle geometries are correlated with terrain characteristics such as obstacle avoidance, water hazards, or any other necessary terrain geometry characteristics.

The vehicle performance parameters group is a section in which all necessary vehicle actions are included. This section is used to define the basic performance functions of the UGV for the given mission. The template that was developed intentionally leaves this area rather vague so that the user can set specific threshold values and determine the most important performance characteristics.

The final section is the vehicle's instrument sensitivity parameters. This category is used to describe any necessary sensors or sensor sensitivity that is required for the mission operating criteria. These sensitivities are correlated to mission requirements and must be defined by the user because of the vast range of sensing solutions and sensitivity ranges.

The next step in using the MMM to evaluate various vehicles for a specific mission is to assign each mission category a level of importance. This allows the matrix to be customized to mission requirements. Connections that are made between a vehicle parameters and mission need are assigned a level of impact which can be high, low, or negative impact. To avoid any coupling between characteristics in which the vehicle parameter overlap, priority is given to the parameter that encompasses the other. One simple example is the relation between tractive effort and vehicle weight. In this case priority would be given to tractive effort because the vehicle weight in considered in the tractive effort vehicle parameter. Various vehicles are rated and a relative score is given to each vehicle. This relative score allows for a direct and efficient comparison between a large numbers of vehicles. This allows the vehicle candidate pool to be narrowed in a quick thorough manner.

The levels of weighting given to a correlation between mission and vehicle parameters represent how one effects the other during a given mission performance. A high positive correlation (H) describes a direct and beneficial dependency between criteria. A low positive correlation (L) describes a beneficial dependency between criteria but is not direct, or of great enough importance to necessitate a high positive value. A negative correlation (A) represents a correlation where the vehicle parameter will adversely affect the desired mission characteristic. Each of these correlation categories is assigned a specific weighting using the indexing function. Worley notes that this method is based in part on the Quality Function Deployment and indexing function associated with the House of Quality [6, 53].

The final step in the MMM process is to apply the indexing function. The indexing function facilitates a computational approach to the direct comparison of different mobility platforms. The established mission parameters are divided into T groups according to their level of threat/important, $l_{T/I}$. These levels are defined by the MMM user. Within each level of the T/I group, vehicles are ranked for mission suitability, initially by the important of each vehicle parameter to the mission criteria and then by the vehicles comparative abilities to fulfill the desired vehicle parameter. The values of vehicle parameters must be normalized to minimize any unwanted effects when comparing vehicles. The indexing function allows for this normalization and rates vehicles against each other with a zero-to-ten relative rating. For each vehicle metric the user selects the ideal of best vehicle candidate from the vehicle candidate pool. The best candidate must be chosen according to the mission criteria or according to the empirical data. In each case however, the vehicle with the maximum performance for the given criteria should be chosen. As each i^{th} vehicle is scored for the j^{th} vehicle parameter, $p_{i,j}$, it is compared to the best level of performance for all vehicles for that metric, $p_{best(V)j}$. Ranking in this manner allows for the relative vehicle performance to be normalized against the best vehicle performance. This dictates that the best vehicle for a specific metric receives a default score of 10. The vehicle rank is formulated according to,

$$rank_{i,j(k)} = \frac{p_{i,j}}{p_{best(V),j(k)}} * 10 \qquad 3.1$$

In order to weight the amount of correlation of a specific parameters, p_j, to a given mission T/I group we employ two factors. These factors are an *n*-factor and its respective weighting factor. The *n*-factor is equal to the frequency in which a metric *j* is shown in the MMM to be related to the k^{th} group of mission needs. As previously mentioned these can be related by a high, low, or adverse correlation. The *n*-factor is combined with its respective weighting function to determine the importance of a specific vehicle parameter to the mission parameter. The two factors are combined and an importance is determined based on the following equation,

$$importance_{j(k)} = (w_l n_{j(k),l} + w_h n_{j(k),h} + w_a n_{j(k),a} \qquad 3.2$$

The weighting functions values are to be determined by the user. These weighting values can be based on the number of vehicles to be compared or the level to which the vehicles must be eliminated from the general pool. One exception must be noted and that is, for a negatively correlated relationship the value of the weighting function must also be negative. This is important because if you do not assign a negative weighting factor this relation will appear to be a positive relation and will give a skewed vehicle comparison. It must be noted that as of now there is no established method for determining these weighting function and each user must establish his or her own system. If a large weighting factor is used then there will be a large variation of computed values. An example produce by Worley cites that an commonly employed set of values used in industry product development would be set as a 9 for a strong positive, a 3 for a weak positive and a -3 for a medium adverse relation.

Using the threat/importance levels provides the user with a good measure of a specific mission parameter effect on the overall mission and illustrates the final step in comparison of mission needs and vehicle performance. This allows all the importance markers and weighting factors to be combined and a cumulative rank is produces that allows a direct comparison to all vehicles in the candidate pool. The vehicle rank is given by the equation,

$$Q_i = \sum_{k=1}^{T} 1_{\frac{T}{I},k} \sum_{j=1}^{M} \left\{ (w_l n_{j(k),l} + w_h n_{j(k),h}) \left(\frac{p_{i,j}}{p_{best(V),j(k)}} * 10 \right) + w_a n_{j(k),a} \left(11 - \frac{p_{i,j}}{p_{best(V),j(k)}} * 10 \right) \right\} * 3.3 \qquad 3.3$$

Use of this equation allows the mission specific rank, Q_i, of the i^{th} vehicle to be computed which is its mission performance as compared to all vehicles in the candidate pool. The MMM was used and adapted to this specific case study. This involved a customization of the vehicle parameters and will be presented in depth in chapter 4.

The Mobility Metric Matrix is a valuable tool to directly compare vehicle performance across several different vehicle platforms. Because of this it will be included in this vehicle mobility analysis to directly compare the vehicle in a tracked versus wheeled configuration. The MMM template will provide the starting point for the analysis but will be adapted for this specific study. The goal of using and adapting the MMM for this analysis will be to further develop and refine the MMM to produce a more advanced version that can be specifically applied to vehicles that are on the robotic scale. This refinement will produce a MMM that more focuses on mobility performance of vehicles in this size range and present a more distinct and definitive set of vehicle metrics. This set of more individualize metrics will help make a more precise comparison and will produce a more accurate vehicle performance contrast. With this more refined MMM greater insights can be gained and a more suitable vehicle can be selected or designed.

3.3 Case Study Vehicle

The case study proposed is aimed at examining the mobility characteristics of a small unmanned ground vehicle. This ground vehicle is going to be tested in a wheeled configuration and a tracked configuration. Changing the running gear will allow for a direct comparison between the mobility of each specific running gear. The vehicle will be tested in a variety of operating scenarios and environments. These scenarios and environments will be discussed in detail in chapter 4. The vehicle being used for testing was generously provided by Virginia Tech's Vibration and Acoustics Laboratory (VAL) Professor, Alexander Leonessa.

The test vehicle is a small unmanned ground vehicle that is teleoperated via a controller program connected through X-Bee wireless communication devices. The vehicle is a kit robot that was produced in Korea. The robot was purchased for the VAL Laboratory a few years ago and has been occasionally employed for a select few research projects thus far. The vehicle has remained in the VAL Laboratory for the duration of its use. Unfortunately much of the vehicles original documentation and specifications have been

lost throughout this time. This presented a slight hurdle as some parameters were needed, especially regarding the motor characterization. An exhaustive attempt was made to find out more information about its manufacturing, origin, motor characterization, etc. This searched turned up no new information and the effort was aborted to move forward with the project. The specifications and metrics required for this project, such as a motor power relation, were collected specifically for this case study and are assumed to be valid after extensive testing.

The vehicle's basic metrics were collected before testing began. This vehicle is differentially steering in both running gear configurations. The vehicle has six wheels in the wheeled configuration and when converted to the tracked configuration it has 6 sprockets that interface with the track. The basic vehicle dimensions can be seen in figure 3-3, 3-4, and 3-5. The vehicle in a wheeled configuration measures 17 inches in length and has a width of 18.5 inches. The vehicle has a wheel diameter of 5.058 inches and overall height of 5.5 inches with a ground clearance measuring 2.25 inches. The widths of the tires are 2.5 inches leaving 13.5 inches between the wheels. The tread height of the wheels is approximately 0.225 inches. Each wheel on the vehicle has an independent suspension system. This suspension system is very basic and consists of a set of suspension springs and a damping unit connected to the wheel's swing arm. This suspension system has a nominal travel range of approximately 1 inch. The vehicle weighs approximately 16.25 pounds. The springs on the vehicles suspension system are very stiff for the weight of the vehicle and their usefulness is yet to be seen. The tires on the vehicle are made of rubber and are non-rigid. The tires are specifically designed for small vehicles and are not inflated. The tires keep their shape due to the stiffness of the rubber used. This allows the tires to be non-rigid while not holding air or requiring any inflation. This type of tire and suspension system arrangement can be seen on many small unmanned vehicles currently be used today.

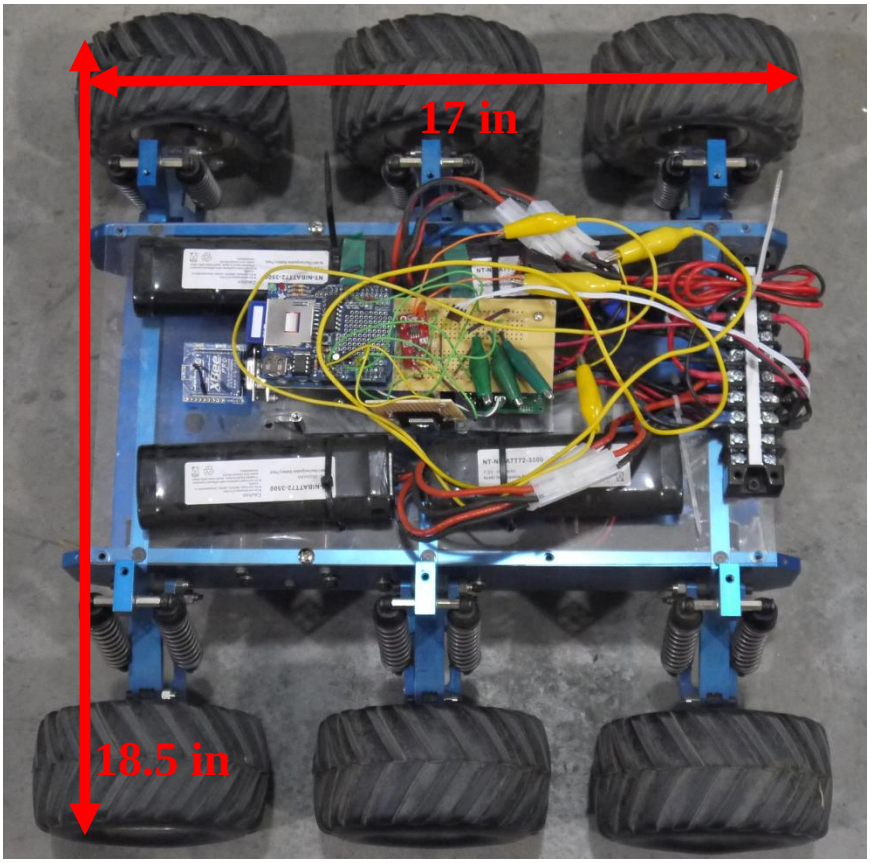

Figure 3-3: Wheeled vehicle dimensions from top

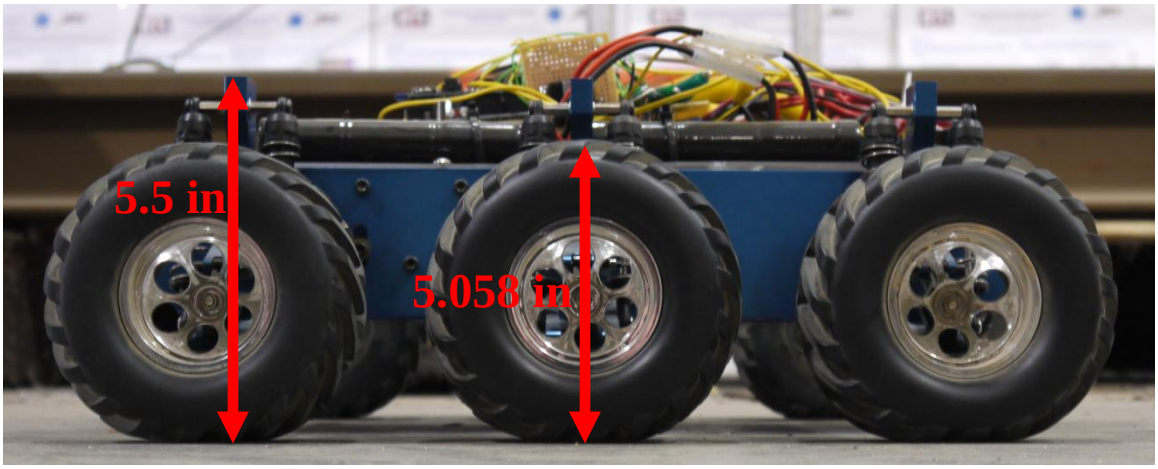

Figure 3-4: Wheeled vehicle dimensions from side

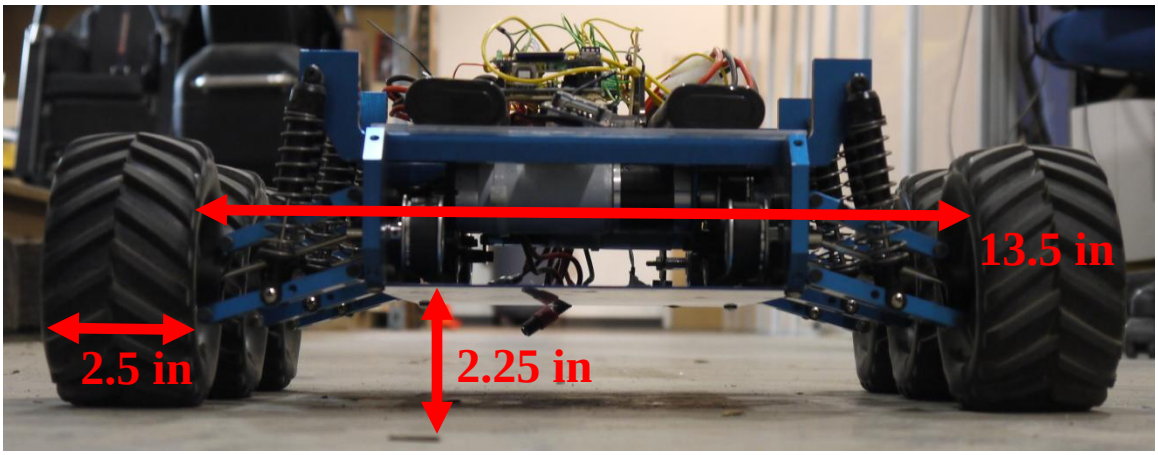

Figure 3-5: Wheeled vehicle dimensions from front

After the wheeled testing is concluded the vehicle is then converted to a tracked configuration. The basic metrics for the tracked configurations were collected before testing began. The conversion between the wheeled and tracked configuration was done in a manner that preserved as many critical dimensions as possible. The tracked vehicle dimensions can be seen in figures 3-6, 3-7, and 3-8. The vehicle in a tracked configuration measures 16 inches in length and has a width of 17.5 inches. The vehicle has a sprocket diameter of 4.5 inches an overall height of 5 inches with a ground clearance measuring 2 inches. The widths of the tracks are 2 inches leaving 12.5 inches between the wheels. The tread height of the wheels is approximately 0.0125 inches. The vehicle in its tracked configuration has a total weight of 16.47 lbs. In the tracked configuration the vehicle has the same suspension travel range.

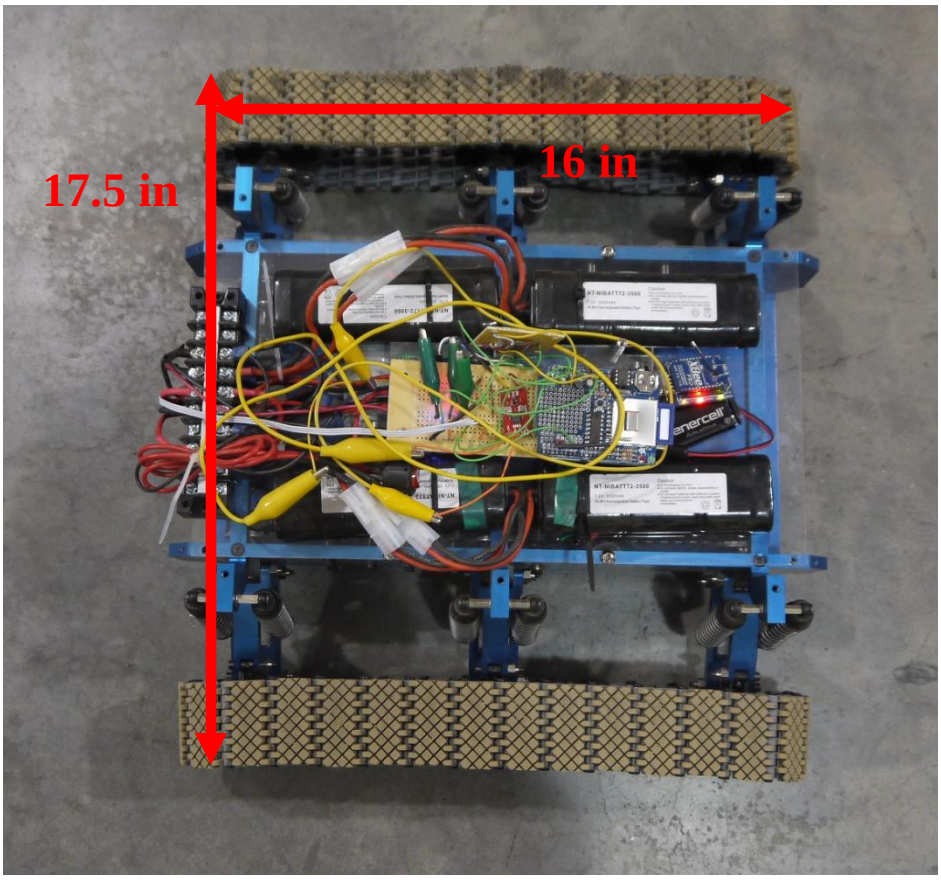

Figure 3-6: Tracked vehicle dimensions from top

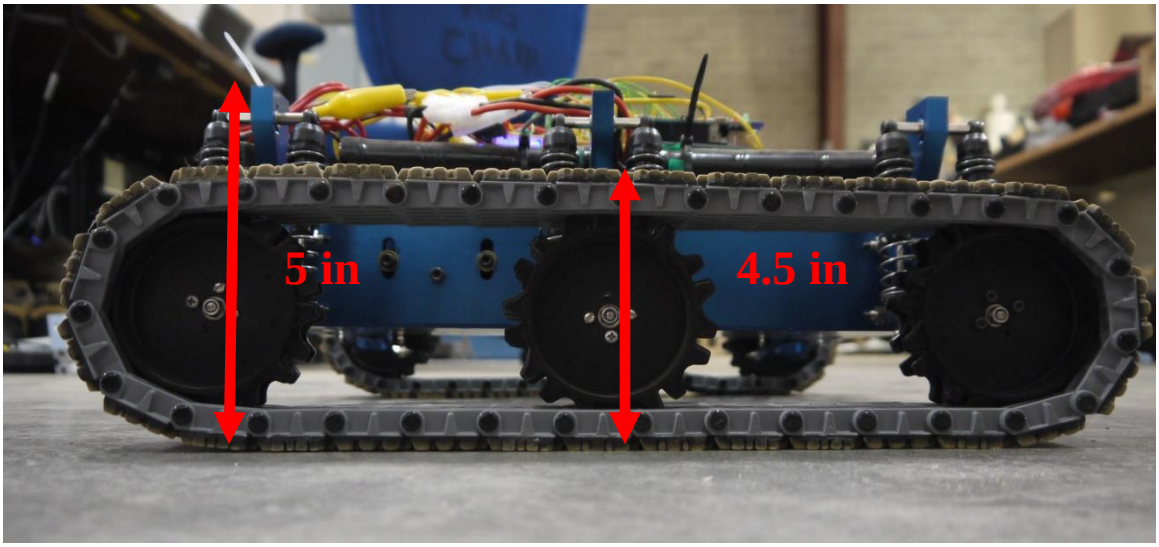

Figure 3-7: Tracked vehicle dimensions from side

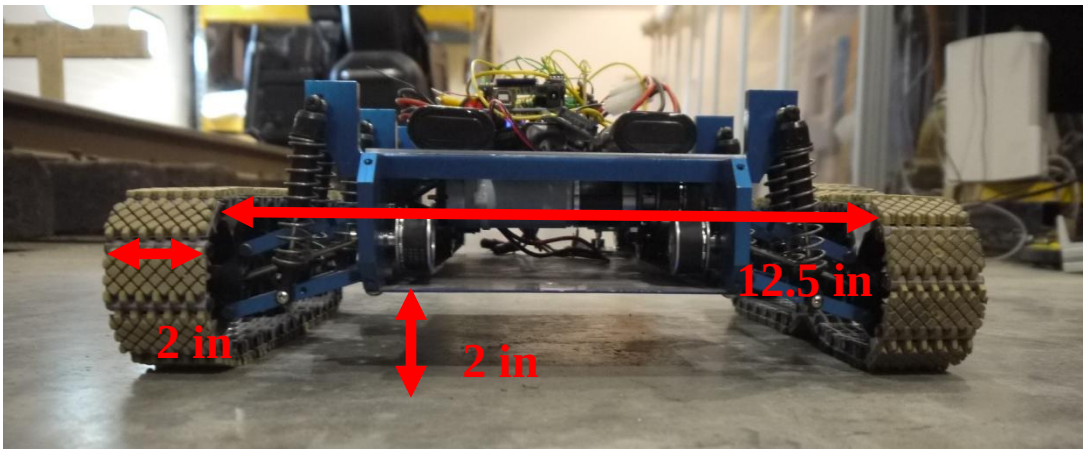

Figure 3-8: Tracked vehicle dimensions from front

As previously mentioned the vehicle is differentially steered in both the wheeled and tracked configuration. Each side of the vehicle is powered by its own individually controlled DC motor. This arrangement facilitates the vehicles differential steering system. The organization of the vehicles power system allows torque to be applied to all six wheels simultaneously. The vehicle's DC motor is mechanically linked to each drive sprocket through a transmission belt. This belt is approximately .08 inches thick and is produced by Mitsuboshi Belting LTD. Mitsuboshi Belting LTD. is a Japan company that specializes in the manufacture of a variety of power transmission belts. The vehicles drive train system can be seen in figure 3-9. The vehicles drive train is powered power four rechargeable nickel-metal hydride battery packs. These batteries are rated for 3400mAh and provide approximately 7.2 volts. These batteries are commercial off-the-shelf parts and are manufactured by the Ovonic Battery Company which has recently been acquired by BASF Corporation. An attempt was made to discover the manufacturer information of the vehicle's DC motors but any identifying marks have been removed by previous students. The manufacturer's stickers on the motors are illegible so the origins of the vehicles motors remain unknown.

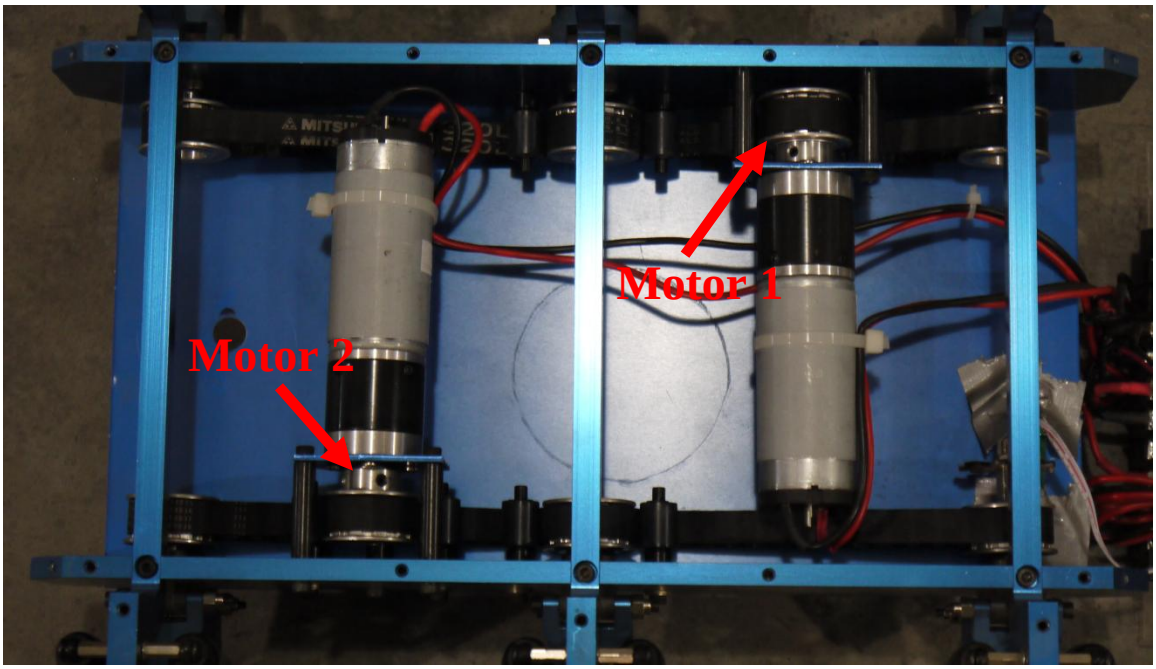

Figure 3-9: The test vehicle's drive train

The vehicle's motors are controlled by the TReX Jr. Dual-Motor Controller produced by Pololu Robotics and Electronics. This motor controller is a versatile motor controller that is designed specifically for use with small and medium sized robots [56]. This motor controller can be used to drive up to three motors, two of which can be driven in a bidirectional manner and one in a unidirectional manner. The control information for these motors is received through five separate input channels. The motor control can be operated using one of three input methods; radio control (RC) servo pulses, analog voltage, or asynchronous serial communication (RS-232 or TTL). In this case study the motor controller is operated using serial communication to receive control inputs and output motor information. The motor controller receives the serial input commands and increases or decreases the voltage on the appropriate channels accordingly. This increase or decrease in voltage will determine the direction and speed of the DC motors. The TReX Jr. motor controller can be seen in figure 3-10. For this case study the power supplied to the motors in controlled by the motor controller through the Pulse Width Modulation Technique (PWM).

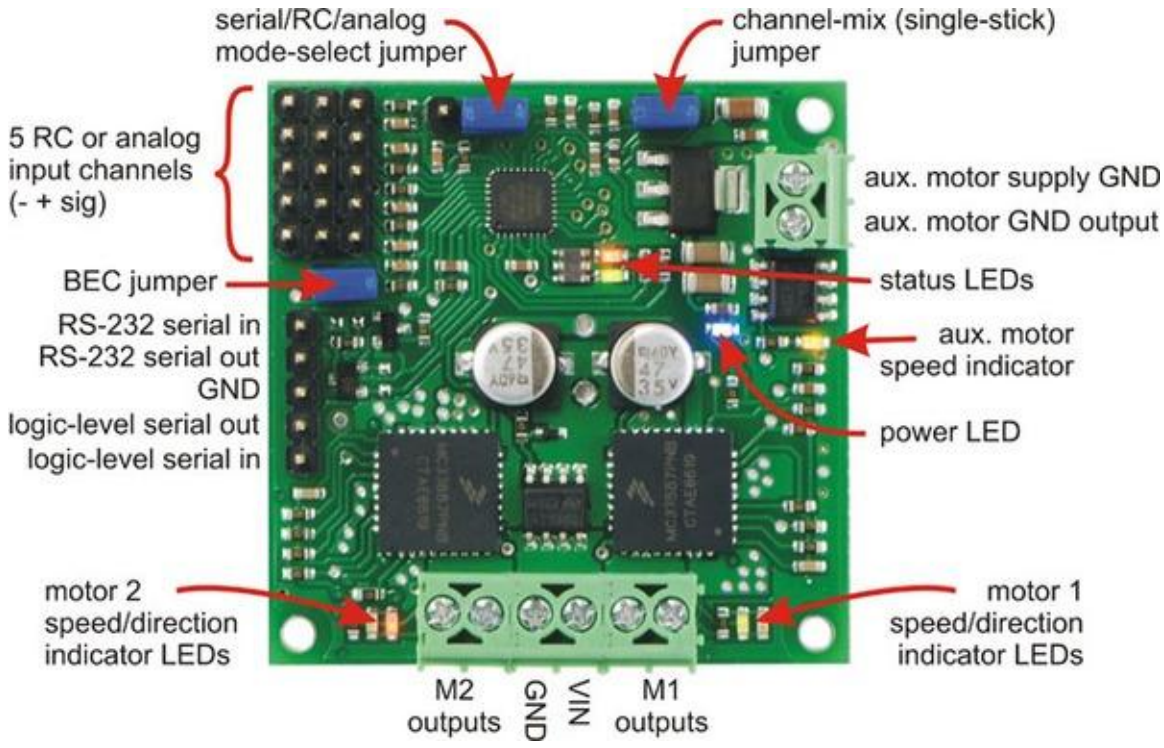

Figure 3-10: TReX Jr. motor controller [57]

PWM is a relatively common technique for controlling the power supplied to an electric motor. The operating principle is fairly simple and relies on switching the power supply on and off at a very high rate to control the average voltage and current available to the motor [58]. The longer that the power supply is switched on compared to switched off then the higher the average voltage and current. The amount of time that the power supply is switched on over the defined time period is called the duty cycle. A duty cycle of 100% would indicate that the power supply is fully on. This principle is governed by the following equation,

$$\bar{y} = \frac{1}{T}\int_0^T f(t)dt \qquad 3.4$$

where $\bar{y}$ represents the average value of the waveform function, $f(t)$. If $f(t)$ is a pulse waveform with a value of either y_{min} or y_{max} and these values have a duration of D, then equation 3.4 can be expanded as,

$$\bar{y} = \frac{1}{T}\left(\int_0^{DT} y_{max}dt + \int_{DT}^{T} y_{min}dt\right). \qquad 3.5$$

Equation 3.5 can be further simplified depending on the application. Because of its simplicity PWM has many advantages as a motor control technique. Some of these advantages are low power losses and an ease of use for digital control situations. An example of the PWM technique can be seen in figure 3-11. In this example PWM is being used to generate an AC signal but the operating principle is the same when use PWM for DC motor control. In the figure below V represents the phase-to-phase voltage pulses and B represents the resulting flux density waveform.

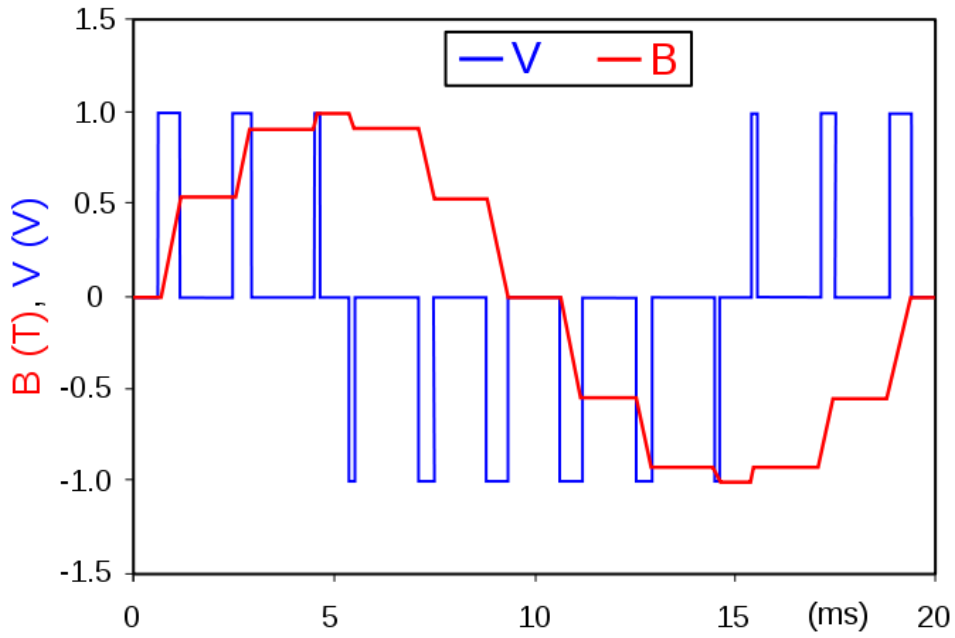

Figure 3-11: PWM being used to generate an AC motor control signal. [59].

The motor controller is produced with a propriety graphical user interface (GUI). This GUI allows for direct control of each motor as well as a number of other parameters. This is very useful because the user can set current limits, acceleration limits, PWM

Frequencies, etc. For this case study I have kept all the settings constant with what previous students using this vehicle had them set to. This decision was made due to a lack of knowledge of the motor characteristics. An example of the GUI can be seen in figure 3-12. The GUI allows motor commands to be received by the motor controller through the computer and are transmitted using an X-Bee-PRO wireless communication system. The motor controller receives commands through this propriety controller program that is operated from a computer.

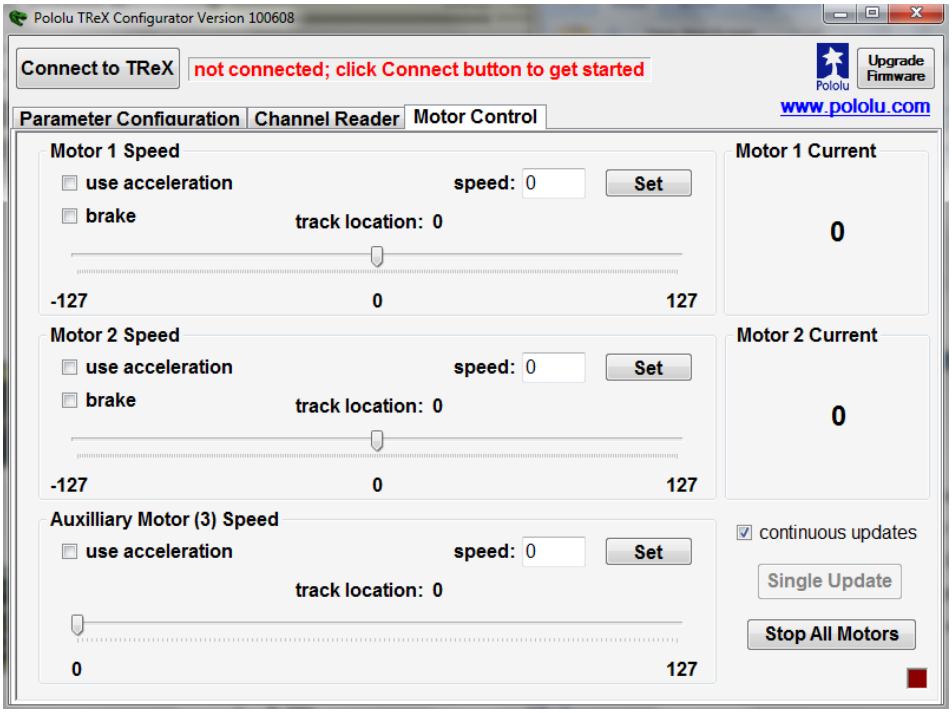

Figure 3-12: TReX Jr. motor controller GUI

The X-Bee-PRO is an OEM RF module that enables users to wirelessly communicate between various devices. These modules are engineered to meet IEEE 802.15.4 standards. This wireless communication devices interfaces directly with the computer and provides a direct link to the vehicles motor controller. The wireless communication range is approximately 300'. X-Bee-PRO can transfer data at a rate of 115200 bps but for this case study the data transfer rate was set at 9600 bps to prevent computer lag from an overly high data rate. The X-Bee-PRO module can be seen in figure 3-13.

Figure 3-13: X-BEEPro wireless communication device [60]

4. Design of Experiment

This chapter contains an in-depth description of the design of experiment used for this study. The experimental objectives are outlined in the first section. The motivation and reasoning behind these objectives are explored next. Following this section, a presentation of the parameters selected for the study is given. This section includes all the collected parameters and highlights all the information planned to be used in the analysis section. The next section discusses the specific testing scenarios implemented in this study, as well as the motivation behind these scenarios. The final section in the design of experiment chapter is a thorough exploration of the experimental methods applied and settings selected. In this section the soil preparation method is discussed in addition to the testing procedure and suite of sensors used to collect the selected parameters.

4.1 Experimental Objectives

The main experimental objective of this study is to assess and classify the mobility and key performance parameters of small unmanned wheeled and tracked vehicles. Thus, the work conducted is aimed providing both quantitative and qualitative analyses of these mobility and performance parameters. As concluded from the review of literature conducted, while there have been numerous studies in which mobility performance for large vehicles has been investigated it has still to be explored if these same relations can be successfully applied to small unmanned vehicles. This is a significant gap in practical understanding and as the use of these unmanned vehicles grows, the need for an accurate description of their mobility grows as well; the U.S. Army and NASA have seen an increase in the use of UGV's and this trend is very likely to increase as time moves forward. In addition, the study presented in this thesis is aimed at highlighting the characteristics unique to each type of the two running gears considered. This will allow users to determine this correct vehicle configuration for a given set of operating requirements and environments. This objective will be further explored through the use of the Mobility Metrics Matrix discussed in earlier chapters and first developed by

Worley [6]. With further work with regard to the MMM, this case study will help developers quickly compare vehicle configurations in a direct and intuitive manner. Finally it is the hope of the author that the work presented in this study will lay the foundation for future work in the area of small unmanned ground vehicle mobility and will lead to a better understanding of their operating characteristics.

4.2 Parameters Selected for Study

After the thorough and complete review of literature and the state-of-the-art in vehicle mobility assessment, a select of selected vehicle parameters were highlighted for investigation in this study. These parameters were selected since there were considered to be in order to give a complete and accurate picture of vehicle mobility performance and have been used in previous studies dating back to the original work done by Bekker and Wong [5, 7, 33, 34]. These vehicle performance measures were intended to give the most complete picture possible while still maintaining a feasible scope for this project. The parameters collected in this study are the drawbar pull, slip, sinkage, current consumption, vehicle speed, roll, yaw, and ground pressure. These parameters also allow a number of terramechanics and vehicle performance relations to be employed because these are common inputs for many of these classic relations. These parameters were collected by a sensor suite outfitted on the vehicle.

Drawbar pull has long been a parameter of interest and has been used since the early 1960's to characterize an off-road vehicles mobility performance [34]. This parameter wasn't thoroughly studies and well understood until the 1970's when it saw increased use and dedicated research. As researchers and user groups begin to search for better small unmanned vehicle designs the drawbar pull continues to be a vital parameter. The Army currently uses drawbar pull to characterize the traction capabilities of all of its vehicles to make better decisions for vehicle selection for a specific mission [2]. Another benefit of selecting the drawbar pull in this case study is that it allows some insight into the vehicle's maximum tractive effort as well as the vehicle's internal resistance. The

drawbar pull relation is expressed in equation 2.11. It has long been accepted that there are noticeable differences in performance of the drawbar pull for wheeled and tracked vehicles and it is hoped that this difference will be highlighted in this case study and allow discernible conclusions to be drawn regarding the specific operating criteria that each vehicle is better suited for. Because of these factors and its relevance in research today, the drawbar pull was a parameter of interest and included in this case study.

Depending on the operating conditions the vehicle sinkage can be a significant parameter of interest. For off-road applications the vehicle sinkage is a key parameter and can greatly impact overall mobility. This parameter along with vehicle ground pressure has long been studied and was one of the first parameters to be researched in the early work done in the late 1950's [5]. Bekker's relation between pressure and sinkage has been used for decades and laid the foundation for many researchers to follow (equation 2.2). Vehicle sinkage and ground pressure have a big impact on mobility especially in an off-road operating environment where vehicle floatation can be preferred and the difference between mobility and immobility. Vehicle ground pressure is directly related to vehicle sinkage and is included in most mobility analysis performed to date. Such relations are still under investigation to assess their feasibility for applying them on robotic scale vehicles. Thus, it seemed like an obvious element for this case study and was included.

The final parameters selected that are considered classic vehicle mobility parameters are running gear slip and vehicle speed. The slip of the vehicle's running gear can have a huge impact on the mobility characteristics. The basic slip relation can be seen in equation 2.6 and 2.7 and is generally defined as the ratio between the forward speed of the running gear and the actual forward speed of the vehicle. The slip of the vehicle has been a research interest for quite some time and can be related to numerous operating condition factors such as tire or tread design, terrain characteristics, vehicle speed, and many others [7]. Because of its direct relation to vehicle slip and it being a parameter included in almost all vehicle mobility studies, the vehicle's speed was included. The speed of the vehicle can be useful in helping to characterize the vehicle's mobility performance and is generally a parameter of interest. While the vehicle speed is usually

easy to measure, the vehicle slip is quite difficult to measure and several different methods have been used for heavy vehicle but wheel slip has yet to be measured directly for robotic vehicles. The available experimental data for heavy vehicles suggests that the maximum tractive effort occurs around 15% to 20%. Slip for a wheeled and tracked vehicle is characterized slightly different and the mobility performance differences between these two running gears would be of great interest and would provide valuable insight into the mobility performance of each running gear. The factors mentioned have all contributed to the decision to include this performance parameter in this case study.

As small unmanned vehicles continue to be used, vehicle range and continuous operating time will see an increased importance. Currently small unmanned vehicles are limited by their energy storage capabilities but also by their energy efficiency. A main goal of this case study is to study the energy needs for a wheeled versus tracked vehicle, while they perform similar tasks. This comparison will provide a great insight into the energy efficiency of each running gear style and can be used to design more energy efficient vehicles. Because of this research goal current consumption was deemed a parameter of significance and included in this case study. By studying the current consumption, a direct comparison can be made regarding power requirements for each running gear while they perform similar task. This information can be used in the future to help design more efficient vehicles that will have increased range and operating characteristics.

The final parameter selected in be included in this case study is the vehicle's roll and yaw. These terms were developed to describe flight dynamics but are applied here to describe the motion of the SUGV as it traverses over unprepared terrain. Roll is generally defined as the rotation along the X axis and the yaw is defined as the rotation along the Z axis. Knowing the orientation of the vehicle will allow the other vehicle parameters to be correlated to the vehicles position. This will be beneficial when comparing vehicle speeds and current consumptions. A diagram of the axes of rotation with respect to the test vehicle can be seen in figure 4-1. Because of the potential insights gained by included the vehicle orientation in this case study it was deemed a parameter of interest.

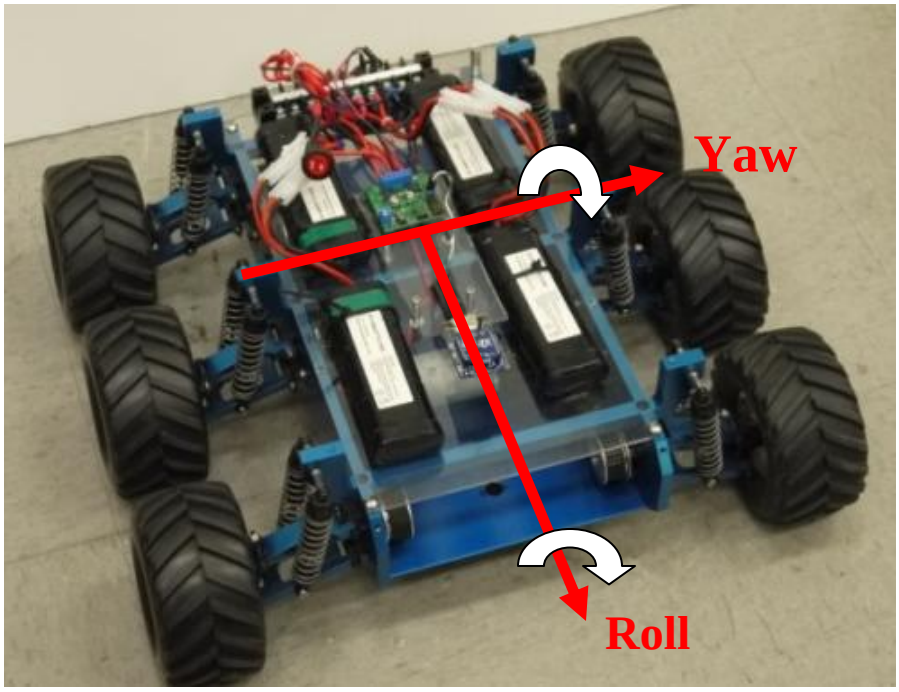

Figure 4-1: Yaw and roll axes

The parameters included in this study have all been carefully selected after a thorough review of literature and are intended to give the most accurate representation of vehicle mobility performance possible. Many of these vehicle parameters have been used for decades in vehicle mobility research and have long been proven valuable in vehicle mobility comparisons. While many more parameters could have been included, this study was limited to these parameters to maintain a scope that was reasonable to accomplish in the time period allotted to this study. These parameters will all be measured by a suite of onboard sensors and sensors embedded in the testing environment. The method of measuring these parameters is discussed in section 4.4.

4.3 Case Study Scenarios

The study scenarios for the case study were carefully selected in order to gain the most accurate measure of vehicle mobility performance. The study scenarios were design so that all the testing could be conducted at the Advanced Vehicle Dynamics Laboratory

(AVDL), at Virginia Tech. This allowed testing to continue throughout the year and any inclement weather would not affect the testing schedule. The vehicle used in the testing belonged to the Vibration and Acoustic Laboratory (VAL) at Virginia Tech.

In total there were eighteen different scenarios that were identified and used for testing. The bulk of the scenarios occurred on either rigid surface or sandy silt loam. The vehicle was tested on flat surfaces, incline surfaces, and in obstacle negotiation situations. A summary of the testing scenarios that were utilized can be seen in table 4-1. While the scope of the testing was significant, all the scenarios were necessary to facilitate a complete analysis. The scenarios in which the vehicle was tested, where there were no obstacles present included in this case study are: flat rigid surface, flat sandy silt loam, incline rigid surface, incline sandy silt loam, random rough vegetated terrain. These scenarios were all tested at varying speeds. The scenarios in which the vehicle was tested for obstacle negotiation included: negotiation of a 1.5 inch square bar with one side of the running gear, negotiation of a 1.5 inch square bar with both sides of the running gear, negotiation of a 1 inch square bar with one side of the running gear, negotiation of a 1 inch square bar with two sides of the running gear, negotiation of a triangular cleat with one side of the running gear, and negotiation of a triangular cleat with both sides of the running gear. An example of these scenarios can be seen in figures 4-3 and 4-4.

Table 4-1: A summary of testing scenarios

Testing Condition	Sandy silt loam	Rigid Surface	Random Vegetation
Level Surface	✓	✓	✓
Inclined Surface	✓	✓	✓
Obstacle Negotiation with One Side	- 1.5 in square - 1 in square - triangular cleat	- 1.5 in square - 1 in square - triangular cleat	
Obstacle Negotiation with Both Sides	- 1.5 in square - 1 in square - triangular cleat	- 1.5 in square - 1 in square - triangular cleat	

The testing on a sandy silt loam surface was carried out on the terramechanics rig in the AVDL lab. The terramechanics rig was developed in the mid 2000's and developed to perform single wheeled tests on soft soil indoor. While the measurement systems mounted to the rig were not utilized for this project, the rig was used extensively for pre-run soil preparation. The terramechanics rig can be seen in figure 4-2.

Figure 4-2: The terramechanics testing rig at the AVDL Laboratory

The testing that occurred on a rigid surface was conducted on a concrete testing strip located in the AVDL laboratory. This strip of concrete was free of obstruction and allowed the various obstacles to be secured to the framework of the terramechanics rig. This was convenient because the obstacles needed to be secured or they would be pushed aside by the vehicle as the testing was being conducted. The rigid surface testing area can be seen in figure 4-3.

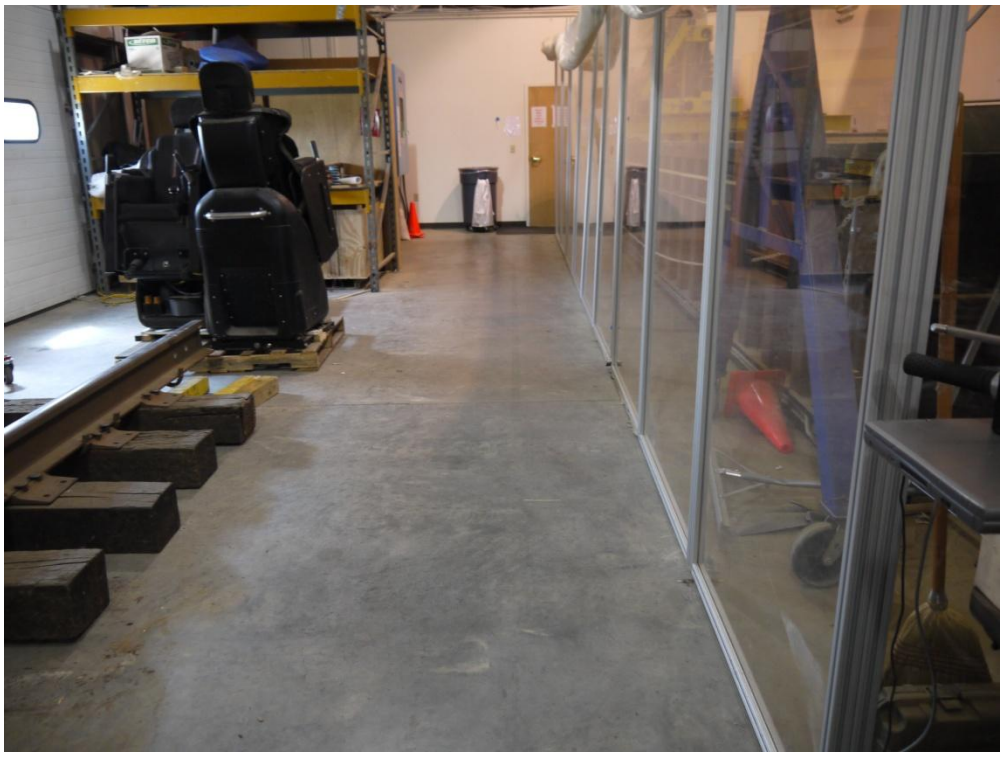

Figure 4-3: Rigid surface testing area

As previously mentioned various obstacle negotiation scenarios were included. These obstacles were tested with one running gear traversing the obstacle and then with both running gears traversing the obstacles. In figure 4-4 you can see the test vehicle traversing an obstacle with one running gear. In figure 4-5 the vehicle is negotiating the same obstacle but with both running gears.

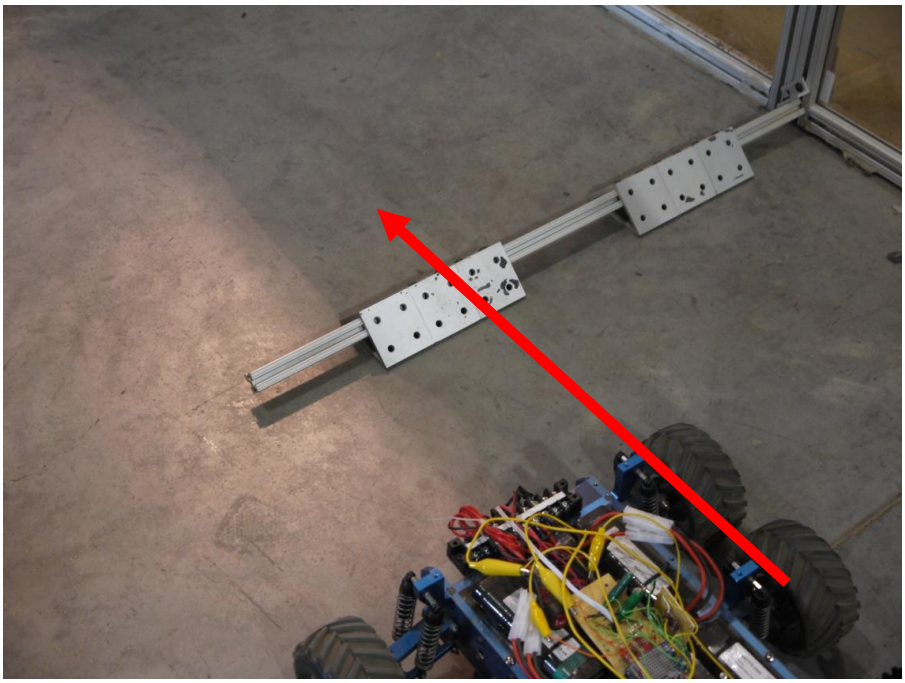

Figure 4-4: The test vehicle negotiating an obstacle with one running gear

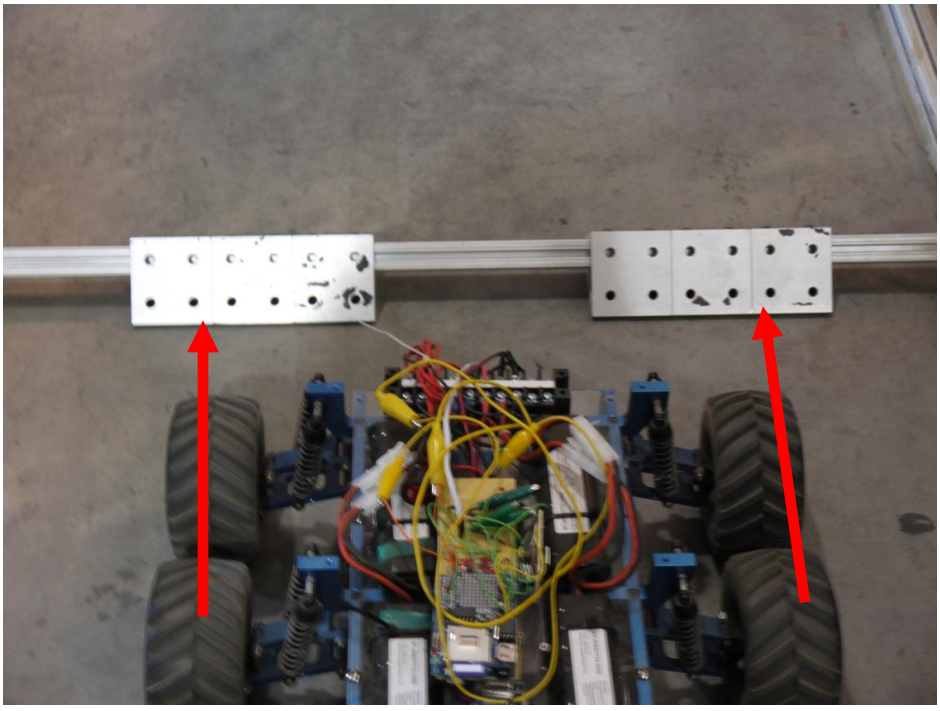

Figure 4-5: The test vehicle negotiating an obstacle with both running gear

Three different obstacles were used in the various obstacle negotiation tests. These obstacles include a 1.5 inch square bar, a 1 inch square bar, and a triangular cleat. Both the square rod obstacles have an approximate length of 17 inches. The triangular cleat used for these tests had a height of approximately 2.29 inches, a width of 2.29 inches, and a base length of 4.19 inches. There are three triangular cleats secured in a row for each side of the running gear with a gap of six inches between each set of cleats. These obstacles can be seen in figures 4-6 to 4-8.

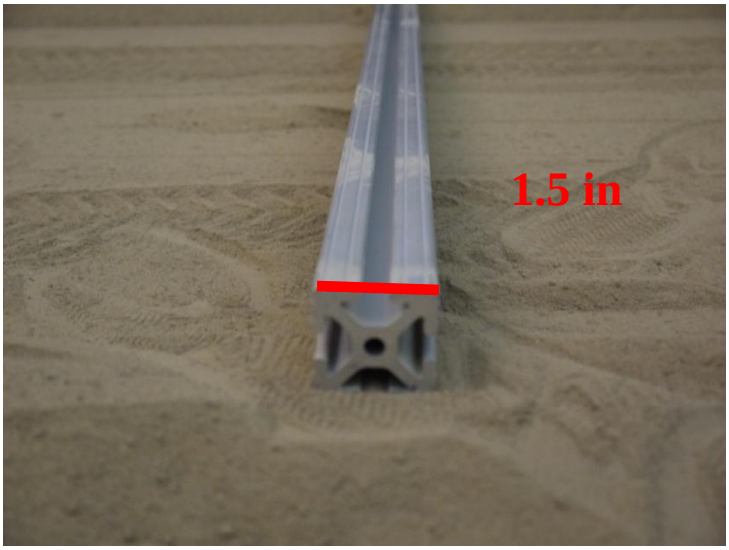

Figure 4-6: 1.5 inch square rod obstacle

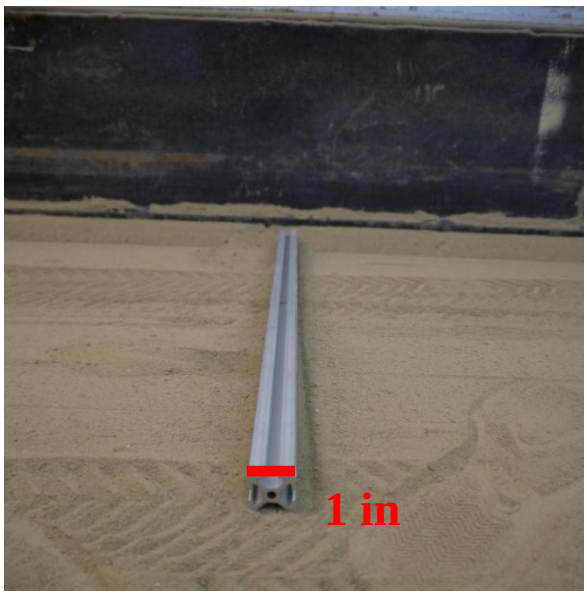

Figure 4-7: 1 inch square rod obstacle

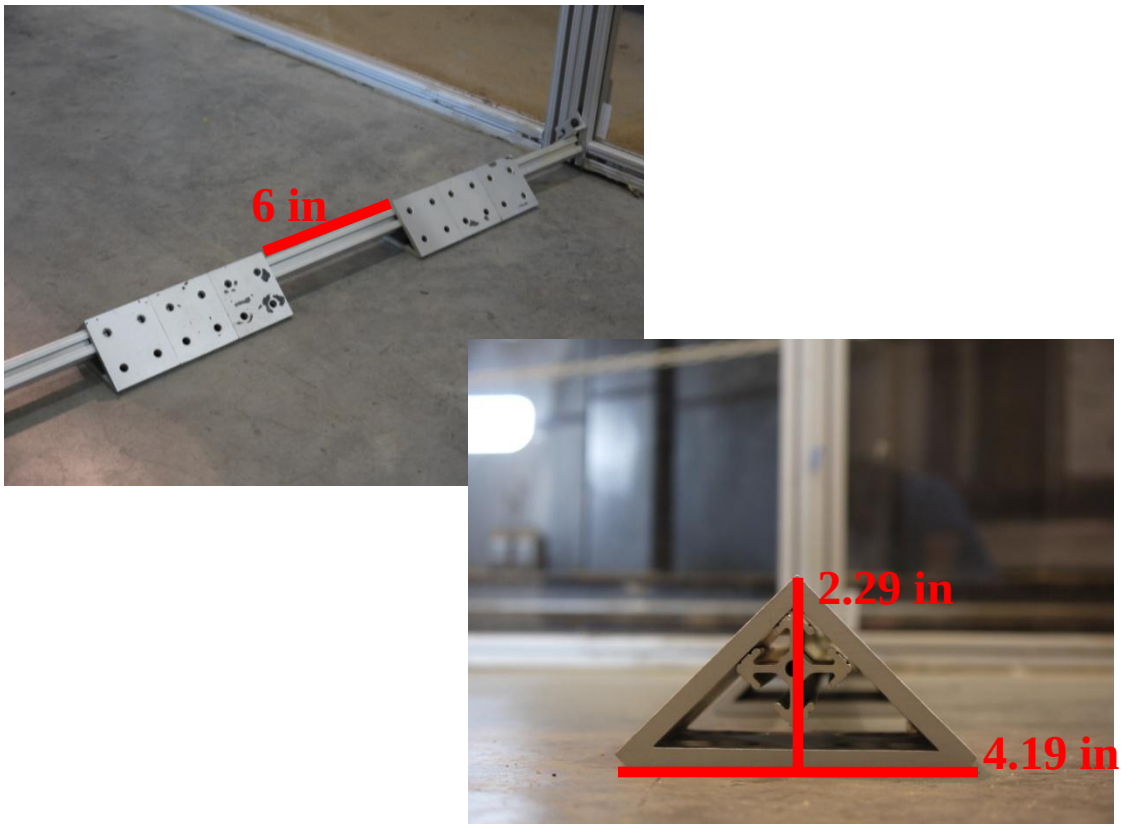

Figure 4-8: Triangular cleat obstacle

These eighteen scenarios were selected to give a relatively complete picture of vehicle mobility. They were selected after a thorough review of the state-of-the-art in vehicle mobility assessment and also from feedback from various user groups. These scenarios were selected to highlight differences in mobility characteristics between the wheeled and tracked configuration. The obstacle negotiation tests were included because SUGV's are seeing an increased use in urban areas as well as environments that have uneven and unprepared terrain. This makes obstacle negotiation of keen interest. If the vehicle cannot negotiate minor obstacles than it will either become immobilized or its path of travel will have to be altered to avoid these minor obstacles. In an urban environment many obstacles will be present such as stairs, bricks, and other loose rubble. By including these multiple scenarios it is hoped that a very complete picture of mobility will be presented.

4.4 Experimental Methods and Settings

This case study was conducted in a manner that allowed each test to be as similar and repeatable as possible. In order to achieve this goal, a rigid experimental method was followed throughout the experimental study. The experimental method included consideration of as many factors as possible, from soil preparation to post run procedures.

Pre-Run Soil Preparation

The soil was prepared prior to each run conducted on the sandy silt loam surface. The testing procedure was performed in a manner so that the soil conditions remained the same for every run. To begin the soil preparation method, the soil was first spayed down with water using a garden hose. This was done in order to reduce the amount of dust that was introduced into the air from the soil preparation procedure. Next the soil was tilled with an electric tiller to loosen up any compaction and soil clumping that occurred due to the introduction of moisture. This was done so that each section of soil received two passes from the tiller. This step is illustrated in figure 4-9. The tiller had a width of 10

inches and the testing area had a total width of 30 inches. This means that three rows of tilling passes must be made to till the total testing surface.

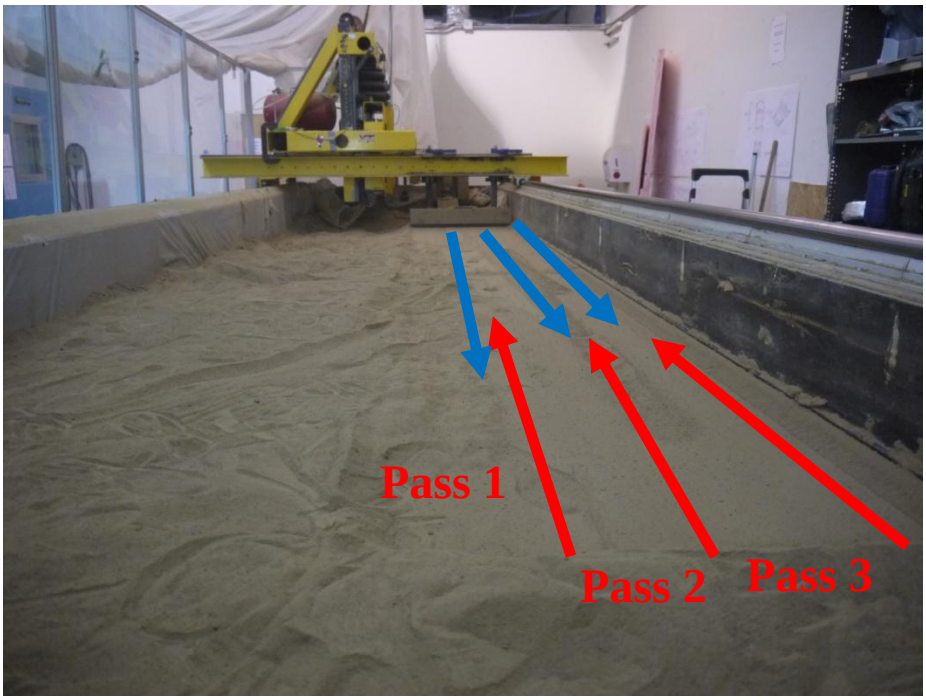

Figure 4-9: Pre-run soil tilling procedure

Following the tilling of the soil, the soil was then raked. This was done to roughly level the testing area to prevent any soil mounds and to achieve an even soil compaction. After the soil was raked a 300 pound roller was used to compact the soil in an even manner. The roller was rolled down and then back to its original position. This step in the soil preparation procedure can be seen in figure 4-10.

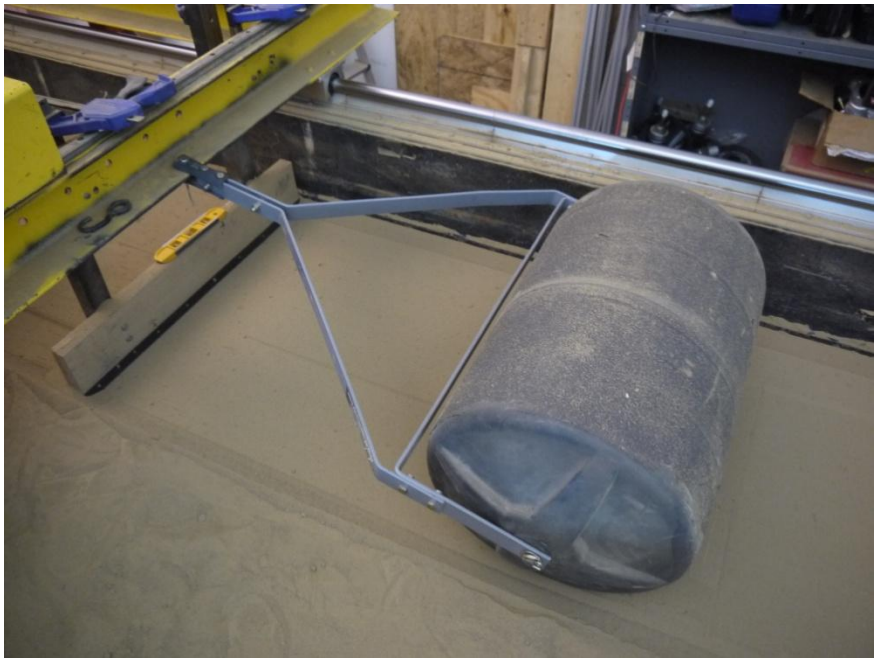

Figure 4-10: Soil compaction using a lawn care roller

The final step in the pre-run soil preparation procedure involved leveling the soil in order to have a nice flat surface to commence testing on. A leveling device is attached to the terramechanics rig and utilized for this case study. The leveling device was set in place using a tubular spirit leveler. This step in the soil preparation procedure can be seen in figure 4-11. Once the soil was level the vehicle test could then be performed.

Figure 4-11: Leveling the soil, the final step in the pre-run soil preparation

Case Study Run Procedure

In both the wheeled and tracked configuration the run procedure was identical. The vehicle is teleoperated from a computer using a program included with the vehicles motor controller. The vehicle direction of travel and speed can be controlled using the program. The vehicle speed is set as a percentage of available power. When the vehicle's motors are set to 100 this means that all the available power is being provided to the motors. Before the run can be started the vehicle must be connected to the computer through the X-Bee PRO wireless communication modules. To begin the run the test vehicle was first place in the test area pointing in the desired direction of travel. If testing on the sandy silt loam the vehicle was place on the prepared soil in a manner that allowed the greatest available testing space. Once the vehicle was in position, power was provided to both motors according to the desired testing speed. If the initial power that was set was not enough to overcome the initial motion resistance and no motion occurred then the power was gradually increase until the test vehicle began moving. Once the vehicle began moving down the testing area, the direction of travel was monitored and corrected, if needed, using the direction control function on the computer. All testing scenarios were

performed with the intention of steady-state, straight line motion. Corrections were sometimes necessary however, as the obstacles would sometimes cause the vehicle to alter its direction of travel. The vehicle tests were performed to run the entire length of the available testing surface. The vehicle was stopped and power cut from the motors when the vehicle reached the end of the testing surface or if the vehicle encountered an obstacle that it could not traverse. If the vehicle could not traverse an obstacle, power was cut after approximately 10 seconds or if it was absolutely clear that the object was immobilized.

Post-Run Procedure

Following a testing run, the data was collected in the same manner each time and the soil was tested using a cone penetrometer to verify that the soil conditions remained the same throughout the case study. After a run was completed the data that was collected by the onboard data collection system was transferred to the computer. The data collection system stores information on an SD card. This allows for quick and easy transfer of data to the computer. The collected data is transferred to the computer and quickly reviewed to ensure that there are no anomalies or discrepancies. Once this step is complete then sinkage measurements are taken if the run occurred on the sandy silt loam and was a parameter of interested for that particular testing scenario. Sinkage measurements are taken using a millimeter scale ruler and are measured from the bottom of the tire grouser imprint to a horizontal marker that is placed on the surrounding soil and extended to the testing site. This horizontal marker is placed so that it is perpendicular to the direction of travel. The true sinkage measurement is then obtained by subtracting the height of the horizontal marked from the measured sinkage. This measurement represents the different in the undisturbed soil height to the height of the soil after a vehicle has made a pass at the grouser. For each run, the sinkage was measured at ten different locations. These ten sinkage measurements were taken at equal intervals along the entire length of the testing area. This measurement method can be seen in figures 4-12 and 4-13.

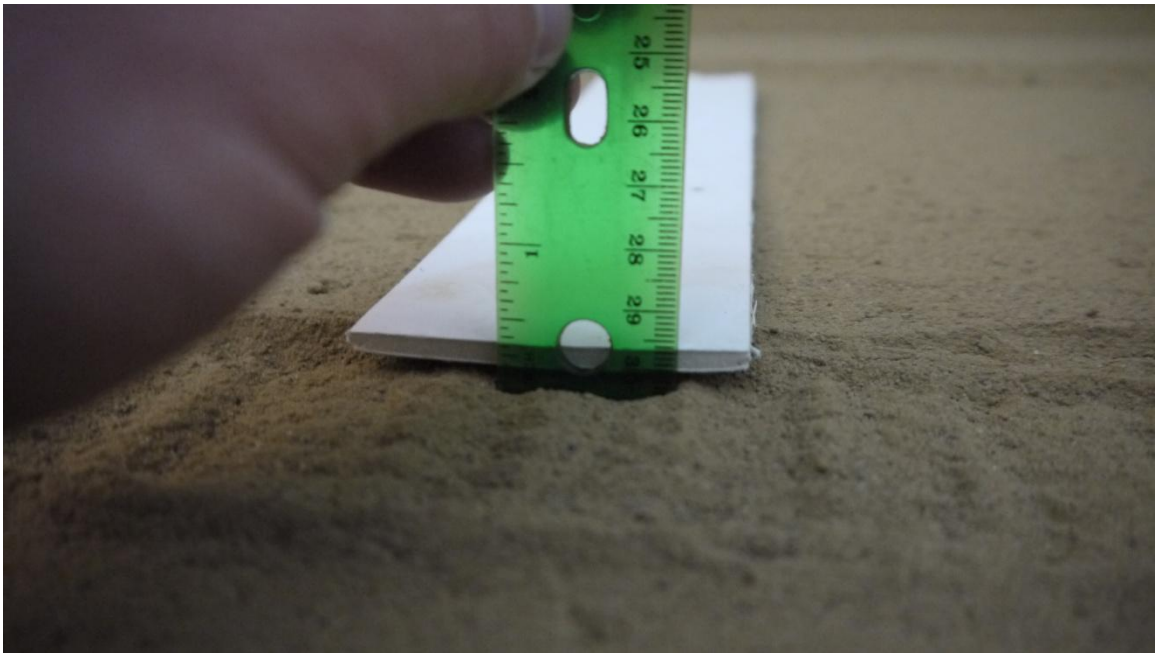

Figure 4-12: Recording a sinkage measurement

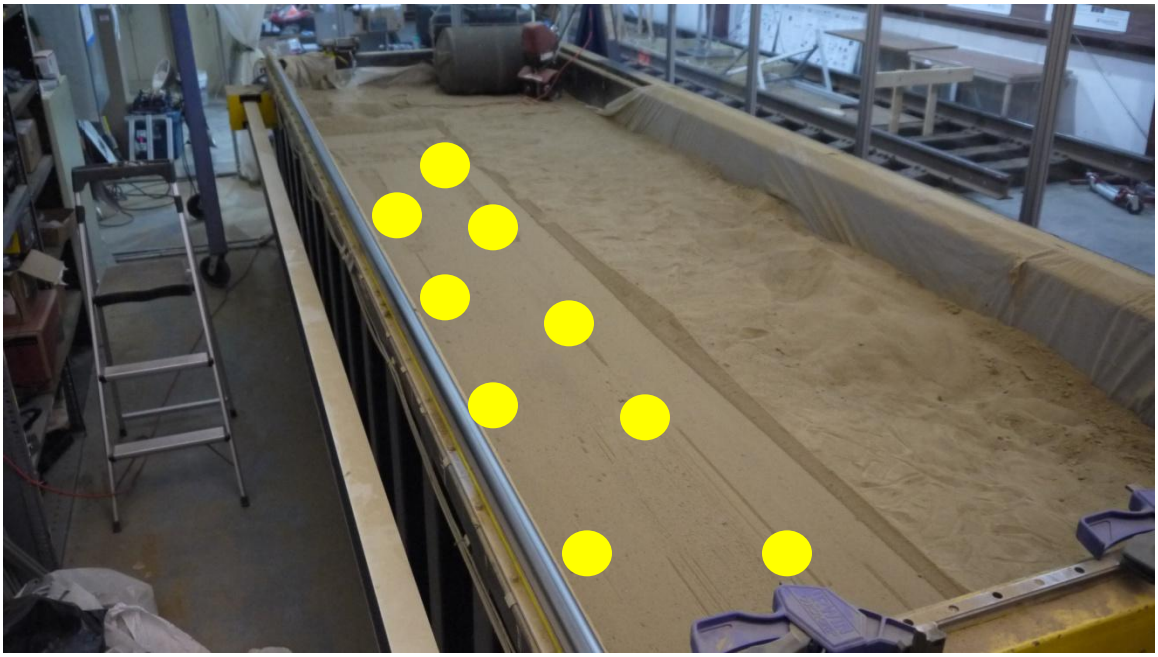

Figure 4-13: Sinkage measurement locations

In addition to the sinkage measurements, following each run, the soil is tested using a cone penetrometer to ensure that the soil conditions are as close as possible for each run. The soil was tested using a Rimik Electronics CP40II Cone Penetrometer. The cone penetrometer measures the soils resistance to the penetration of a right angle cone as it is driven into the soil. This measure of soil compaction has been used since the 1960's and is generally regarded as an acceptable method to characterize soil for vehicle mobility purposes or soil trafficability [5, 33, 34, 42]. This particular cone penetrometer records insertion depth as the operator drives the cone into the soil as a constant speed. The depth is measured using an ultrasonic distance sensor mounted to the body of the cone penetrometer. This allows the cone index (CI) reading to be correlated to a specific insertion depth. In order to take a measurement the operator first starts with the cone tip of the penetrometer above this soil. This registers a negative insertion depth reading. As the operator drives the cone into the ground, the insertion depth goes from a negative value to a positive insertion depth. The zero value corresponds to the point at which the cone is just touching the top soil particles. In this case study it was decided to limit the maximum insertion depth to 150 mm. This was done to increase measurement efficiency and this depth seemed reasonable because the vehicle has very minimal sinkage. The cone penetrometer used in this case study can be seen in figure 4-14.

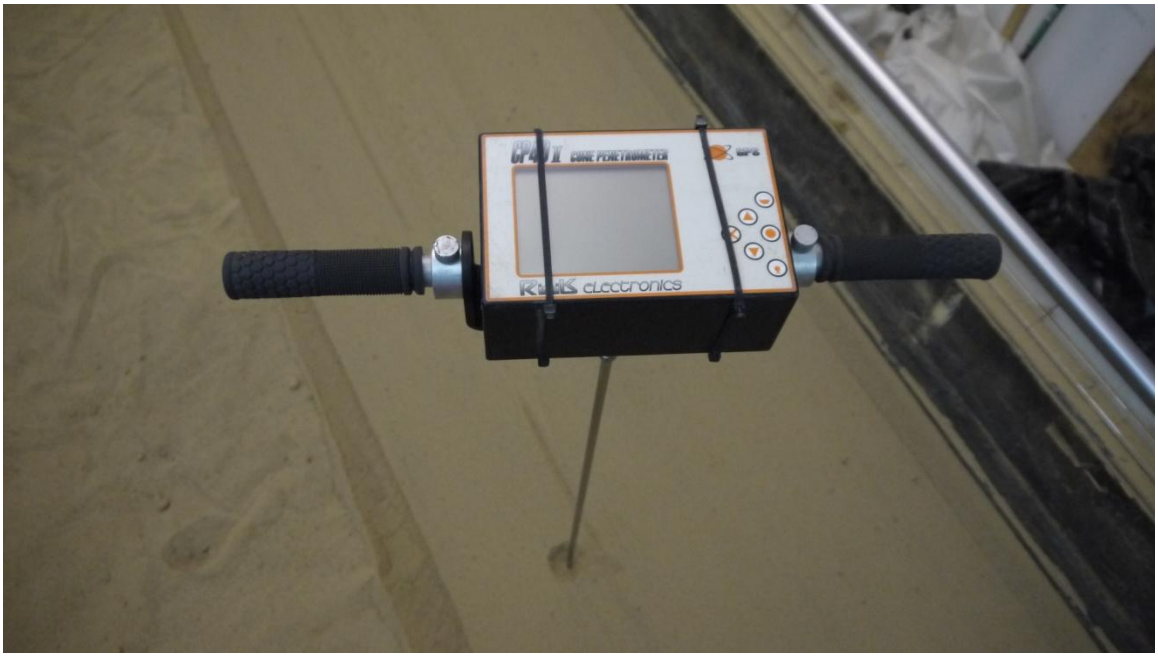

Figure 4-14: Cone penetrometer used for case study

The cone penetrometer was used to record approximately eight readings per run. These readings were recorded at various even spaced intervals along the testing area. Also these readings were alternated between the right and left track area. When taking these measurements it was important to find an area of soil that was undisturbed by the sinkage measurements. While this might not have had a huge impact on the readings, this procedure was maintained for consistency. This testing protocol is illustrated in figure 4-15. Following the collection of the cone penetrometer data for a specific run, it was compared to the previously collected cone penetrometer data to ensure that the soil conditions were acceptable.

Figure 4-15: Cone penetrometer testing areas

Test Run Vehicle Speed

For all tests conducted in this case study the vehicle was operated at three different speeds. This achieved a broader picture of the vehicle's mobility performance and allowed curve fitting of the data to be possible which allowed any trends in performance to be more distinctive. Because the vehicle's speed is controlled as a function of percent power, the three speeds used for the test were 50%, 75% and 95% power. The vehicle was not tested at 100% power in most cases because at 100% power the steering of the vehicle becomes more difficult due to the differential steering mechanism. In some rare

cases during the obstacle negotiation tests, if the vehicle could not traverse an obstacle as 95% power then the vehicle was tested at 100% power. This was only done if the vehicle had failed at traversing the obstacle at the other three testing speeds.

Vehicle Analysis Sensing Methods

The testing parameters were collected by a combination of onboard sensors and stand alone sensing devices. Through the combination of several sensors, all the desired vehicle parameters could be collected in an efficient and accurate manner. The majority of the sensors were located onboard the test vehicle and included a gyroscope, current sensor, rotary wheel encoded and load cell. The sensing devices that were not located on board the vehicle was a Rimik Electronics CP 40II , a Tekscan I-Scan 3150 pressure sensor, and a LIDAR measurement system that was developed in house at Virginia Tech. The sensor that the vehicle parameters of interest were captured with can be seen in Table 4-2. Following the table is a description of the stand alone sensing devices followed by a description of the onboard sensor suite.

Table 4-2: Sensing solution with corresponding vehicle metric

Sensing Device	**Analysis Metric**
Rimik Electronics CP 40II	Cone index value
Tekscan I-Scan 3150 and Fujifilm Prescale Film	Pressure and contact patch area
ACS712 Low Current Sensor	Current consumption
LPY503AL Dual Axis Analog Gyroscope	Roll
LPY503AL Dual Axis Analog Gyroscope	Yaw
Cytron Technologies RE08A Rotary Encoder	Speed
Standard rule with millimeter divisions	Sinkage
Measurement Specialties FC22 Compression Load Cell	Drawbar pull

LIDAR Measurement System	Slip

Tekscan I-Scan 3150

The Tekscan I-Scan 3150 is an ultra-thin, tactile pressure sensor. This sensor is used in the analysis to record the pressure distribution beneath the running gear. The Tekscan pressure sensor comes in a wide variety of sizes and pressure ranges. Proper calibration allows this sensor to be used for a variety of applications.

The Tekscan I-Scan 3150 has a width of 17.16 inches and a height of 14.52 inches. The sensor can detect a maximum pressure of approximately 125 psi. While this is well outside the required range for the vehicles used in this study, by following the calibration guide this device can be used for any pressures up to 125 psi. The actual sensor is extremely thin but in order to protect it and prevent any damage, the sensor is housed in a black plastic supporting structure. The structure is 24 inches by 23 inches and is 0.25 inches thick. This black plastic support protects the sensor while having no effect on the sensor accuracy. In addition to the black support structure a thin plastics sheet is placed over top the sensor to further protect the sensor from damage. This thin plastic sheet is adhered to the black plastic support structure and provides a water tight seal. The Tekscan pressure pad is comprised of a 52 by 44 matrix of pressure sensing pixels generating a total of 2, 288 pressure pixels or 9 pixels per square inch. The Tekscan pressure sensing device can be seen in figure 4-16.

In order to get as accurate a reading as possible the Tekscan pressure sensor must be equilibrated and calibrated. Equilibration is performed by inserting the sensing pad into a equilibration device produced by Tekscan that applies an even pressure distribution across the entire sensor. This is done by inflating a bladder housed in the equilibration device to the desired equilibration pressure. This pressure applies an evenly distributed force and allows the sensor to be equilibrated. The equilibration process is performed to ensure that all the sensors are reacting to a uniform pressure with a uniform reading. This is done prior to calibration.

Tekscan provides calibration instructions in their user manual and it is recommended that the sensor be calibrated using two points. These two points should be roughly 20% and 80% of the maximum expected sensing load. These loads were determined using the known vehicle weight of 16 pounds. It was assumed that the vehicle weight would be evenly distributed along each of the 6 tires or along the entire length of the tracks. This assumption means that the maximum expected load would not exceed 3 pounds for each tire. Using this assumption the sensor was calibrated with 80% and 20% of the expected load using known weights. The weight was distributed over a majority of the testing surface in order to avoid any loading spikes.

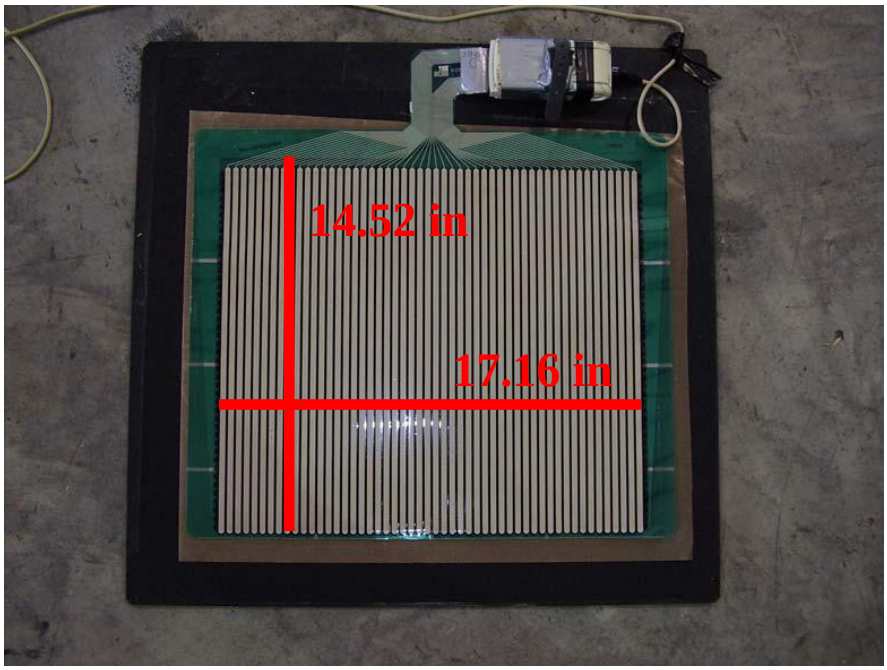

Figure 4-16: Tekscan I-Scan 3150

Fujifilm Prescale Film

In order to develop an alternative technique to measure the vehicle's pressure distribution Fujifilm Prescale Film was used. This film is a thin flexible, single-use film that is used to create a peak pressure snap shot. This film indicates pressure distribution through

changing degrees of color intensity. The film is mylar based and contains a thin layer of tiny microcapsules. As the vehicle passes over the film the pressure causes the film's microcapsules to rupture which causes a permanent high resolution image to appear in the shape of the pressure distribution. On the processed film, a darker more vivid color indicates a higher magnitude of pressure. This film comes in seven pressure ranges and can be rated for pressure ranges of 7.25 psi to 43,500 psi depending on your desired application. This film is extremely thin, approximately 200 µm. After the vehicle passes over the film and the pressure distribution is reveled the user can determine the pressure magnitude by using the supplied color scale. The color scale allows the user to determine a pressure magnitude based on the color of the developed film. For a more accurate analysis of the pressure film you can send the film to Fujifilm and they will perform an in depth analysis. An example of an exposed pressure indicating film can be seen in figure 4-17.

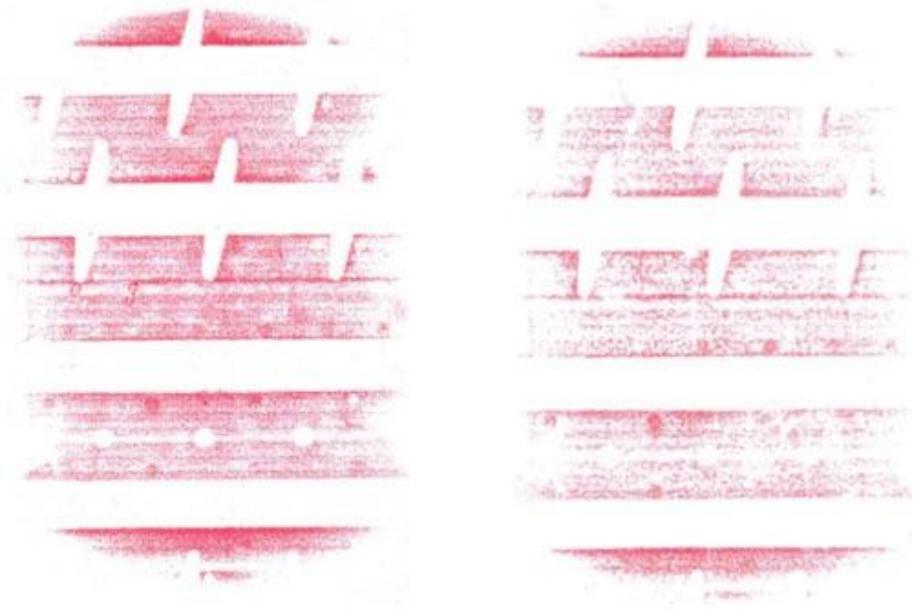

Figure 4-17: Fujifilm Prescale Pressure Film measuring tire contact patch [61]

LIDAR Slip Measurement System

A novel system for the measurement of wheel slip has been developed at Virginia Tech by Dr. Carvel Holton [62]. While this measurement apparatus was originally developed to measure the slip at the tire/wheel-running surface contact for large vehicles, an attempt has been made in this study to adapt it for the small robot used in the project. This measurement system is an optical device that uses LIDAR to determine the vehicle's longitudinal slip. This system is used for this project to measure the longitudinal slip on flat sandy silt loam and a flat rigid surface. The operating principle behind this system is that a beam of light is aimed at the vehicles tire and another beam of light is focused on the test surface immediately adjacent to the tire. Using the light beams to measure the induced Doppler shift from the incident light allows for the slip measurement to be made. The first laser beam is directed at the wheel or track and is used to measure the tangential velocity of the rotating running gear. The second laser beam is direct at the ground and is used to measure the translation velocity of the vehicle. The slip is then a function of the ratio of the vehicles tangential speed of the running gear versus the speed of the translation speed of the entire vehicle. This relation is expressed in equation 2.6 and 2.7. The setup of this system mandates that the LIDAR units must be a minimum of 21 inches away from the desired measurement site. This is due to the fact that 21 inches is the minimum focal length. The operating principle behind this measurement system can be seen in figure 4-18.

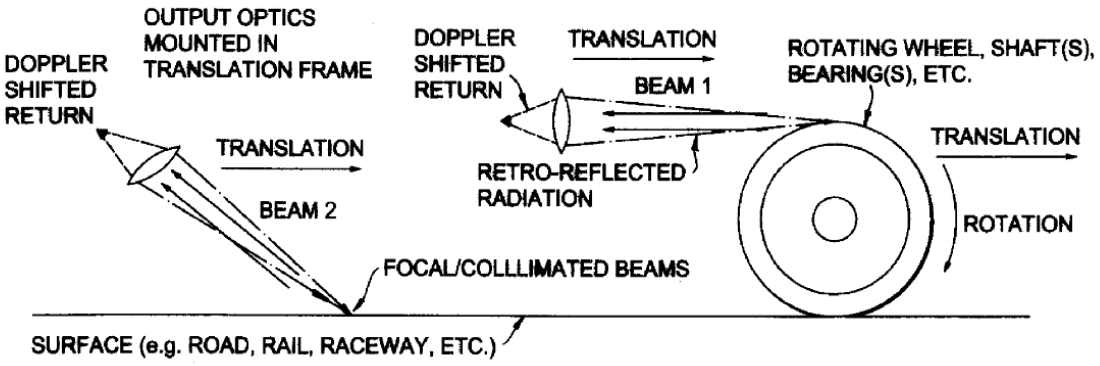

Figure 4-18: LIDAR vehicle slip measurement system [62]

Onboard Sensor Suite

In addition to the stand alone sensing devices used in this analysis, the vehicle was outfitted with a suite of onboard sensors. These sensors were mounted to the vehicle to provide a relatively easy method for sensing motor current, vehicle speed, drawbar pull, and vehicle angular position. The on board sensor suite is built around the Arduino open source microcontrollers. Arduino microcontrollers can be used for a variety of prototyping and project purposes. For this analysis it will be used to fuse the data from the on board sensors and record it for later analysis.

Arduino makes microcontroller boards with many different configurations and sizes. For this analysis an Arduino Uno microcontroller is used. The Arduino Uno is a microcontroller based on the ATmega328 chip. The ATmega328 chip is a Atmel 8-bit RISC-based microcontroller that combines read-while-write capabilities, a built in A/D converter, 23 general I/O lines, as well as many other useful features. The Arduino Uno is built around this chip and includes 14 digital input/output pins of which 6 can be used as PWM outputs, 6 analog inputs, and a 16 Hz internal clock. The Arduino Uno can be seen in figure 4-19.

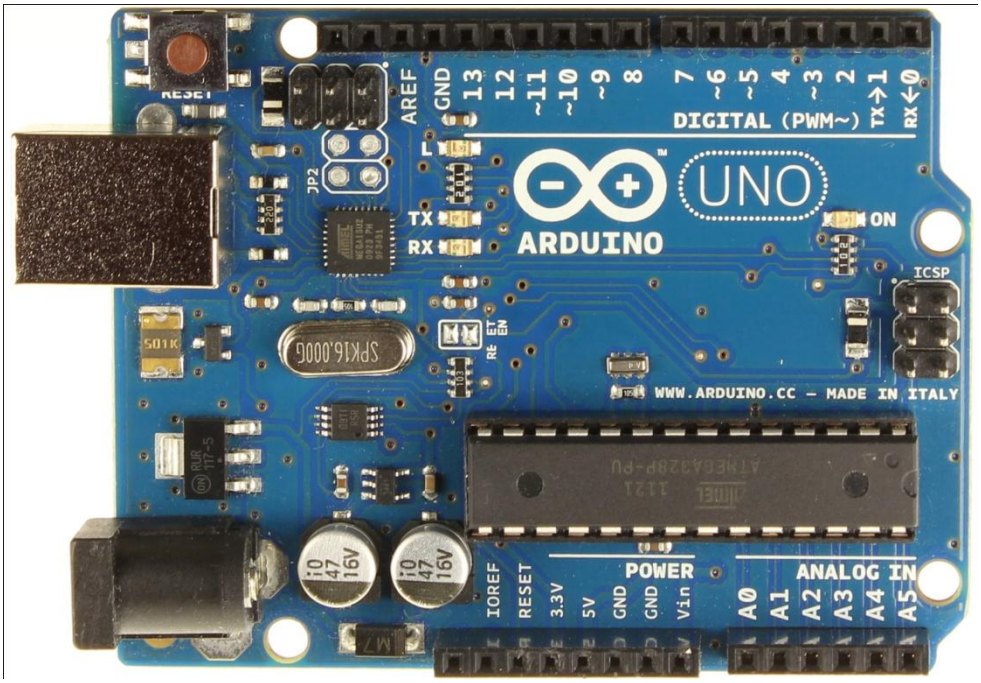

Figure 4-19: The Arduino Uno microcontroller [63]

The Arduino Uno allows the data from the four onboard sensors to be collected and stored for later use. While the Arduino Uno has a built in flash memory, at 32 KB it is too small for the amount of data that is collected for each run of this analysis. Because of this a data logging shield was built and installed on the Arduino Uno.

The Arduino microcontroller platform has been developed as an open source prototyping platform. This has allowed outside developers to create various shields. A shield is a separate printed circuit that sits on top of the Arduino and connects directly to the input pins of the Arduino. For this analysis a data logging shield was used to store the data from the sensors. The data shield allows the user to store any type of data on an SD card. This is very versatile and with the use of a large SD card many days worth of testing can be stored on a single SD card. The data shield used can be seen in figure 4-20. The data shield is a kit produced by Adafruit Industries. By using this data logging shield you are limited to four analog inputs because the shield uses two analog inputs in its process to read and write to the SD card.

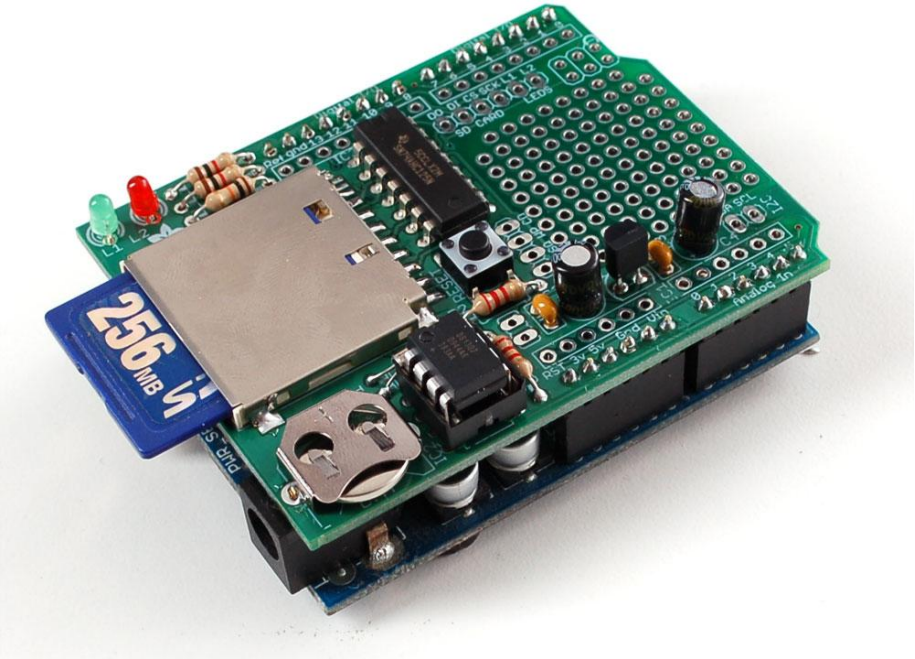

Figure 4-20: SD data logging shield for Arduino Uno [64]

The Arduino is programmed with an integrated development environment that is a cross-platform application produced in Java. This programming environment is derived from an earlier version also produced by Arduino. It is design with new programmers in mind and has many features to aid software developers unfamiliar with programming. The programming language features syntax very similar to the C++ coding language. An example of this programming environment can be seen in figure 4-21. Before a program can be loaded onto the Arduino Uno board it must be compiled and checked for errors. Another feature of this software development tool is that during the compilation process any errors in your code will be specified and pointed out. This makes debugging very easy because the exact location of the code error is known. Once the program is error free it can be uploaded to the Arduino Uno. The programs are uploaded to the Arduino Uno over a RS-232 serial connection. The direct connection to the Arduino Uno is a USB-to-Serial cable which provides power while connected to the computer as well as the I/O method to the microcontroller.

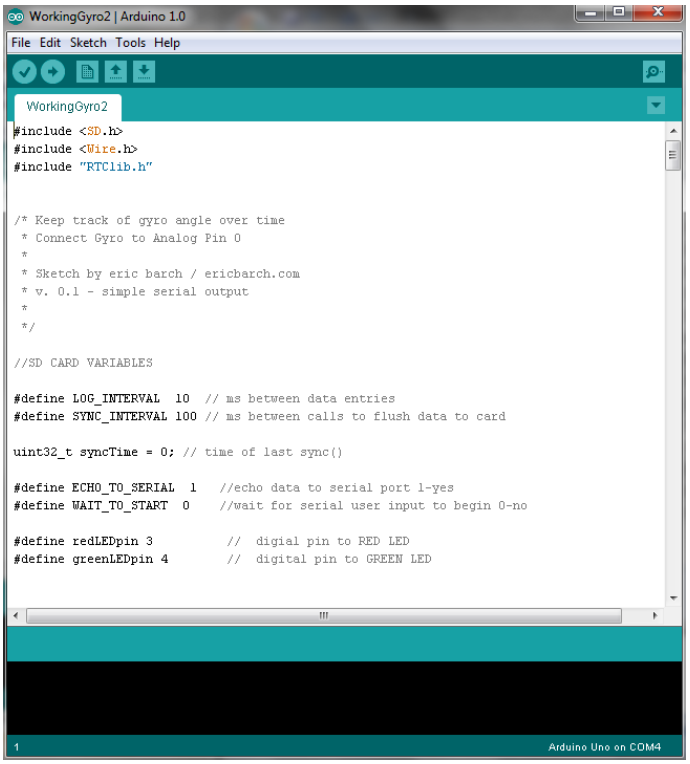

Figure 4-21: Arduino programming environment

Measurement Specialties FC22 Compression Load Cell

The first onboard sensor that will be discussed is the load cell used for the measurement of the drawbar pull. The load cell can be seen in figure 4-22. The load cell used in this analysis is a compression load cell produced by Measurement Specialties. This load cell is made for measuring a compressive load but a load cell housing has been created to convert the compressive load into a tension load. The load cell housing can be seen in figure 4-23. This load cell is rated for a 0 to 10 pound force load range. It measures direct force and is not subject to lead-die failure fatigue commonly associated with other types of load cells. The sensor operates on a 5 volt supply voltage and has a output range of 0 to 4.5 volts. This sensor is quite convenient because it is produced be calibrated and includes a built in amplifier. In order to check the sensors calibration it was tested using known weights included 25%, 50%, 75%, and 100% of the operating range. This

calibration test results proved to be very accurate and verified that the sensor had been pre calibrated.

Figure 4-22: Load cell used for drawbar pull measurements [65]

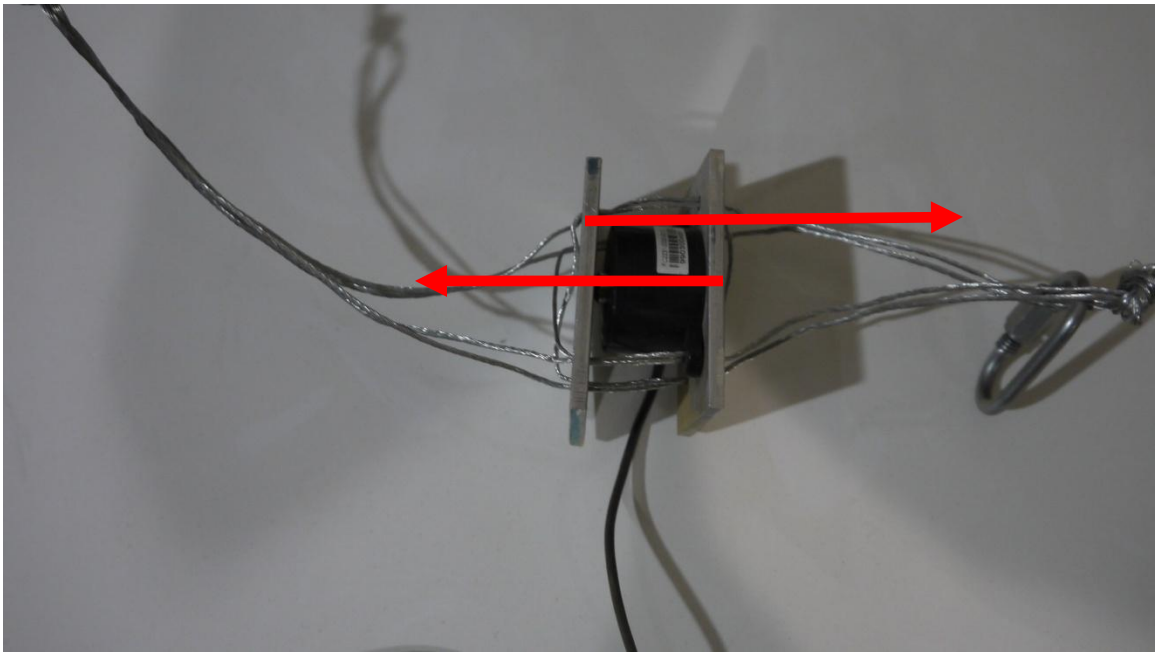

Figure 4-23: Housing used to convert tensile force of drawbar pull to a compressive force

ACS712 Low Current Sensor

A key aim of this analysis is to examine the power requirements and energy efficiency of robotic vehicles in a wheeled and tracked configuration as they perform similar maneuvers. To accomplish this goal the current was deemed a parameter of interest and must be recorded and observed. The ACS712 low current sensor was used to measure and record the current as the vehicle performed the various maneuvers. This current sensor is produced by Allegro MicroSystems, Inc. This sensor can be seen in figure 4-24.

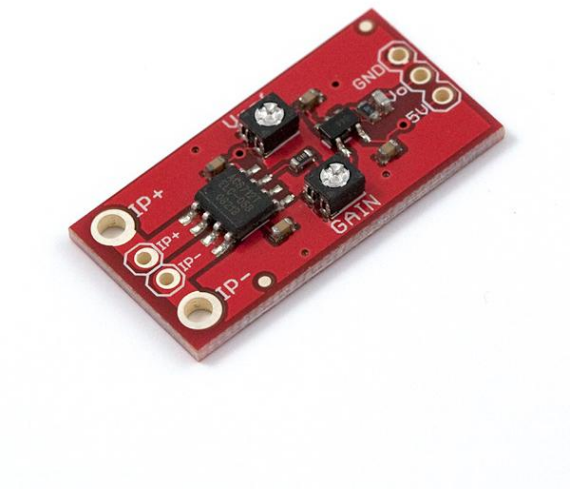

Figure 4-24: ACS712 low current sensor [66]

This current sensor gives an accurate measure of current for both AC and DC signals. For this case study it will be used to measure the DC current provided to the motors by the battery packs. This sensor operates by using the Hall Effect principle. The Hall Effect is the phenomenon in which a voltage difference in produced across an electrical conducted in a transverse direction to the electrical current in the conduction. The voltage difference is proportional to the current in the conductor. This allows the voltage difference to be used as an indirect measure of the current. The ACS712 low current sensor consists of a precise, low-offset, linear Hall sensor circuit which uses a copper conduction path. The

output of this sensor has a positive slow with an increased current flow. It is optimized by its design with having the Hall transducer in very close proximity to the die that houses the conductor in which the current is being measured. This sensor operates at 5 volts and a range of -5 to 5 volts. The maximum current output of the batteries falls well within this range and will provide an acceptable resolution for this case study. The resolution of this sensor is 10 mA with a response time of 5µs. This current sensor also features an adjustable gain that allows for very small current measurements. The gain can be manually adjusted and set between 4.27 and 47. For this case study the gain on the current sensor was set to the lowest possible, 4.27, because of the relatively wide range of measured currents with respect to the sensors total overall range. While there are more accurate current sensors produces this sensor will suite the purposes of this analysis because of the fact that the max current is well within the operating limit and while testing the chosen scenarios the vehicle will be operated at a constant speed where limited current fluctuation is expected.

In the sensor's datasheet there was no mention of any calibration methods or techniques. In order to verify the accuracy of the sensor a simple calibration was performed. A ammeter was connected in series to the current sensor. A function generator was used to produce an accurate DC current output that was then measured by the ammeter and the current sensors. These readings were compared and facilitated the calibration of the sensor. The function generator was used to produce a signal that was 25%, 50%, 75%, and 100% of the total positive range for the sensor. The calibration proved very useful and allowed more accurate current measurement. While the response was typically linear, at the extremes of the total range, approximately 95% of total range, the response would exhibit some non-linear behavior. This non-linear behavior was very slight and is assumed to not affect the accuracy of the analysis results because the vehicle will not be operating close to that mark in the overall sensor range.

LPY503AL Dual Axis Analog Gyroscope

In order to measure the vehicles angular position as the traverses through the various testing scenarios a gyroscope was included in the onboard sensor suite. Gyroscope have been used for hundreds of years but the last few decades have seen an gyroscopes being produced on very small scales. A gyroscope is a device used for measuring or maintaining a vehicles orientation. In this case it will be used to measure orientation along two axes; this gyroscope can be seen in figure 4-25. The gyroscope used in this study is a LPY503AL MEMS gyroscope. This gyroscope is a dual axis gyroscope that can measure up to a maximum of $\pm\ 30^{\circ}/s$.

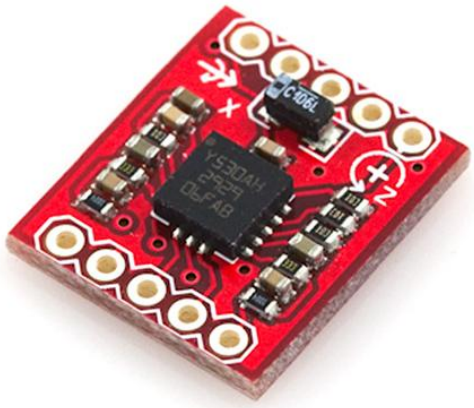

Figure 4-25: LPY503AL Dual Axis Analog Gyroscope [67]

This gyroscope was used to measure the angular position of the vehicle as it moves through the testing scenarios. The two axes of rotation can be seen in figure 4-1. The LPY503AL is a MEMS device that combines one actuator and one accelerometer that are integrated into a single structure. It includes a sensing element that contains a single driving mass kept in continues oscillation that is able to reaction to an change in angular

momentum based on the Coriolis principle. A CMOS IC outputs the measured angular rate as an analog output voltage. This particular gyroscope has a sensitivity of 8.3 mv/∘/s and operates on a 3.3 supply voltage. This device is the only sensor on the onboard sensor suite that runs on 3.3V. The Arduino Uno has a power regulator that operates on a 5V and a 3.3V output. There was a resolution issue however, when converting the analog signal to a digital signal. Because the A/D convert onboard the Arduino Uno has a reference voltage of 5V, if you have a device with a voltage reference lower than 5V you will sacrifice some resolution and range in the analog to digital conversion process. The choice was made to sacrifice the resolution and range on the gyroscope rather than running the other three sensors on a 3.3V reference. Running the other sensors would have caused many calibration issues and it was preferred to have a loss of resolution and range to having to calibrate and adjust the other three sensors. Because the obstacles that were being used were relatively small and a small angular change was not expected, this loss in resolution and range was deemed acceptable. Gyroscope output change in angular velocity in degrees per second but in this case study it was desired to have the angle off of the horizontal as an output so an algorithm was developed to track and output the angle and is formulated through a series of logic statements. The process is displayed in the Arduino programming environment in figure 4-26.

Figure 4-26: Code syntax to track vehicle orientation

By using this angle tracking algorithm, the output of the gyroscope can be convert to an absolute angle.

Cytron Technologies RE08A Rotary Encoder

The final sensor included in the suite of onboard sensors of a rotary wheel encoder produced by Cytron Technologies. This rotary encoder is specifically design for use in robotic vehicle applications and can be seen in figure 4-27. A rotary encoder is a sensor that is used to convert rotary motion data into a series of electrical pulses that can be readable by a controller. The rotary encoder that is used for this project contains a slotted

disk that has an outside diameter of 35mm. This slotted disk has 8 slots with provides 16 transitions as the disk is rotated. This disk is mounted directly to the running gear shaft and rotates one time with every one rotation of the wheel or drive sprocket. While most rotary encoders used for experimentation have vastly greater resolution, on the order of 10,000 divisions, for this case study the vehicle will be operating at very slow speeds in relation to other vehicles and this resolution will be sufficient to derive the vehicle's average velocity.

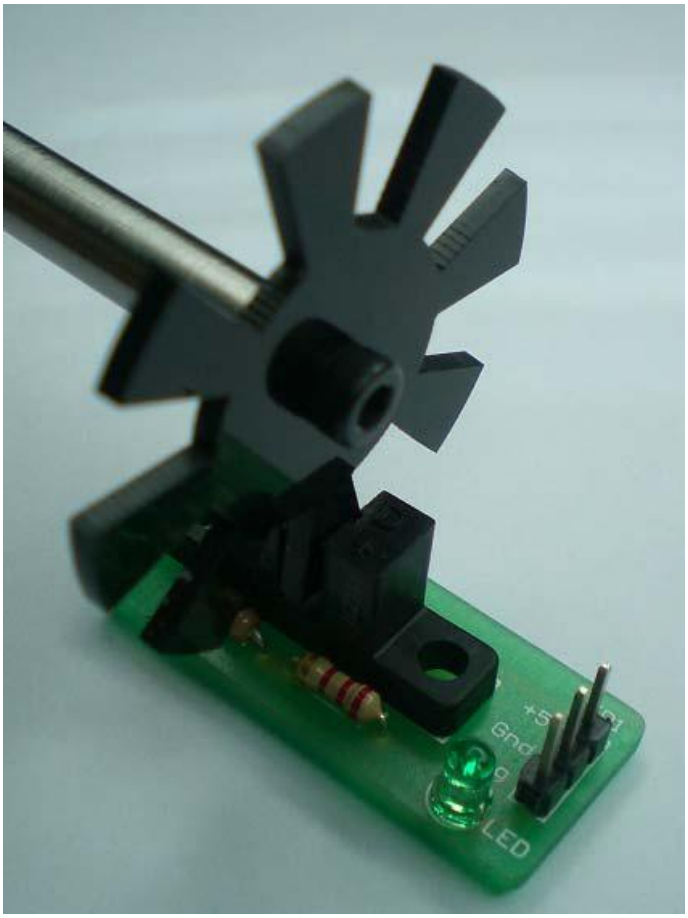

Figure 4-27: Cytron Technologies RE08A Rotary Encoder [68]

The rotary encoder operated on a 5V power supply and can have a pulse rate up to 1000 pulse/sec. This rate is much greater than the top speed of the vehicle can produce. In

order to derive the vehicle speed an simple equation was produced and can be seen in equation 4.1,

$$V = \frac{(C * 0.0785 + T * 0.6283)}{t_{total}} \qquad 4.1$$

where C represents a click, T represents a turn, V is the vehicle velocity, and t_{total} is the total elapsed time. A click is one pulse division where a turn is an entire revolution of the rotary encoder. The values of 0.0785 and 0.6283 are the distance in meters the vehicle will travel for one click and turn respectively. This equation will provide the velocity in meters per second as the vehicle travels through the scenario and will be an average velocity across the testing scenario. This method is limited in that is will not detect minor fluctuation in velocity but because these scenarios are tested at a constant speed this will not have a major effect on the results. This is the final sensor on the onboard sensor suite.

5. Experimental Study

This chapter presents the results of the comparative analysis of lightweight robotic wheeled and tracked vehicles.

The experimental results for the vehicle in a wheeled configuration are first presented and discussed. These trials are qualitatively analyzed and initial observations are considered. The obstacle negotiation test results are presented in the terms of a GO, NO-GO determination on whether or not the vehicle traversed the obstacle. Following this are the initial case study results for the vehicle in a tracked configuration. These trials are also qualitatively discussed along with the initial observations and obstacle negotiation results.

The data processing is presented following the qualitative comparison. In this section the parameter data is processed and displayed in an intuitive format. Included in this data presentation are the sinkage, current consumption, and drawbar pull results. Presentation of these parameter results allow other parameters to be formed. This presentation of the collected data allows quantitative comparisons to be made between the two vehicle configurations. By using the qualitative and quantitative observation made an in depth comparative analysis is presented.

The final section of this chapter includes a discussion of the comparative analysis between the two included running gear in the context of a customized Mobility Metrics Matrix (MMM). In this section the results are utilized to formulate a customized MMM that is better suited to make vehicle configuration decisions for a given set of mission criteria. This new customized MMM is then tested against a fictional operating scenario in order to display the MMMs effectiveness.

5.1 Parameter Collection

The vehicle testing for this comparative analysis was conducted during the winter and spring of 2011-2012. During this testing period the vehicle was tested in the wheeled and tracked configuration. The vehicle performed the same maneuvers and the same vehicle parameters were collected in both cases. The vehicle was tested through a series of scenarios outlined in the previous chapter. In these scenarios the same obstacles and testing conditions were used to ensure that the scenarios matched as closely as possible.

Wheeled Configuration Testing Observations

In the winter of 2011-2012 the testing of the vehicle in its wheeled configuration was completed. The test vehicle operated adequately throughout the duration of the winter testing. The vehicle was testing in the eighteen scenarios outlined in the previous chapter. The vehicle parameters that were collected were; sinkage, drawbar pull, vehicle speed, current consumption, and vehicle orientation. These parameters allowed for other direct comparisons to be made as well.

The vehicle in its wheeled configuration was able to navigate over most obstacles but there were a few obstacles that the vehicle could not negotiate. The results of the obstacle negotiation tests on a go no-go basis are displayed in table 5-1. The vehicle was tested in the obstacle negotiation scenarios at 50%, 75%, and 95% available power. If the vehicle could not negotiate the obstacle at any of these power levels then the vehicle was tested at 100% power to make a final comparison about the robots ability to traverse a certain obstacle. If the vehicle did traverse the obstacle at any of the lower three power levels then the vehicle was not tested in that obstacle negotiation scenario at 100% power. It appears throughout the testing that a major limiting factor of the vehicle was its overall power. Many of the obstacles that the vehicle could not traverse seemed to be due to a lack of power. One obstacle in particular is the inclined surface on sandy silt loam. The vehicle would approach the obstacle and begin to climb the incline but could not traverse the obstacle due to lack of power. This phenomenon is attributed to a lack of power

because the vehicle would not lose traction while navigating the incline. In figure 5-1 you can see the approximate position in which the vehicle would become immobilized.

Figure 5-1: Vehicle in wheeled configuration immobilized on inclined sandy silt loam

Another major difference in mobility was observed when comparing the obstacle negotiation results for the vehicle on a rigid surface and the sandy silt loam. The vehicle could not negotiate the same obstacles in the sandy silt loam at the same speeds. For the cases of: the 1.5 inch obstacle with both running gear, the 1 inch obstacle with one side of the running gear, and the 1 inch obstacle with both running gear, there were noticeable and repeatable differences. The vehicle could not negotiate these obstacles at 50% power on the sandy silt loam, while the vehicle had successfully negotiated the obstacles on a rigid surface. This is attributed to the fact that the vehicle is experiencing more resistance to motion on the sandy silt loam surface due to sinkage. The vehicle's sinkage increases the resistance to motion because the vehicle must displace the soil in front of the running gear and/or compact the soil underneath the vehicle in order to move forward. This

causes an increase in the resistance to motion and the vehicles speed is affected. In these three cases the vehicle could not maintain a high enough speed to negotiate these obstacles.

One further observation in the mobility differences between the vehicles mobility performance on the sandy silt loam versus the rigid surface is the vehicle's ability to negotiate the 1.5 inch with one side of the running gear and the triangular cleat with one side of the running gear. During the vehicle testing on rigid surface the vehicle would become immobilized on these obstacles after one wheel have successfully traversed the negotiated the obstacle and as the second wheel was coming into contact with the obstacle. The vehicle had lost speed while the first wheel was traveling over the obstacle and therefore the vehicle did not have sufficient speed to continue traveling. This would cause the second wheel to become stuck in front of the obstacle. The side of the running gear that was not in the path of the obstacle would keep applying power and the vehicle would turn until the vehicle would become completely immobilized. This phenomenon was not observed in the testing on sandy silt loam. On sandy silt loam the vehicle would not experience any of the rotation that was displayed on the rigid surface. If the vehicle on sandy silt loam did not traverse the obstacle then it seemed due to insufficient speed or motor power and not due to loss of traction or rotation. The vehicle's tires have a deep grouser patter that increased the vehicles traction in the sandy silt loam and provided greater obstacle negotiation ability. In figure 5-2 and 5-3 you can see the sequence of events as the vehicle becomes immobilized on the triangular cleat obstacle while trying to negotiate this obstacle with one side of the running gear.

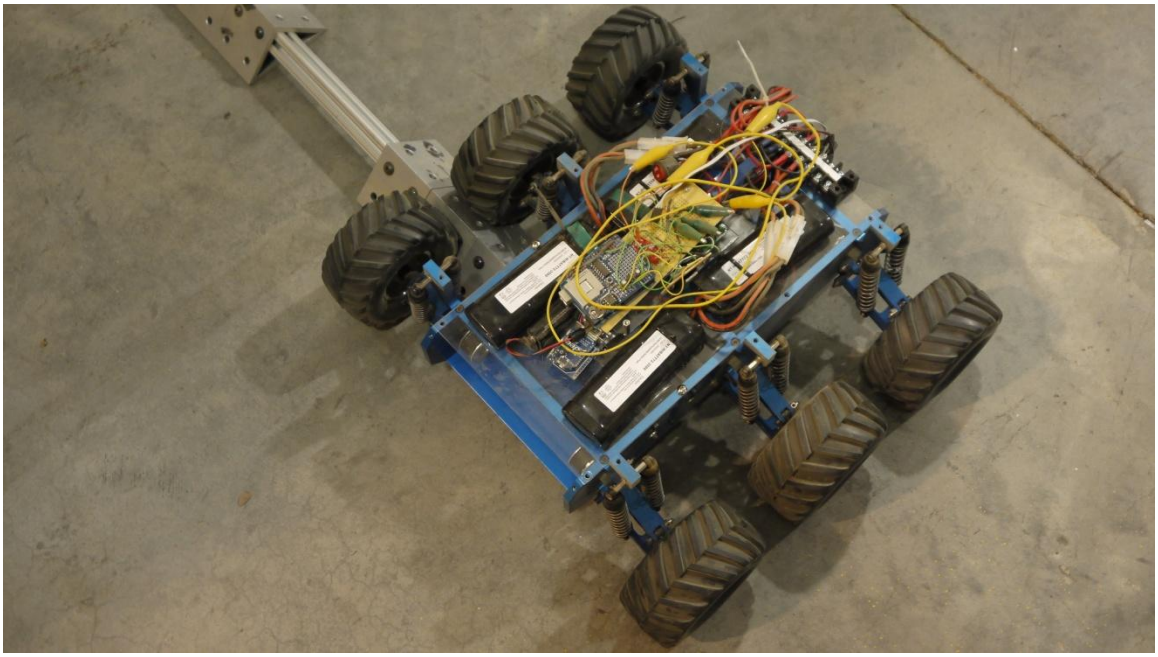

Figure 5-2: Vehicle's first tire negotiates obstacle

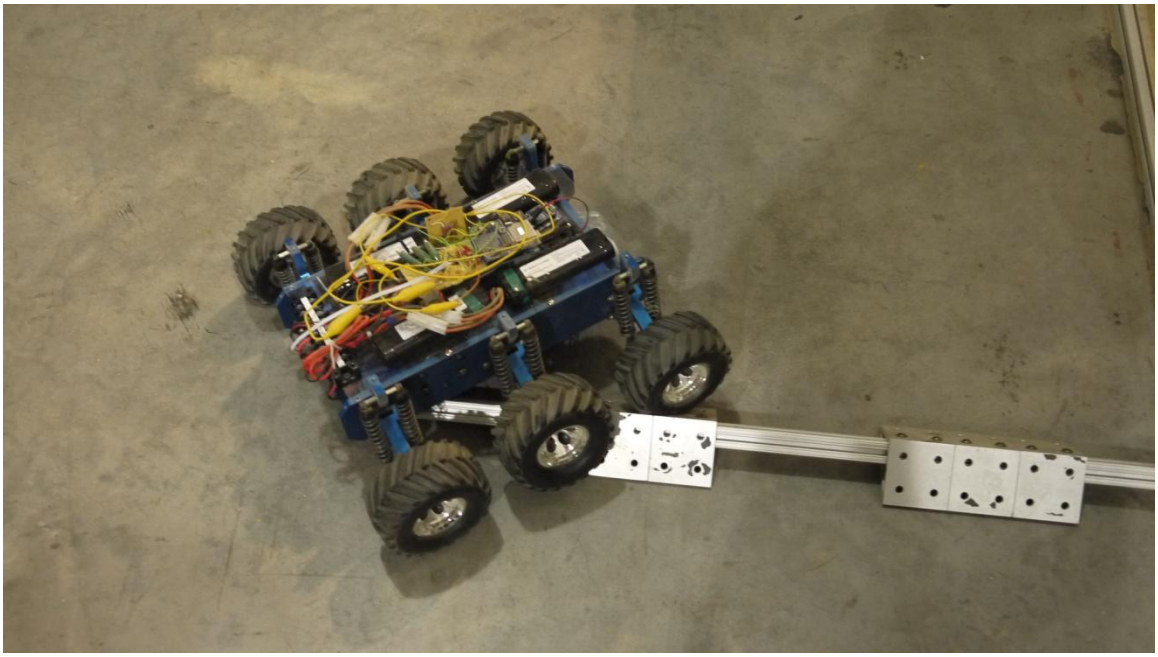

Figure 5-3: Vehicle begins to rotate and is quickly immobilized

Table 5-1: Wheeled obstacle negotiation tests go, no-go determination

	Sandy silt loam				Rigid Surface			
Available Power	50%	75%	95%	100%	50%	75%	95%	100%
1.5 inch obstacle, 1 side of running gear	NO-GO	GO	GO	N/A	NO-GO	NO-GO	NO-GO	NO-GO
1.5 inch obstacle, both running gear	NO-GO	GO	GO	N/A	GO	GO	GO	N/A
1 inch obstacle, 1 side of running gear	NO-GO	GO	GO	N/A	GO	GO	GO	N/A
1 inch obstacle, both running gear	NO-GO	GO	GO	N/A	GO	GO	GO	N/A
Triangular cleat, 1 side of running gear	NO-GO	NO-GO	GO	N/A	NO-GO	NO-GO	NO-GO	NO-GO
Triangular cleat, both running gear	NO-GO	NO-GO	GO	N/A	NO-GO	NO-GO	GO	N/A
Inclined surface	NO-GO	NO-GO	NO-GO	NO-GO	GO	GO	GO	N/A

Tracked Configuration Testing

In the spring of 2012 the testing of the vehicle in its tracked configuration was conducted. The test vehicle operational performance was satisfactory. The vehicle in its tracked configuration was tested in all scenarios and the same vehicle parameters as compared to the wheeled configuration were collected.

While performing the tracked testing some initial observations were developed. The vehicle in its tracked configuration experienced significantly more internal resistance to

motion due to the tracked running gear. While the vehicle in the wheeled configuration on a rigid surface at 50% power, the vehicle could negotiate some of the obstacles. In the tracked configuration the vehicle would not have enough torque at 50% power to induce motion. This was the first and most obvious initial observation. The fact that the internal resistance was high enough to cause the vehicle to be immobile at 50% power could be due to the fact that all three sprockets on each side of the running gear is powered. In typical situations for heavy vehicles, only one sprocket is driven while the other sprockets act as idlers. By powering all the sprockets there could have been some added track tension which could be accountable for the increased motion resistance. Due to the nature of the vehicles drive train, it was not possible to convert the other two sprockets to idler gears. Also because in the wheeled configuration the vehicle had all six wheels powered, it seemed appropriate to power all six sprockets.

The tracked vehicle exhibited overall, a greater mobility performance. The tracked vehicle negotiated all the obstacles with ease, the only exception being the inclined surface on sandy silt loam. In the wheeled testing the vehicle could not negotiate the triangular cleat with one side of the running gear because the vehicle would lose traction and rotate. This did not happen with the vehicle in a tracked configuration. The vehicle negotiated the triangular cleat obstacle very efficiently and displayed none of the tendencies to rotate. This can be attributed to the added traction and flotation of the vehicle. The vehicle in this configuration never broke contract with the obstacle and maintained ample traction throughout allowing the vehicle to carry out the obstacle testing with ease. In figure 5-4 the vehicle is overcoming the triangular cleat obstacle. This added traction and flotation also allowed the tracked vehicle to traverse the obstacles as a slower speed. This could be a valuable performance attribute that will have an impact on the vehicles energy efficiency.

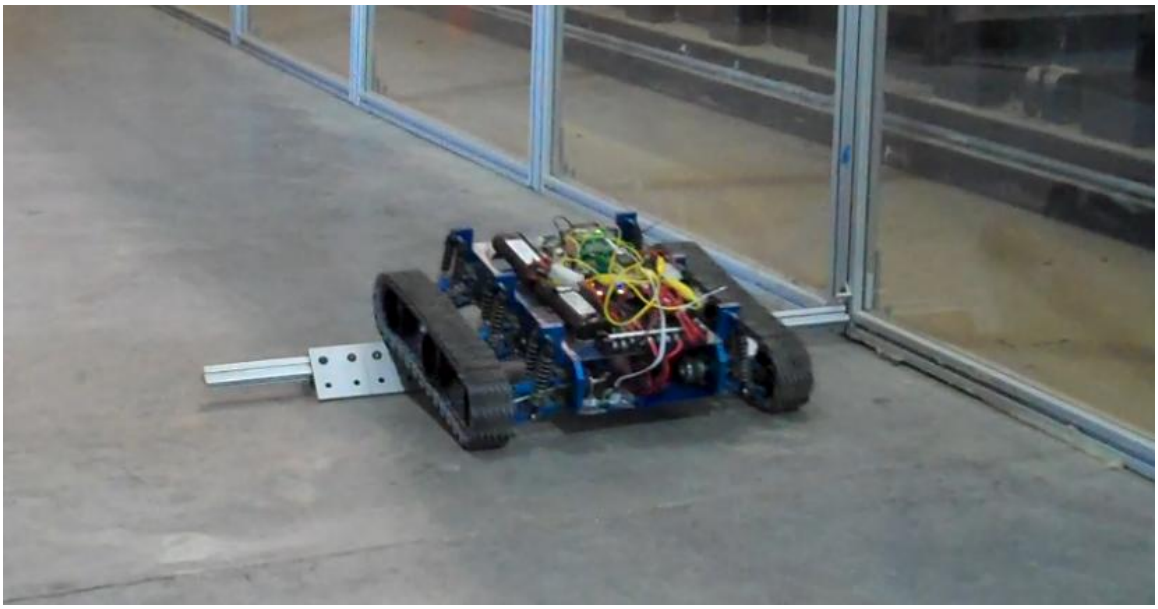

Figure 5-4: Tracked vehicle negotiating triangular cleat obstacle

Table 5-2: Tracked obstacle negotiation tests go, no-go determination

	Sandy silt loam				**Rigid Surface**			
Available Power	50%	75%	95%	100%	50%	75%	95%	100%
1.5 inch obstacle, 1 side of running gear	NO-GO	GO	GO	N/A	NO-GO	GO	GO	N/A
1.5 inch obstacle, both running gear	NO-GO	GO	GO	N/A	NO-GO	GO	GO	N/A
1 inch obstacle, 1 side of running gear	NO-GO	GO	GO	N/A	NO-GO	GO	GO	N/A
1 inch obstacle, both running gear	NO-GO	GO	GO	N/A	NO-GO	GO	GO	N/A
Triangular cleat, 1 side of running gear	NO-GO	GO	GO	N/A	NO-GO	GO	GO	N/A
Triangular cleat, both running gear	NO-GO	GO	GO	N/A	NO-GO	GO	GO	N/A

Inclined surface	NO-GO	NO-GO	NO-GO	NO-GO	NO-GO	GO	GO	N/A

5.2 Data Processing

Sinkage

The sinkage of the unmanned vehicle was tested on flat sandy silt loam for straight line, steady state motion. The sinkage was tested at the three power settings of 50%, 75%, and 95%. There appears to be no statistical difference in the sinkage results when comparing the same running gear sinkage to the different testing speeds. It was expected that a difference would present itself but due to the low speeds of the vehicle and the very small sinkage values no difference was noticeable. The results from the sinkage tests for the wheeled vehicle can be found in figure 5-5, and the results for the tracked vehicle can be found in figure 5-6. The sinkage results have been displayed in a histogram format to accurately represent the measurement distributions. A normal curve fit has been applied to gather some conclusions on how normal the measurement distributions are.

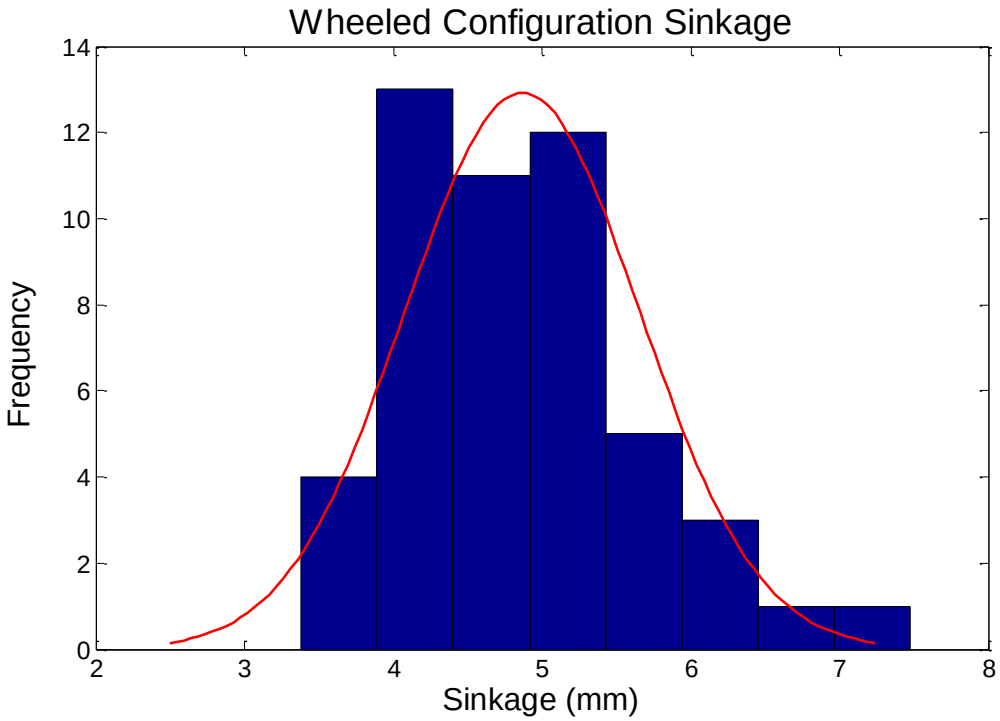

Figure 5-5: Wheeled sinkage results

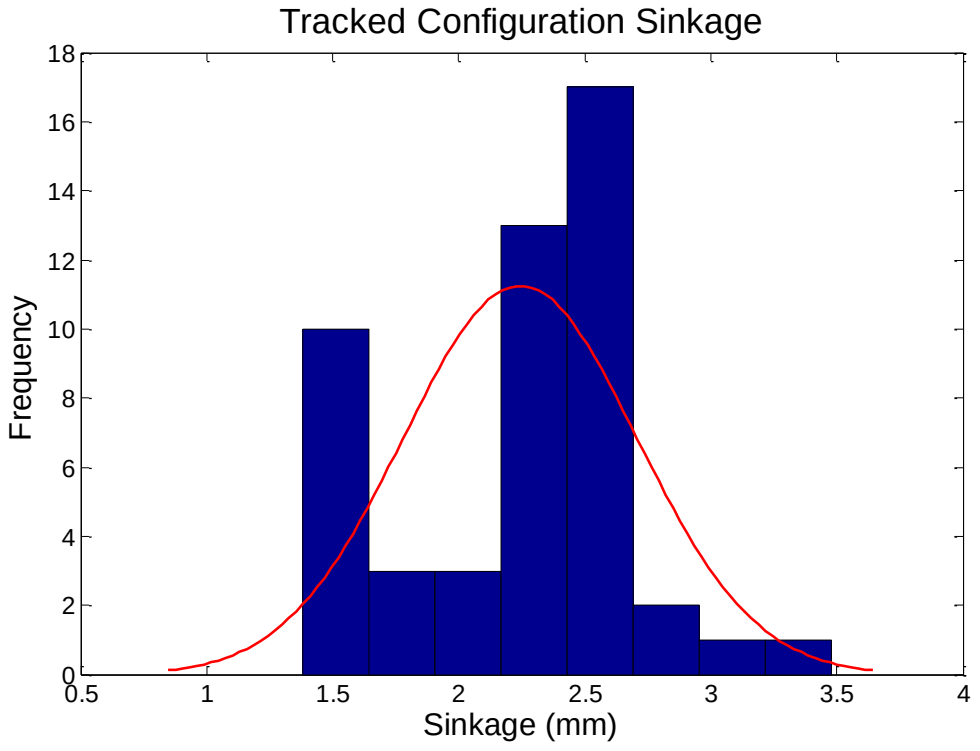

Figure 5-6: Tracked sinkage results

Throughout the testing the wheeled vehicle had a noticeably greater sinkage value. The average sinkage for the wheeled vehicle was 4.868*mm* and the tracked vehicle had an average sinkage of 2.244*mm*. A greater sinkage was expected for the wheeled vehicle because the load of the vehicle is distributed over a smaller contact area. The tracked vehicle's normal load is distributed over the entire length of the vehicle's running gear and therefore has a lower ground pressure which results in less sinkage.

The sinkage for the wheeled vehicle was measured in the winter of 2011-2012. This data set appears to follow a normal distribution fairly well. The sinkage was measured for the tracked vehicle during the spring of 2012. This set of data does not appear to follow a normal distribution very well. The set of data appears to fit more of a bimodal distribution. A normal distribution was expected for both data sets. It is possible that the sample size was too small at 50 data points, for a true normal distribution to form. With further testing, generating a larger sample size, it is expected that a normal distribution would form.

From of previous research performed on heavy vehicles and presented in the literature, wheeled vehicles have been known to exhibit a greater sinkage value [7]. This trend is present in this case study for light vehicles and would be expected to be observed for vehicles of any scale. This is an important realization because the vehicle sinkage could have an extensive impact on a SUGV's mobility depending on the operating environment. Typically in an off-road application a lower sinkage value would be more desirable. In this case study the tracked vehicle exhibited a lower value of sinkage and a greatly improved performance when faced with an obstacle negotiation scenario. These two factors could be correlated because the mechanism that allows the tracked vehicle to have a lower sinkage value, such as lower ground pressure resulting in a better floatation on sandy silt loam, appears to also be a contributing factor in the tracked vehicles improved performance in the obstacle negotiation testing. Moreover, the ability of the tracked vehicle to "bridge" over an obstacle also contributes to its enhanced mobility.

To ensure that the soil conditions were as close as possible for all tests, the soil procedure outlined in chapter 4 was followed and the soil compaction was tested following each sinkage testing run. The soil compaction testing was used to compare conditions and the results of the cone penetrometer testing are displayed below in figures 5-7 to 5-9.

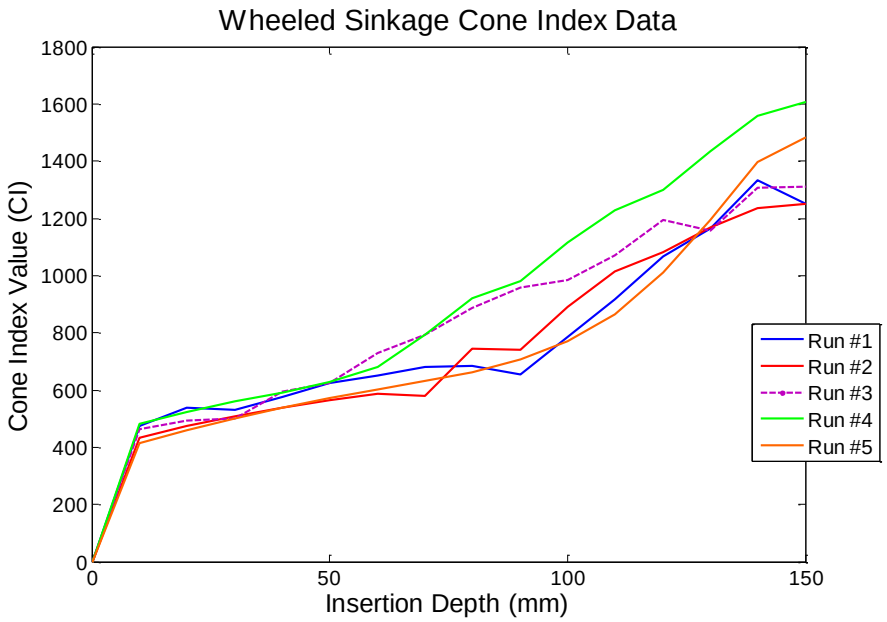

Figure 5-7: Cone index data for wheeled testing

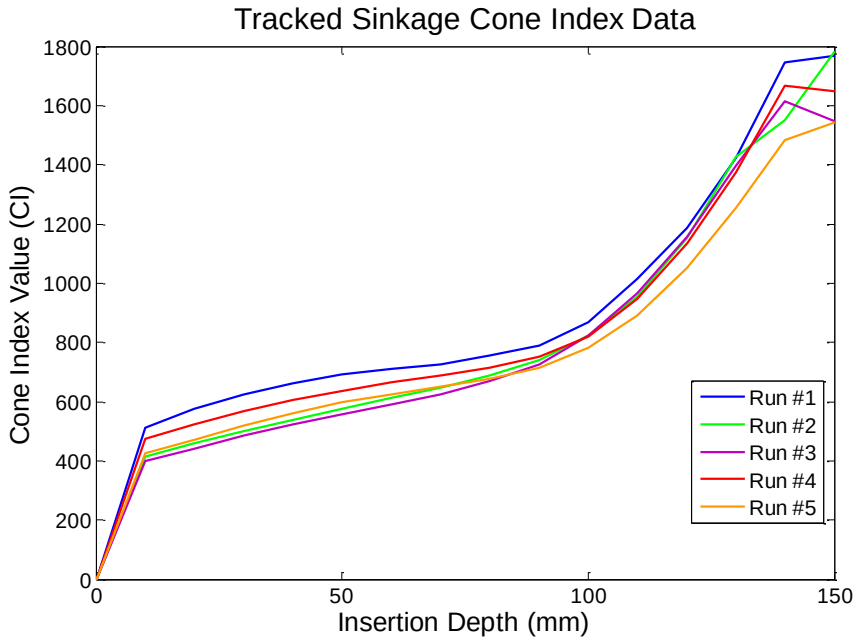

Figure 5-8: Cone index data for tracked testing

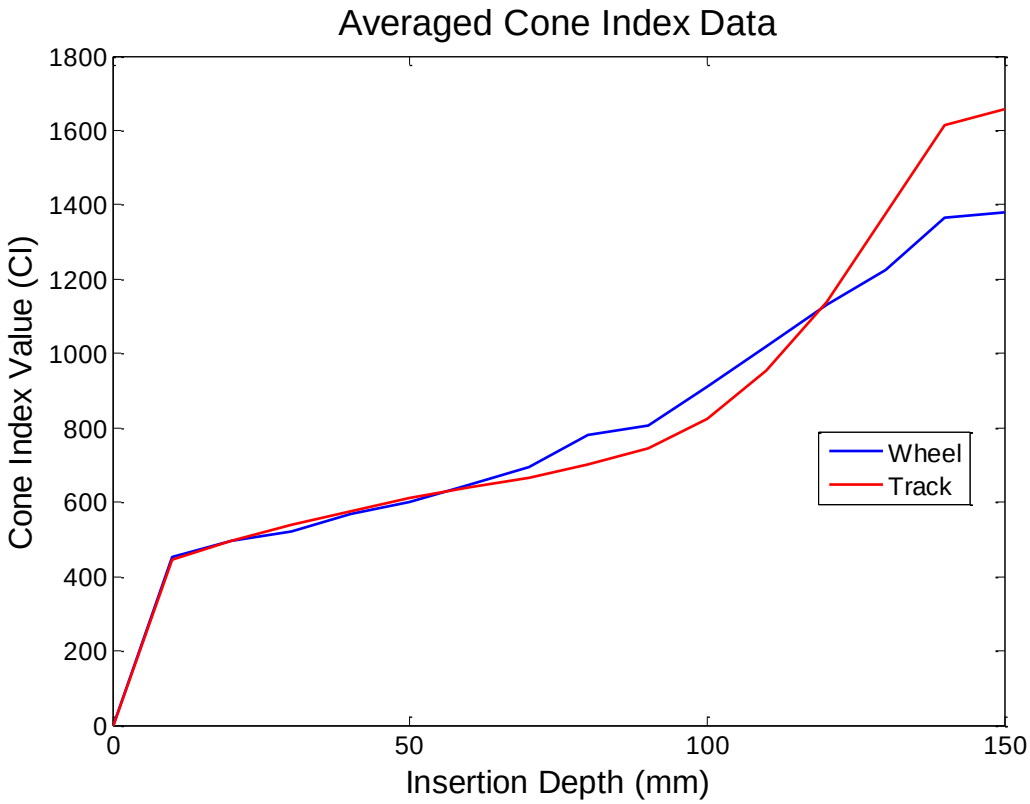

Figure 5-9: Averaged cone index data

The cone index data was used to compare the soil conditions during the wheeled and track testing. It was deemed important to have as close to identical soil conditions for both cases so that the sinkage data could be compared directly. In addition to the sinkage testing, the soil conditions were tested for all trials conducted on the sandy silt loam. Only the results for the sinkage tests will be displayed. This is for proof of concept purposes as it wasn't seen as necessary to include cone index data for each testing run. Figure 5-7 displays the cone index data for the wheeled testing. Each plot line represents the averaged cone index data for each separate run. After each run a total of 8 to 10 cone index measurements were taken. Figure 5-8 displays the cone index data for the tracked vehicle testing. By comparing the results it can be shown that the soil conditions are very similar and the sinkage results can be directly compared. In order to further analyze the CI data the averaged data from the entire set of wheeled and track testing was compared in figure 5-9. The averaged data sets appear almost identical. This is very encouraging and confirms that the soil preparation procedure is adequately replicating the soil conditions for each testing run. The soil preparation procedure is followed for all testing that was performed on the sandy silt loam testing surface.

Random Rough Vegetated Terrain

In order to make some qualitative comparisons regarding the vehicles ability to traverse rough vegetated terrain, the vehicle was tested on various unprepared areas. In these areas the vegetation ranged from 1 inch to 16 inches in height and consisted mostly of grass and small shrub like plants. The terrain had a variety of vegetation thickness which ranged from less than 1 millimeter thick to several millimeters thick. The incline of the area ranged from level to + or – 5 degrees. This testing surface allowed for many different paths of travel to be taken.

The wheeled vehicle was tested in the winter of 2011-2012. During this testing period there was no snow present in the testing area. The tests were conducted only when the temperature was approximately 45 degrees Fahrenheit or above. This was done to ensure

that no differences in results between the wheeled and tracked vehicle could be attributed to freezing conditions. The wheeled vehicle performed marginally on the rough vegetated terrain. The vehicle would routinely become immobilized in vegetation over approximately 5 inches in height. The density of the vegetation played a major role in the vehicles ability to traverse the terrain. If the vegetation was spare then the vehicle could traverse vegetation that had a thicker diameter and greater height. The wheeled vehicle was consistently unable to overcome any vegetation that was greater than 15 millimeters thick. The wheeled vehicle did not appear to have enough power available to overcome vegetation of this thickness or greater.

In the spring of 2012 the tracked vehicle was tested while operating on the random rough vegetated terrain. Overall the tracked vehicle exhibited a superior mobility performance. The tracked vehicle was able to traverse vegetation that was thicker and more densely packed than compared to the vehicle in its wheeled configuration. The tracked vehicle could overcome vegetation that was thicker then the vegetation that routinely caused the wheeled vehicle to become immobilized. Another interesting observation is that the tracked vehicle would not sink as far into the vegetated terrain as the wheeled vehicle would. It appeared that because of the greater pressure distribution due to the increase in contact area the tracked vehicle had a much greater floatation characteristic. This would allow the vehicle to traverse vegetation that was much denser. Finally the tracked vehicle tended to not disturb the terrain as much as the wheeled vehicle did. The wheeled vehicle caused the vegetation to become noticeably deformed and would break the vegetation as it traveled through. The tracked vehicle however, did not deform the vegetation as much and the vegetation would remain mostly intact. These different operating characteristics could have an impact on vehicle selection and should be considered if the mission parameters included a vegetated environment.

Pressure Distribution

The pressure distribution was measured for both running gears while the vehicle was operating on a flat rigid surface. This parameter was compared among the two cases in order to improve the understanding of the difference in pressure distribution in the contact patch between the running gear and the ground between the two vehicle configurations.

In the winter of 2011-2012 the pressure distribution was measured for the vehicle in its wheeled configuration using the Tekscan I-Scan 3150 pressure distribution measurement system. The vehicle was tested in a static configuration, while the vehicle was place upon the sensor and in a dynamic configuration as the vehicle traversed a testing scenario. The system was equilibrated and calibrated according to the manufacturers guidelines before testing was performed. The vehicle unfortunately, was too light to get an accurate pressure distribution reading. The sensor is rated for a pressure range of 0 to 125 psi but the test vehicle did not activate enough of the pressure sensels to maintain an accurate reading. An example of the data collected can be seen in figure 5-10. As it can be seen there is a distinct contact patch area for the two outer wheels, but the inner wheels are barely exerting any pressure, just a single sensel, according to the Tekscan readings. These results were deemed invalid as they did not provide an accurate enough reading. The total force that the Tekscan system was reading was quite lower than the measured weight of the vehicle. This trend was also present when the vehicle was tested in a dynamic configuration with the vehicle traversing over the pressure sensor.

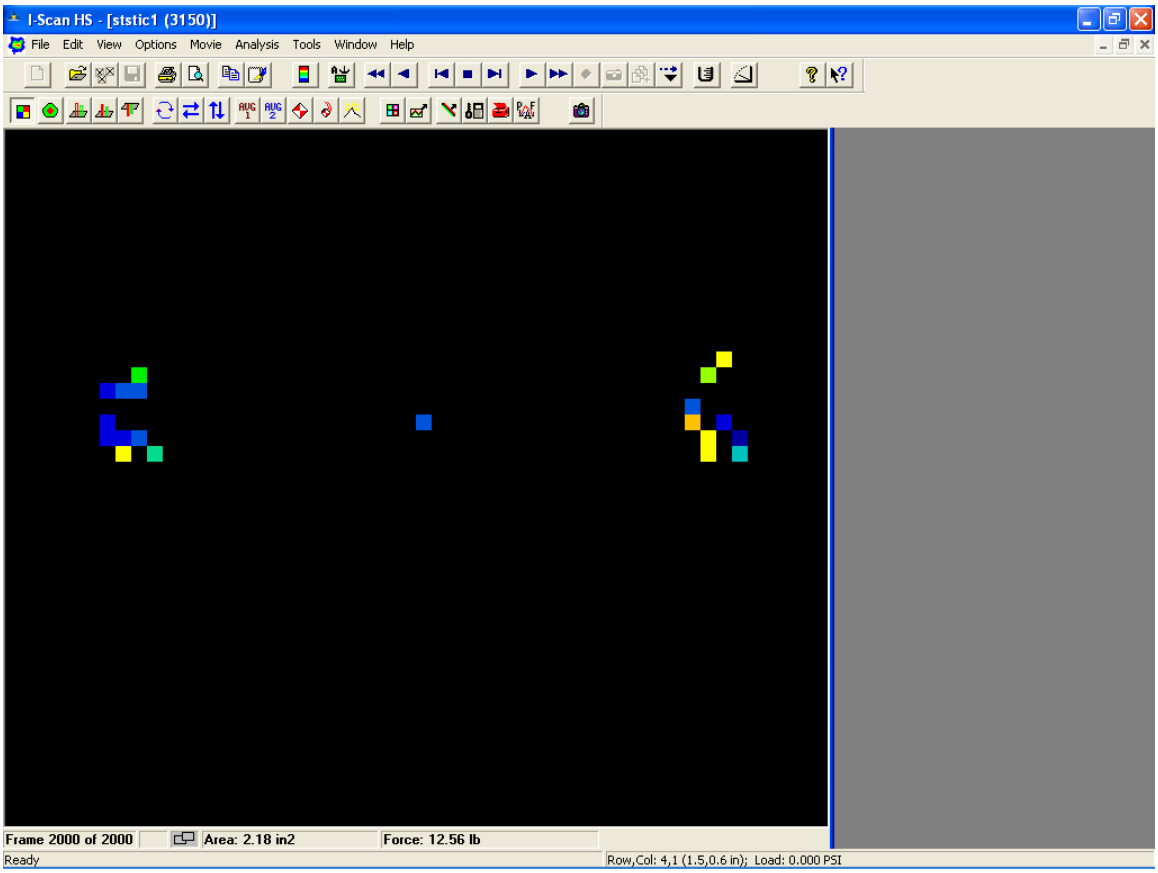

Figure 5-10: Pressure distribution results example

In an attempt to formulate an alternative method to measure the pressure distribution Fujifilm Prescale Film was employed. This film is a pressure sensitive film that reacts when a pressure distribution is applied. The film that was used is rated for use up to 28 psi. The Fujifilm Prescale Film did not provide any better results. The test vehicle was once again too light to produce any meaningful results. Following the second attempt at measured the vehicle's pressure distribution, the parameter was abandoned and the analysis was continued focusing on the remaining mobility parameters.

In the spring of 2012 the vehicle in its tracked configuration was tested using the Tekscan system and the Fuijifilm Prescale product. The results were very similar to those measured with the wheeled configuration in that the pressure was not significant enough to produce usable data. After testing and receiving very similar results to the pressure

distribution data collected in the wheeled configuration, the parameter was abandoned for the tracked configuration and testing continued focusing on the other mobility parameters.

Drawbar pull

The drawbar pull was measured for the both running gear configurations on the sandy silt loam surface and the rigid surface. The definition for drawbar pull according to the International Society for Terrain Vehicle Systems (ISTVS) is, "the force available for external work in a direction parallel to the horizontal surface over which the vehicle is moving" [40]. The drawbar pull was measured with the vehicle operating in a straight line steady state motion.

The results of the drawbar pull testing can be seen in figure 5-11 for a sandy silt loam surface and in figure 5-12 for a rigid surface. In both figures a single run that was most representative of the overall data set was selected to be compared to the other running gear. The entire data set can be seen in the Appendix A section.

When operating on sandy silt loam, both the wheeled and tracked vehicle exhibited a lower average maximum drawbar pull when compared to the drawbar pull results on rigid surface. Because of the deep grouser pattern on both running gears it was expected that the vehicles would have a greater drawbar pull on the sandy silt loam surface. The vehicle experiences a greater resistance to motion on the sandy silt loam surface and without the benefit more available power the vehicle cannot produce a larger drawbar pull. When operating on the sandy silt loam surface the drawbar pull would conclude when the vehicle would become immobilized either by loss of traction or because the vehicles motors could not provide any more power to the running gear. In the case were the vehicle could not provide any more power to the running gear the running gear would usually not experience much slip but the force at the drawbar would equal the maximum producible force at the running gear and the vehicle would reach an equilibrium point.

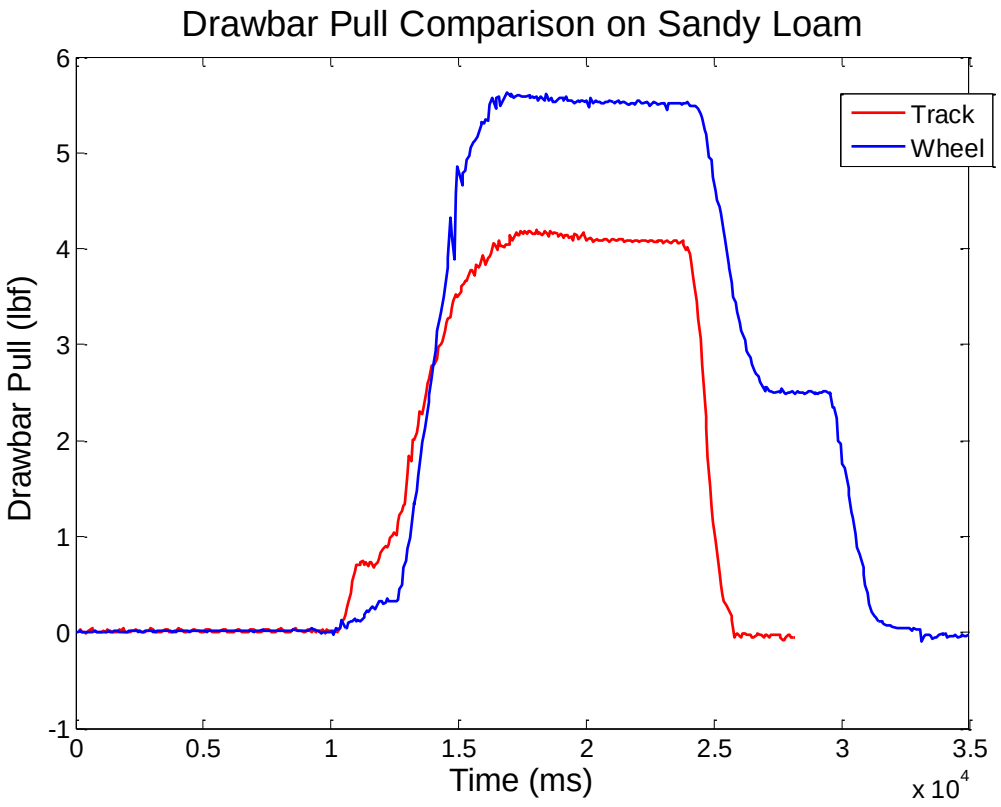

Figure 5-11: Drawbar pull on sandy silt loam

When comparing the drawbar pull on sandy silt loam between the wheeled and the tracked configuration it is clearly shown that the wheeled vehicle has a greater drawbar pull. This trend was present in the entire data set and the average maximum drawbar pull for the wheeled vehicle on sandy silt loam was computed as 5.556 lbf. The wheeled vehicle would quickly reach an optimum slip value to produce the maximum drawbar pull and remain at an equilibrium point for a clearly defined length of time. Continuing through the test and applying more resistance at the drawbar the wheeled vehicle would being to lose traction and the slip would increase. The slip would increase and the drawbar pull would decrease to until it leveled out at a second equilibrium point. At this equilibrium point the vehicle would not be producing any more forward velocity and the test would be concluded by eliminating power to the motors.

The vehicle in a tracked configuration would exhibit a decidedly different behavior during the drawbar pull testing when compared to the wheeled configuration. The tracked vehicle also consistently displayed a lower value for maximum achievable drawbar pull. The average maximum drawbar pull for the tracked vehicle on sandy silt loam was computed as 4.348 lbf. Reviewing figure 5-12 it can be seen that the tracked vehicle's drawbar pull takes longer to reach its maximum value. This is because the tracked vehicle's drawbar pull increases at a slower rate. The slower increase is attributed to the characteristic that in this test it appears that the tracked vehicle increases its slip at a slower rate. This slower rate of slip increase causes the vehicle to maintain better traction throughout the drawbar pull testing and affects the rate of increase in the drawbar pull. The drawbar pull peaks for the tracked vehicle and then only slightly decreases before reaching a noticeable equilibrium point. This slight decrease after reaching a peak drawbar pull value is also present in the wheeled test result. One very noticeable difference in the two drawbar pull results in that the tracked vehicle never produces a second equilibrium point. The drawbar pull for the tracked vehicle peaks and then following a brief equilibrium point decreases to zero. This factor is attributed to the characteristic that the tracked vehicle displayed overall better traction. During the drawbar pull testing the tracked vehicle's running gear would not lose traction and therefore the slip didn't increase as rapidly as the wheeled vehicle. Another factor that could be contributing to the tracked vehicles lower maximum drawbar pull performance is the fact that the tracked vehicle experiences a greater internal resistance due to the larger internal contract area. This larger internal resistance causes the vehicles top speed to be reduced and consumes more of the vehicles available power to be used to overcome this internal resistance. This causes a loss of torque at the running gear. This phenomenon of greater internal resistance has been well documented for large heavy tracked vehicles and is present in this case study as well [7]. A final distinction must be mentioned for the tracked vehicle in that the grouser pattern for the tracked vehicle in this case was much shallower when compared to the wheeled vehicle. When designing this experiment a track with an identical grouser pattern to the wheels could not be found so a track with as similar dimensions as possible was used.

The attributes displayed in the drawbar pull testing for the wheeled and tracked configuration on sandy silt loam allow for some comparisons in mobility performance to be made. In this case study the wheeled vehicle had a larger overall drawbar pull. This characteristic could be desirable if the vehicle is operating in an off-road environment. This higher drawbar pull must be weighed against the tracked vehicles better mobility performance and slower rise to a maximum drawbar pull value. If operating at lower speeds with a relatively small value of drawbar pull expected compared to the vehicles maximum drawbar pull, then the tracked vehicle could be more beneficial in this scenario. Throughout the duration of the tests the wheeled vehicle maintained a higher drawbar pull value for a longer period of time. The tracked vehicle peaked and then quickly fell back to zero. Maintaining a higher drawbar pull value for a longer period of time could cause the wheeled configuration to be better suited for operating on sandy silt loam with few obstacles. Generally it is an accepted convention that tracked vehicles exhibit a greater drawbar pull value when operating in off-road conditions and it was surprising to see that the wheeled vehicle maintained a higher value of drawbar pull [7]. In this case study it became apparent that a huge limiting factor in terms of mobility was the maximum output of the motor. In the tracked configuration the vehicle seemed underpowered after the added internal resistance. This factor seems to have contributed to the drawbar pull results on sandy silt loam.

The results for drawbar pull on a rigid surface can be seen in figure 5-12. In figure 5-12 one data set most representative of entire collection is displayed to compare the performance of each running gear. In the case of the drawbar pull on concrete, both the wheeled and tracked configuration exhibit a greater maximum drawbar pull value when compared to the drawbar pull results on sandy silt loam. This is due to the fact that on a rigid surface there is much less resistance to motion. The decrease is motion resistance allows more torque to be transmitted to the running gear which increases the drawbar pull. Many of the same characteristics that were seen in the drawbar pull testing for the vehicle on sandy silt loam are present for the testing on rigid surface. In the case of the rigid surface drawbar pull testing, the tracked configuration has an average maximum

drawbar pull of 6.742 lbf. The wheeled configuration has a maximum average drawbar pull value of 6.28 lbf.

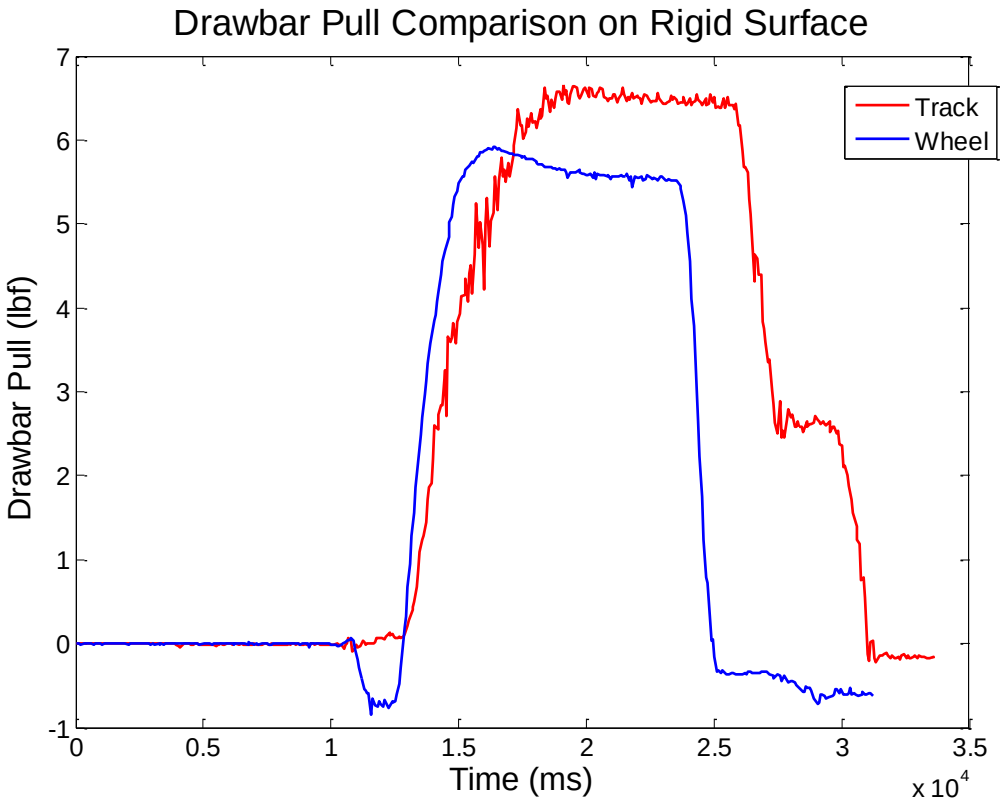

Figure 5-12: Drawbar pull on rigid surface

On a rigid surface the vehicle in its wheeled configuration displayed a lower overall drawbar pull across all trials when compared to the tracked configuration. The characteristic shape of the drawbar pull curve is slightly different for the wheeled vehicle when comparing the wheeled performance on sandy silt loam and rigid surface. On the rigid surface the vehicle does not display a second equilibrium point as it did on the sandy silt loam. The wheeled drawbar pull quickly reaches a maximum value and then slightly decreases to an equilibrium point. After this equilibrium point the vehicle continues to increase in slip and then the drawbar pull quickly drops to zero. This occurs because during the testing the vehicle would quickly reach a point where it would

become immobilized but there would not be very much wheel slip. At this point the available power from the motors would reach an equilibrium point with the force at the drawbar and the vehicle would cease to make any more forward progress; at this point the test was concluded. This characteristic is present for all the wheeled data sets on rigid surface and seems to indicate that on a rigid surface the wheels have a greater traction then on sandy silt loam and less wheel slip is present. The wheeled data set for a rigid surface seems to closely resemble that of the tracked configuration on sandy silt loam. This is an interesting phenomenon and could have implications for the vehicles mobility performance.

When assessing the tracked vehicles performance on rigid surface there are some characteristics that are not present when operating on sandy silt loam. On the rigid surface the tracked vehicle once again displays a slower rate of drawbar pull increase then the wheeled vehicle. This is attributed to the fact that the tracked vehicle increases its slip at a slower rate because it is able to maintain a greater degree of traction. The tracked vehicle reaches a maximum peak value and then slightly decreases into an equilibrium position. This peak drawbar pull value corresponds to a optimum value of slip. When the slip is optimized then the drawbar pull will reach a max value. For heavy vehicles it has been proposed that this optimum slip value occurs between 15% and 20% [7]. This equilibrium position is held for a definitive length of time and then the drawbar pull value decreases as the slip continues to increase, until a second equilibrium point is reached. This second equilibrium point is maintained for a short period of time until the drawbar pull finally decreases to zero. This characteristic is displayed for the wheeled vehicle operating on sandy silt loam and is surprising to find it displayed for the tracked vehicle on rigid surface. The fact that this curve characteristic is present for the tracked vehicle operating on a rigid surface seems to indicate that the tracked vehicle was experiencing a greater value of slip then the wheeled vehicle operating on rigid surface. This is consistent with qualitative observations made during the vehicle testing. The greater maximum drawbar pull value is caused by the decrease in motion resistance attributed to changing the operating environment from the sandy silt loam to the rigid surface.

Following the review of the results from the drawbar pull on rigid surface, some mobility performance comparisons can be made. For operating on a rigid surface, the tracked vehicle obtained a higher average maximum drawbar pull value. This characteristic is consistent with the literature and this characteristic can be deemed to be present for vehicles of any scale. One very interesting phenomenon that presented itself in the testing is that the wheeled and tracked drawbar pull had a similar second equilibrium point when comparing the tests for sandy silt loam and concrete. This can be attributed to the differences in traction between the wheeled and tracked vehicle. During testing of the wheeled vehicle on sandy silt loam, it was observed that the wheeled vehicle reached second equilibrium point that was accompanied with a high rate of wheel slip. The wheeled vehicle operating on sandy silt loam experienced a high rate of wheel slip as the vehicle was reaching a point of immobilization. This same characteristic was present when operating the tracked vehicle on a rigid surface. During drawbar pull testing for the tracked vehicle on a rigid surface, the vehicle also experienced a high rate of wheel slip as it approached a point of immobilization. This high rate of wheel slip in both cases caused a second equilibrium point to be achieved. The other testing configurations, the tracked vehicle on sandy silt loam and the wheeled vehicle on a rigid surface, did not experience this high rate of running gear slip and in both these cases a second equilibrium point was not observed. The lack of high wheel slip in the latter two cases suggests that the vehicle experienced a greater degree of traction than its counterpart. This is an important distinction and leads to the determination that the tracked vehicle performs better in off road mobility situations while the wheeled vehicle experiences less slip when operating on a rigid surface and could result in greater mobility on a rigid surface. These distinctions in mobility performance are important to consider when choosing a vehicle for a given set of mission criteria.

In order to create a non-dimensional comparison of the vehicles mobility the coefficient of traction is used. The coefficient of traction as described by Wong is the ratio of the drawbar pull to the normal load on the driven wheel [7]. This parameter is widely used to

assess the mobility performance of vehicle operating in an off-road environment. This relation is expressed as,

$$\mu_{tr} = \frac{F_d}{W_d} \qquad 5.1$$

where F_d is the force at the drawbar, W_d is the normal load on the driven wheels, and μ_{tr} is the coefficient of traction. Seen in figure 5-13 and 5-14 are the coefficient of traction graphs for both the sandy silt loam and the rigid surface. The coefficients of traction for rigid surface was included for comparison purposes in order to form a more complete picture of mobility.

In both cases the differences in slopes as the coefficient of traction's rise to a peak value are much more similar than in the drawbar pull graphs. This can be seen quite clearly in figure 5-14, where the coefficient of traction is plotted for a rigid surface. In figure 5-14 it appears that the slope of coefficient of traction as it rises to a peak value are very similar between the wheeled and tracked vehicle. This is due to the fact that the tracked vehicle is slightly heavier and therefore will have a reverse correlation to the coefficient of traction. The tracked vehicle has a maximum coefficient of traction on sandy silt loam of 0.226 and the wheeled vehicle has a maximum of 0.348. On a rigid surface the tracked vehicle has a maximum coefficient of traction of .411 and the wheeled vehicle has a maximum of 0.323. The coefficient of traction can be compared for vehicles of any scale because of its non-dimensional nature and conclusions regarding the traction of an SUGV can be compared with that of heavy vehicles.

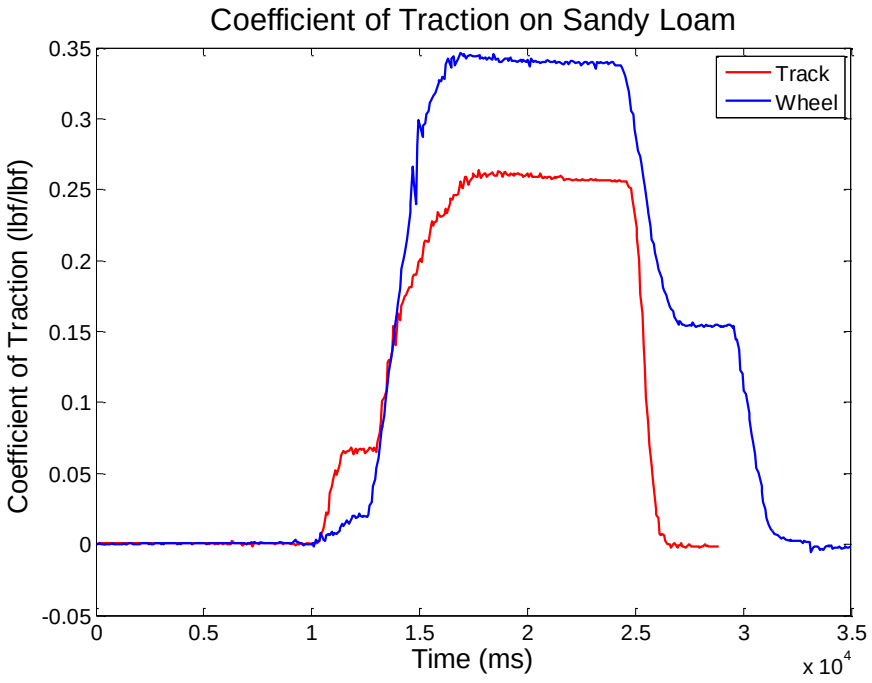

Figure 5-13: Coefficient of traction on sandy silt loam

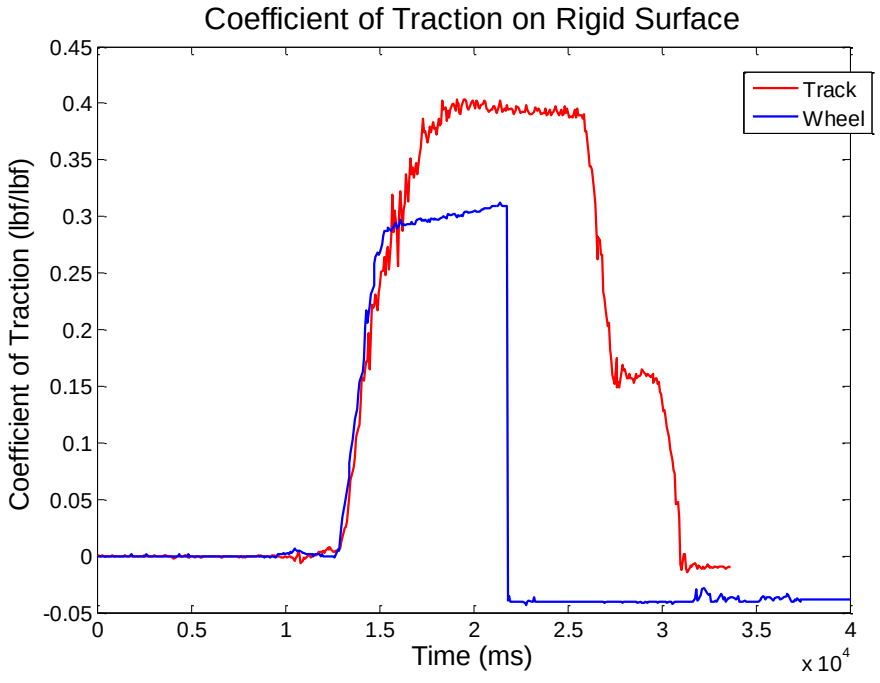

Figure 5-14: Coefficient of traction on rigid surface

Energy Profile

The current consumption was measured for all testing conducted in this comparative analysis. The current was measured in order to gain some insight into the vehicles energy efficiency in the wheeled and tracked configuration. This was done to see if any conclusions can be drawn about differences between the two running gears. In figure 5-15 and 5-18 you can see a profile of the vehicles power as it navigates through the testing scenario in which the vehicle negotiates a 1.5 inch square rod with both running gears. In these scenarios both the tracked and wheeled vehicle are traveling at a constant speed of approximately 2 mph.

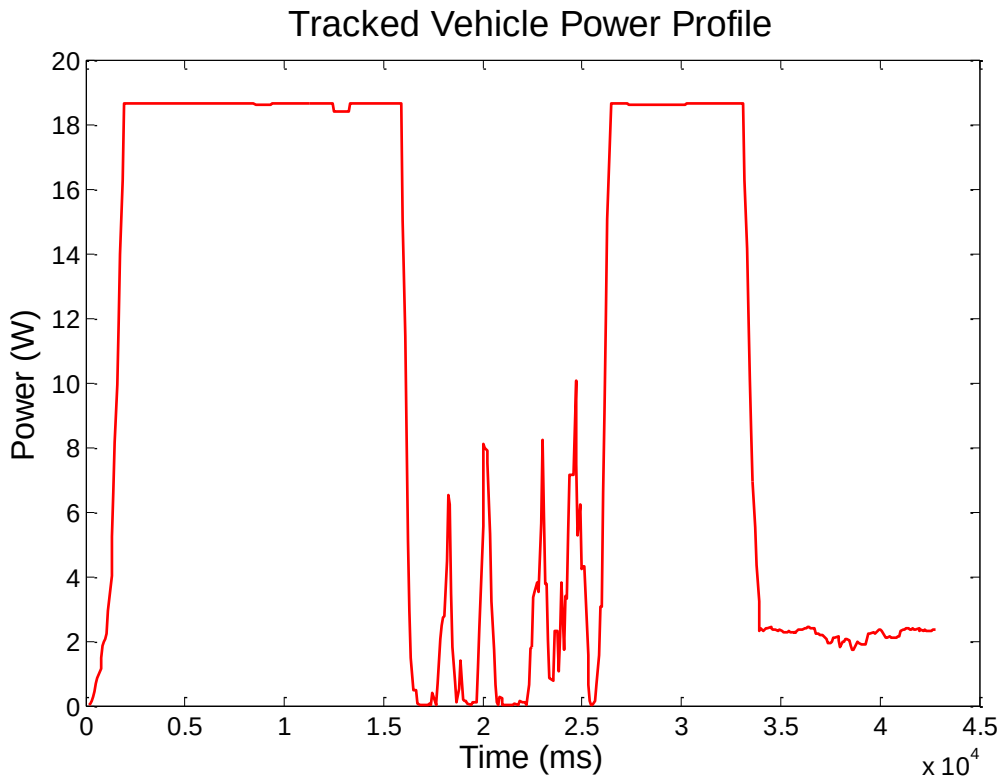

Figure 5-15: Tracked vehicle power profile while traversing a 1.5 in obstacle

When looking at the power profile of the tracked vehicle while traversing the 1.5 inch obstacle with both running gears at approximately 2 mph some trends are noticeable. While current was recorded for every trial only one profile is presented that best

represents the data set as a whole. The trends and conclusions draw from this power profile apply to the data set in general. It can be seen that the vehicle applies power to the motor very quickly and there is not much of a power ramp up period. This is noticed through qualitative observations in that the vehicle accelerates to its steady state speed very quickly. The tracked vehicle operates at steady state for a few brief period of time and then comes into contact with the obstacle. There is large noticeable area in which the current drops significantly. This is due to the fact that the vehicle travels up the obstacle until the midpoint of the vehicle in which is then lurches forward once the center of gravity shifts. This is what is cause the brief drop in current because the force due gravity carries the vehicle over the object. This sequence of events can be seen in figures 5-16 and 5-17. During this significant drop in power there were also many brief spikes. It is believed that this is due to the amount of vibration that is induced when the vehicle is in its tracked configuration. Until the smooth operation of the wheeled vehicle, as sections of the track bend over the drive sprockets there is a considerable amount of vibration introduced. Another aspect to be considered is that during steady state forward motion at approximately 2 mph the tracked vehicle has a power consumption of approximately 18.4 watts. After the vehicle traverses the object the power returns to its steady state value until the power to the vehicle is cut off.

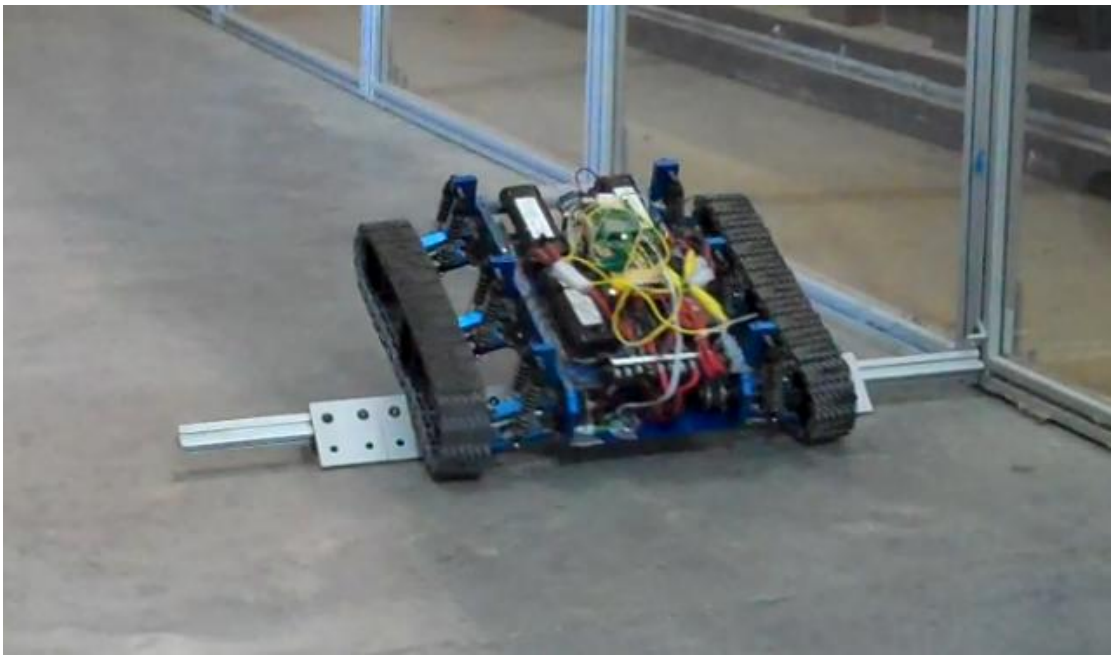

Figure 5-16: Tracked vehicle beginning to traverse obstacle

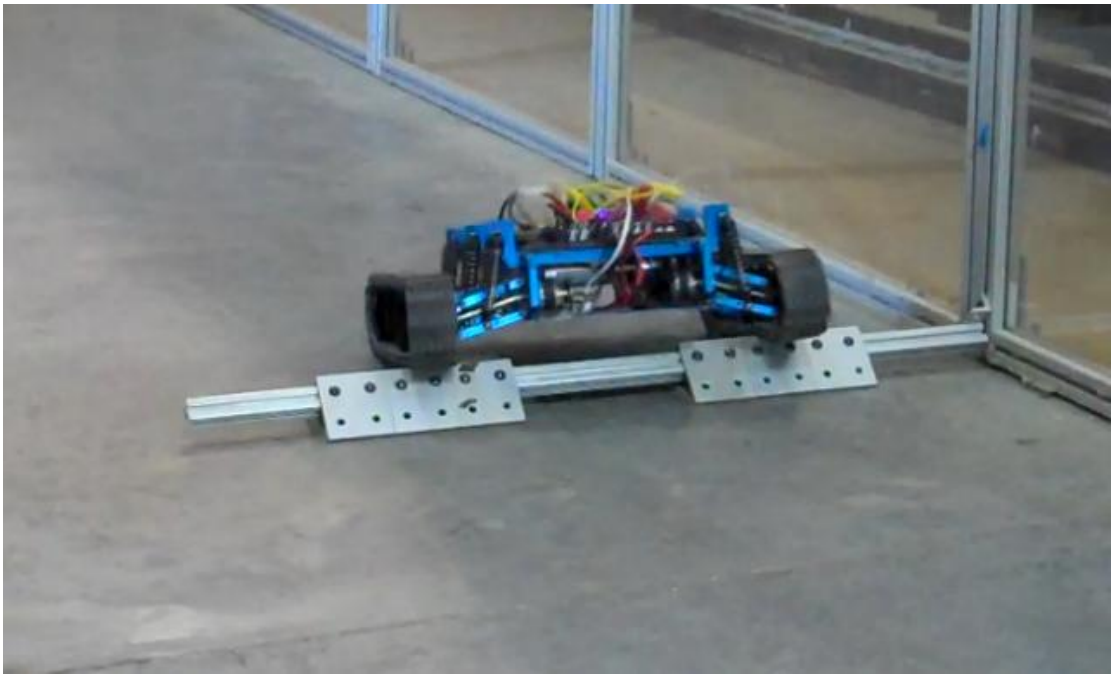

Figure 5-17: Tracked vehicle's center of gravity shifts

The power profile for the wheeled vehicle while negotiating the 1.5 inch obstacle with both running gears is displayed in figure 5-18 and presents some interesting trends. The first trend that is evident in the wheeled vehicle's power profile is the very brief drop in power when the vehicle encounters the obstacles. When the wheeled vehicle was negotiating the obstacles it displayed a very different traversing characteristic. The wheeled vehicle would maintain a fairly level orientation as it negotiated obstacles and there was not a large shift that was displayed for the tracked vehicle. Because the dip in power is so brief for the wheeled vehicle it is hard to determine if there are the minor spikes as seen for the tracked vehicle profile. The overall operation the vehicle in its wheeled configuration was much smoother with much less vibration induced. After the wheeled vehicle overcomes the obstruction it very quickly returns to its steady state power level while moving forward at 2 mph. One last observation that was made was that while operating at steady state at approximately 2 mph the wheeled vehicle has a power level of 13.7 watts.

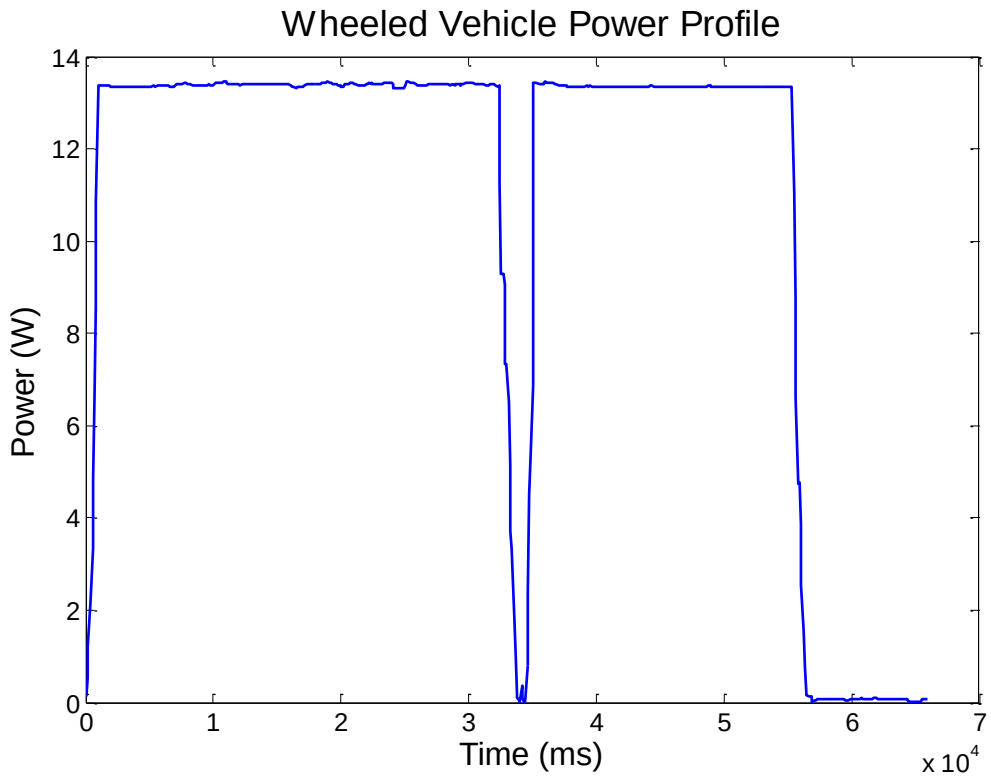

Figure 5-18: Wheeled vehicle power profile while traversing a 1.5 in obstacle

When comparing the power profiles of the wheeled and tracked vehicle while operating in almost identical situations some conclusions can be drawn. The first and most obvious comparison is that the tracked vehicle requires more power while operating at a similar speed as the wheeled vehicle. This observation was consistent across all tests. This is due to the fact that the tracked vehicle experiences a higher level of internal resistance due to the running gear. Another observation related to this effect is that the tracked vehicle appears to take longer to reach its steady state power value. This leads to a slightly slower time to accelerate to steady state. This can also be attributed to the higher internal resistance to motion for the tracked vehicle.

Another comparison that is made is the difference in power profiles as the vehicle traverses the obstacle. The vehicles have a vastly different power response when traversing obstacles. The tracked vehicle has a much longer dip in power when traversing

obstacles with brief small spikes. The wheeled vehicle has a very short dip in power and quickly returns to steady state. It can be shown that in the brief time the vehicle is in contact with the obstacle the tracked vehicle consumes less power as the dip in power lasts longer. This brief energy savings is quickly overshadowed by the steady state operating power. This presents a trade off in characteristics, while the wheeled vehicle is more energy efficient the tracked vehicle is superior in obstacle negotiation abilities.

Vehicle Operating Speed

One final point of comparison must be address in regards to the vehicles top speed. During all testing scenarios the vehicles top speed was monitored by a rotary encoder. In the case of the vehicles top speed the vehicle is limited by the power provided by the motors. The top speed is also affected by the vehicles resistance to motion from internal resistance and from resistance due to terrain compaction. In all cases the vehicle in a wheeled configuration had a higher top speed. This was due to the fact that the wheeled configuration had much less internal resistance. In table 5-3 the average maximum speed is listed for sandy silt loam and rigid surface. The top speed comparison was made for when the vehicle was operating at a steady state in straight line motion. The top speed was analyzed for both sandy silt loam and rigid surface. This distinction is another aspect that can factor into decisions where a vehicle must be chosen given a given set of operating conditions. If vehicle top speed is an important parameter then the wheeled configuration might be more attractive. After reviewing the power profile, it can be said that the wheeled vehicle has a higher top speed and would be more energy efficient than a tracked vehicle operating at a similar speed.

Table 5-3: Average maximum operating speeds

	Sandy silt loam	**Rigid Surface**
Wheeled	4.354 mph	5.213 mph
Tracked	3.986 mph	4.567 mph

After reviewing the comparative analysis data and drawing some initial observations and conclusions there are some very distinct differences in mobility performance between the wheeled and tracked configuration. In order to weight these difference against one another and chose the best vehicle for the given set of mission criteria the analysis findings were used to form an MMM that is customized for use with vehicles in the SUGV size range.

5.3 Mobility Metrics Matrix Development and Analysis

In order to improve upon the MMM method of vehicle comparison, the qualitative and quantitative comparisons were used to create metrics that are more suitable for vehicles in the robotic scale. The MMM was first created by Worley in 2007 and is based on the business practice of the House of Quality in which attributes are ranked against each other and correlations noted in order to choose the best course of action from a pool of viable options. Worley developed the MMM to help made comparisons between different vehicle platform options for a given set of mission parameters. After performing the comparative analysis and examining the results in order to form a set of conclusions, these conclusions were used to improve upon the MMM. The goal of improving the MMM is to develop a comparison tool to better select a vehicle in the robotic scale for a given set of mission parameters. In figure 3-1, a template for the MMM developed by Worley is displayed. This template will provide the starting point for a more customized MMM.

Terrain Interaction Parameters

The first group of analysis consideration falls under the category of terrain interaction. In this category, terrain characteristics such as Non-disturbance of terrain and type of terrain are considered. This group of terrain parameters is correlated to vehicle-terrain interaction parameters such as tractive effort and sinkage. Many parameters are considered but following the comparative analysis it is proposed that more specific

terrain characteristic should be considered. Today many SUGV are expected to operate in a wide variety of environments including urban environments. Because of this fact it is proposed that average, or expected obstacle size parameter is included. This point of consideration should be included because while operating it might not be feasible or possible for a SUGV to avoid every encountered obstacle by choosing an alternative path of travel. This parameter would have to be user defined for the given set of mission criteria. The user will need to specify an estimated range of obstacle sizes for consideration. However, this will allow a much more customizable selection process and will lead to a better vehicle selection.

A second point of consideration for the terrain characteristics group would be to consider whether or not the vehicle will be traversing a vegetated environment. Vegetated environments can be encountered in virtually any operation setting from urban to off-road. This means that ability to navigate vegetation could be of great importance and should be considered in all vehicle selection processes. This input can be included as a yes or no with regard to vegetated operating environment or the user can define exactly what type of vegetation characteristics are expect. These two additional terrain characteristics parameters will help better characterize the operating environment and help make a more refined vehicle selection.

Geometry Parameters

The second group of analysis considerations relate to the operating environment and vehicle geometry. This group includes considerations such as vehicle contact area, ground clearance, and confined travel path area. The MMM developed by Worley includes a fairly complete consideration of vehicle and terrain geometry parameters [53, 69, 70]. One parameter though should be proposed as a worthy addition. Following the analysis of the drawbar pull results it was seen that the grouser pattern and depth had a great impact. The vehicle with a more pronounced and deeper grouser pattern provided a much greater drawbar pull on sandy silt loam, while the vehicle with very small grousers and a greater area of contact provided a larger drawbar pull on rigid surface. Because of

this difference, the vehicle's grouser depth and tread pattern should be a factor of consideration. This parameter can be included as a simple a criteria as a yes or no regarding whether or not the vehicle has a pronounced tread pattern. This criteria could also be a user defined such as if the vehicle has a grouser depth of over 5 mm. With the addition of this point of consideration the MMM's geometry parameters are all encompassing and no further points of comparisons can be made without further testing and analysis.

Performance Parameters

The third group of vehicle parameters that are considered are the performance parameters. The performance parameters group consists of comparison criteria such as distance of travel, agility, vehicle speed range, and energy consumption. With a focus on vehicles in the range of robotic SUGVs a few other points of consideration much be included with a focus on energy efficiency. Energy efficiency is one of the greatest limiting factors facing SUGVs and should be a focus of comparison.

The MMM currently includes a consideration for energy consumption but it would be more useful to frame this comparison in terms of energy efficiency. Energy consumption appears rather ambiguous, all vehicles consume energy, and a more definitive point of comparison should be used. A comparison point of energy efficiency is substituted for the energy consumption parameter. Energy efficiency is defined as the ratio of useful output to energy input. This specific point of energy efficiency comparison can be defined by the end user but for this analysis is will be framed in terms of distance traveled versus energy consumed while the SUGV is traveling at approximately 2 mph. The velocity of 2 mph was chosen because for this case study the vehicle was routinely tested at 2 mph and a direct comparison can be made between the wheeled and tracked configuration.

Another parameter that is introduced to the MMM with regards to energy is the vehicles energy storage capability. Energy storage capability is a very important point of comparison and all SUGVs are limited by their energy storage capability. Because most

SUGV use some sort of battery energy storage system the storage capability of their battery packs becomes very important and their range is a factor of both their energy storage capabilities as well as their energy efficiency. In addition to the energy storage comparison another parameter could be considered in the vehicles ability to recharge itself. Many SUGV operating as lunar exploration vehicles had a solar recharging system. The ability of a vehicle to either supplement its energy reserve or recharge entirely would be a very important point of comparison. Because the vehicle used in this comparison did not have this capability it will not be included in the customized MMM but should be considered for users who have vehicles with that capability.

Instrument Sensitivity Parameters

The final group of comparison parameters is the instrument sensitivity parameters. This parameter group only has vehicle characteristic and is not related to any terrain qualities. This group includes factors that will affect instrumentation such as vibration, temperature and impact. This group is fairly complete when considering the comparative analysis that was performed but one addition is suggested.

The operating range can have an impact on the vehicles operating characteristic and should be included in the vehicle instrumentation section. The vehicle used in this case study was teleoperated using X-BeePro modules. The wireless modules had an operating range of approximately 300 feet and no onboard cameras to assist in navigation. This means that the vehicle was essentially a line of sight vehicle. This fact should be considered because a vehicle that is line of sight only can insufficient for certain operating scenarios. To this effect the operating range should be considered. Another term for mode of operating is not included because this should be encompassed by the vehicles operating range. If the vehicle's range is several miles it is assumed that the vehicle will have the necessary equipment to allow the operator to successfully operating the vehicle as that range. Overall these additions were deemed as necessary and an improvement to better facilitate a more accurate vehicle selection when considering SUGVs.

Customized MMM

In figure 5-19 a customized MMM is presented. This MMM is based on the analysis performed for this specific study. This customized MMM is aimed at providing a better selection tool for comparing vehicles in the SUGV range. This MMM can be further tailored by the end user by adding or subtracting selection criteria based on the specific needs. For this study, additional proposed parameters have been included. This customized MMM was used to evaluate an example scenario in order to illustrate how this selection tool can be used.

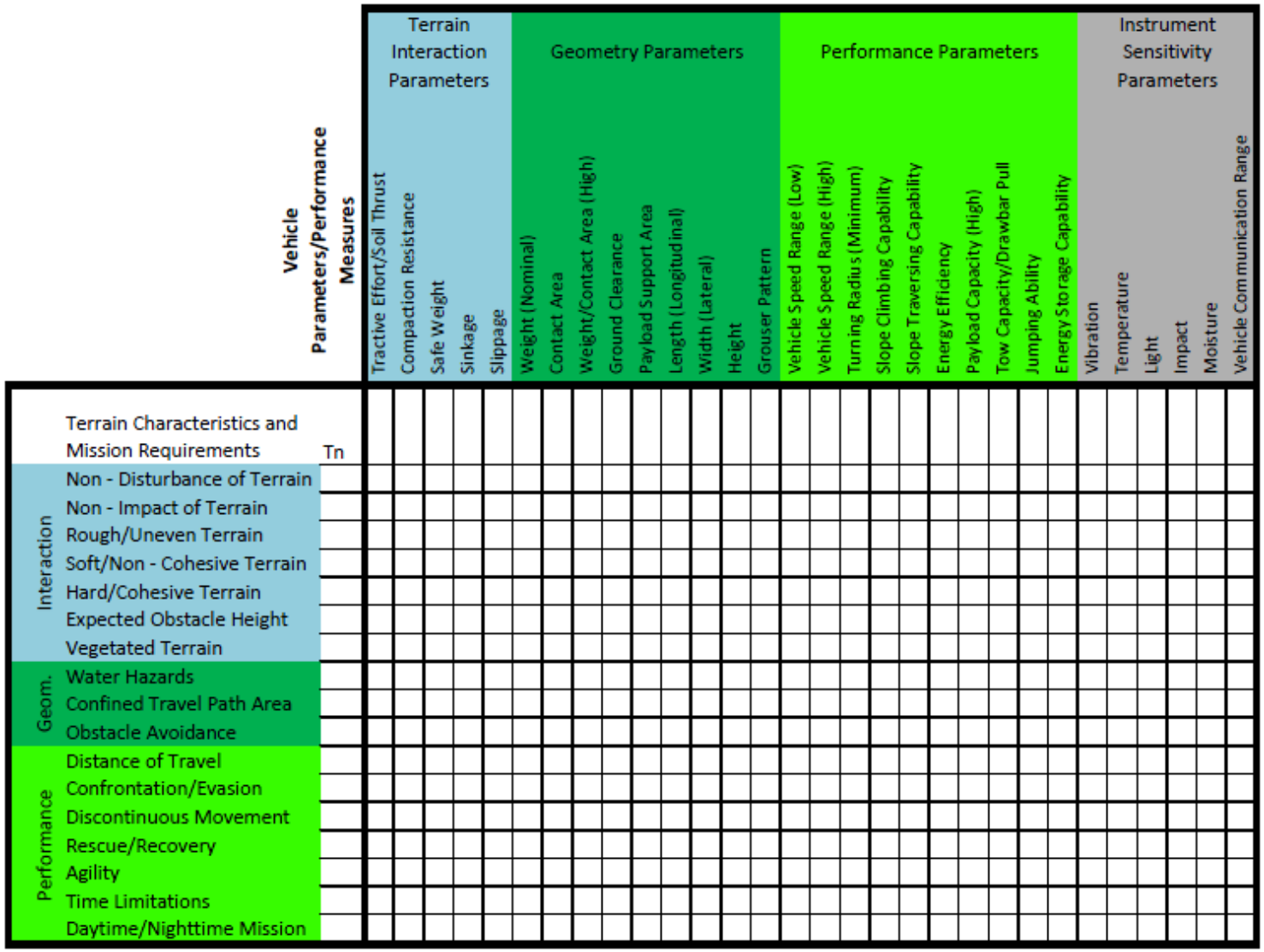
Vehicle Parameters/Performance Measures
Terrain Interaction Parameters
Geometry Parameters
Performance Parameters
Instrument Sensitivity Parameters
Tractive Effort/Soil Thrust
Compaction Resistance
Safe Weight
Sinkage
Slippage
Weight (Nominal)
Contact Area
Weight/Contact Area (High)
Ground Clearance
Payload Support Area
Length (Longitudinal)
Width (Lateral)
Height
Grouser Pattern
Vehicle Speed Range (Low)
Vehicle Speed Range (High)
Turning Radius (Minimum)
Slope Climbing Capability
Slope Traversing Capability
Energy Efficiency
Payload Capacity (High)
Tow Capacity/Drawbar Pull
Jumping Ability
Energy Storage Capability
Vibration
Temperature
Light
Impact
Moisture
Vehicle Communication Range
Terrain Characteristics and Mission Requirements
Tn
Interaction
Non - Disturbance of Terrain
Non - Impact of Terrain
Rough/Uneven Terrain
Soft/Non - Cohesive Terrain
Hard/Cohesive Terrain
Expected Obstacle Height
Vegetated Terrain
Geom.
Water Hazards
Confined Travel Path Area
Obstacle Avoidance
Performance
Distance of Travel
Confrontation/Evasion
Discontinuous Movement
Rescue/Recovery
Agility
Time Limitations
Daytime/Nighttime Mission

Figure 5-19: A customized MMM

Example Analysis Using the Customized MMM

The example scenario is presented in terms of operating conditions and mission criteria and the results of the MMM evaluation are compared with the results from the comparative analysis. The correlations are marked with impact markers as follows: H for a high (strong positive correlation) relation, L for a low (light positive correlation) relation, and A for an adverse relation. These impact markers are used to score the vehicle and are inputs for the indexing function, equation 3.1, in which the markers importance is scored. The importance is a user defined input. Once the markers importance is scored using equation 3.2, the results are used as inputs for equation 3.3, in which a mission specific vehicle rank is formed. For the analysis illustrated here, because there are only two vehicles the mission specific rank will either be 1 or 2.

The example that will be used to evaluate the vehicle is an arbitrary operating scenario. The scenario is that a vehicle is needed to operate in an urban environment in which the vehicle will be responsible for entering a building ahead of the operator to sense for dangerous chemicals. The vehicle will be operating on a rigid surface for 60% of the time and on a sandy silt loam surface for 40% of the time. This operating environment also included an occasional rubble obstacle ranging from 0.5 inches to 3 inches. Because the vehicle does not need to travel far from the operator the vehicle's battery packs can be switched and/or recharged when they get close to depletion. No other scenario parameters are given.

The first step when using the MMM is to evaluate the correlations between parameters in the MMM. After a thorough review of the scenario and using the information gained from the comparative analysis, the MMM has been complete and is displayed in figure 5-20. The vehicle characteristics that have been identified through the comparative analysis have been used to make a more education evaluation of the parameter correlations.

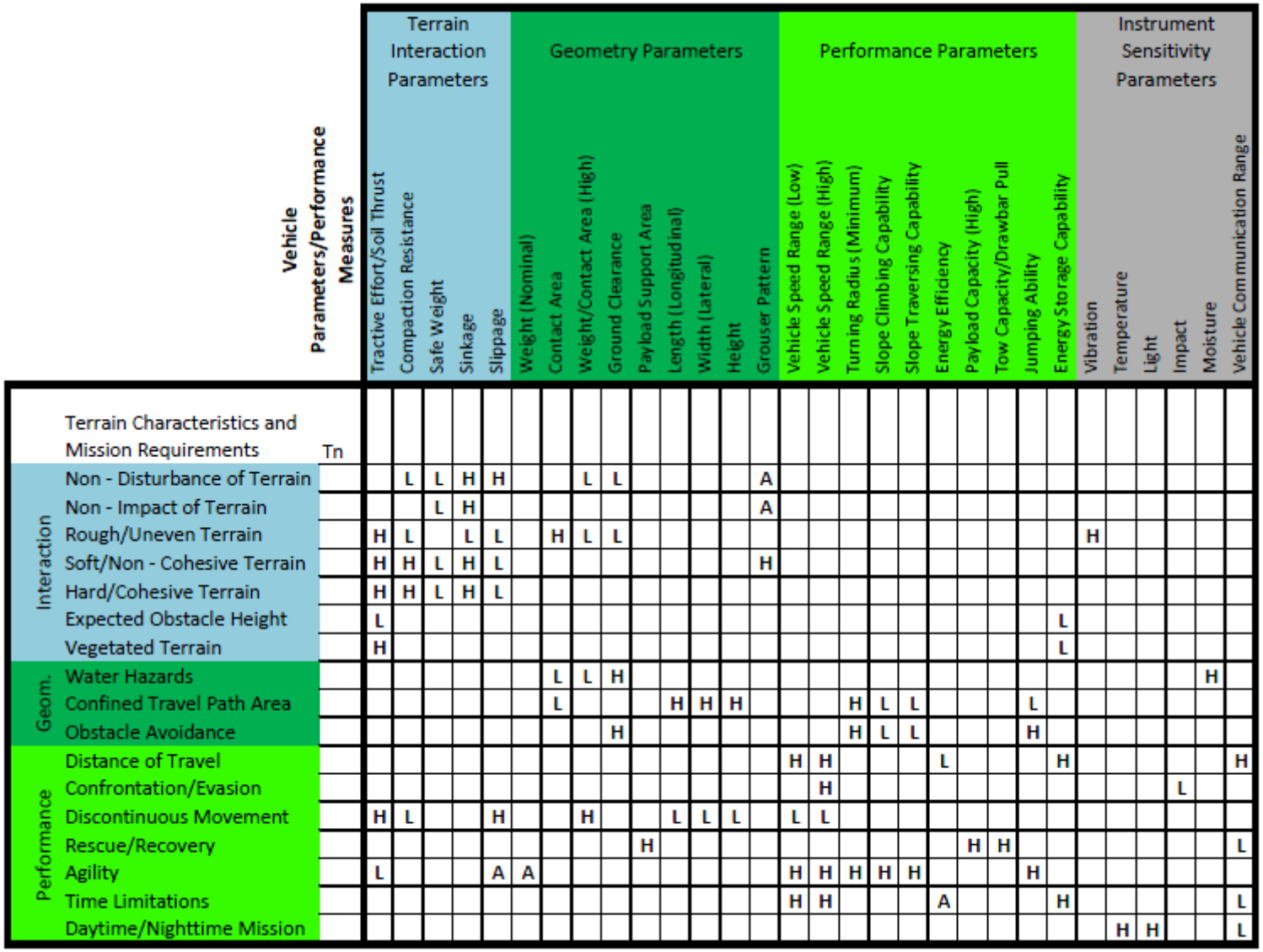
Vehicle Parameters/Performance Measures
Terrain Interaction Parameters
Geometry Parameters
Performance Parameters
Instrument Sensitivity Parameters
Tractive Effort/Soil Thrust
Compaction Resistance
Safe Weight
Sinkage
Slippage
Weight (Nominal)
Contact Area
Weight/Contact Area (High)
Ground Clearance
Payload Support Area
Length (Longitudinal)
Width (Lateral)
Height
Grouser Pattern
Vehicle Speed Range (Low)
Vehicle Speed Range (High)
Turning Radius (Minimum)
Slope Climbing Capability
Slope Traversing Capability
Energy Efficiency
Payload Capacity (High)
Tow Capacity/Drawbar Pull
Jumping Ability
Energy Storage Capability
Vibration
Temperature
Light
Impact
Moisture
Vehicle Communication Range
Terrain Characteristics and Mission Requirements
Tn
Interaction
Non - Disturbance of Terrain
Non - Impact of Terrain
Rough/Uneven Terrain
Soft/Non - Cohesive Terrain
Hard/Cohesive Terrain
Expected Obstacle Height
Vegetated Terrain
Geom.
Water Hazards
Confined Travel Path Area
Obstacle Avoidance
Performance
Distance of Travel
Confrontation/Evasion
Discontinuous Movement
Rescue/Recovery
Agility
Time Limitations
Daytime/Nighttime Mission

Figure 5-20: An MMM completed according to the example scenario

Following the completion of determine the correlations between parameters on the MMM, a level of importance was assigned to each correlation n-factor. The n-factor is defined as the number of correlations made for a given parameters. The level of importance is user defined and is based on the given mission criteria. According to the mission criteria the parameters for hard/cohesive terrain was given an increased weight of 1.6 units because this vehicle will be operating on a rigid surface for approximately 60% of the operating time. The soft/non-cohesive terrain criteria was given an increased importance of 1.4 units because the vehicle will be operating on a sandy silt loam terrain for approximately 40% of the time. One final criteria that was given an increased with was the expected obstacle height criteria because the vehicle will be encountering various rubble obstacles as the vehicle travels through the environment. All other parameters were given a neutral weight of 1 unit. The weights of the units do not have to add to 100% and are based entirely on the user preferences. A larger discrepancy in parameter weight will provide a larger gap between the vehicle's overall score.

After the importance of the vehicle correlations are assessed using equation 3.2, the importance for the tracked vehicle is approximately 1.678 and the importance for the wheeled vehicle is 2.678. The vehicle rank is determined using equation 3.3 in which the importance factors are used to compute the vehicle rank. The vehicle ranks were determined as follows, the tracked vehicle in this scenario scored 1 as the most suitable vehicle for this scenario and the wheeled vehicle scored 2 as the second most suitable vehicle for this scenario. This determination was made following the consideration of parameters that would carry an increased weight because of the specific mission criteria. By using the MMM in this manner and determining vehicle parameter weighting factors based on mission criteria, the user can make a vehicle selection in which the best possible vehicle can be chosen. This will help developers and SUGV users make a more informed and educated selection and will experience an overall better mobility performance form their SUGVs.

6. Conclusions and Future Work

A comparative analysis has been performed in order to gain an understanding of the differences in mobility performance between a wheeled and a tracked robotic vehicle. In this analysis, qualitative and quantitative assessment criteria have been considered. The vehicle was tested first in its wheeled configuration and then converted to the tracked configuration. For both running gears, the vehicle was tested through various obstacle negotiation scenarios. The vehicles drawbar pull, current consumption, speed, sinkage, and ground pressure were all measured. The main contributions of this study are summarized in this chapter.

Mobility Metrics Matrix based assessment. Facilitated by the analysis, the MMM assessment tool, originally developed by Worley, was employed and further improved. This tool provides means to rank vehicles against one another from a given candidate pool for suitability to specific mission parameters. This further allows the user to choose the best vehicle for the respective mission. The vehicle parameters include vehicle-terrain interaction, vehicle performance, vehicle geometry, and instrumentation sensitivity parameters. The user defined mission needs are judged as related to the vehicle parameters by a high correlation, a low correlation, or an adverse correlation marker. The correlation markers are then combined with weighting of the mission criteria to develop a mission specific rank for each vehicle; the importance weighting factor is user defined based on past experience or according to related theory and is customized for each scenario.

In this study the MMM was adapted based on the findings of the comparative analysis performed for the wheeled and tracked vehicle configurations. Following the customization of the MMM an example scenario was developed and the use of the MMM to rank vehicles was presented.

Sinkage analysis on soft soil. Through this comparative analysis performed based on the experimental work conducted as part of this study, many differences were highlighted between the vehicle in its wheeled and tracked configuration. Following the sinkage

testing it was very apparent that the tracked vehicle exhibited a much smaller sinkage. The average sinkage was about half that of the vehicle in its wheeled configuration. This difference is consistent with the research found in the literature review and confirms a fundamental difference. The tracked vehicle had a much larger contact area and is able to distribute the ground pressure much more effectively. This causes the vehicle to experience more floatation and causes a lower average sinkage value. It was concluded through the sinkage testing that the vehicle did not experience a noticeable difference in sinkage when the velocity was varied. This is due to the fact that the vehicle had a very slow top speed compared to other SUGV and the differences in speed was not enough to elicit a response in the sinkage. The lack of sinkage variety could also be attributed to the fact that this vehicle is very light and the increase in velocity was not sufficient to cause a major change in the vehicle center of gravity. While this was the conclusion reached by this case study it would warrant further exploration and validation by conducting this sinkage testing with a larger sample size and with vehicles that have a larger maximum velocity.

Power capacity impact on vehicle performance. Throughout the experimental testing the vehicles power limitations were very apparent. When the vehicle was switched to its tracked configuration the addition of the internal resistance to motion was very apparent. This limited the vehicles top speed significantly and also caused the vehicles batteries to become depleted at a faster rate. Further research should include a vehicle that has ample power and energy reserves in order to limit its affect on the vehicles mobility. This will allow the differences in mobility due to the running gear to become more apparent and cause less variability in the results.

Geometry relevance on traction capability. The grouser height had a major impact on the vehicles total tractive effort. Traditionally it is accepted that tracked vehicles exhibit a greater drawbar pull. This is due to the increase in traction from the larger surface contact area. In this case study the tracked vehicle produces a smaller drawbar pull than the wheeled configuration on sandy silt loam but produced a larger drawbar pull on the rigid surface. This was an unexpected result and needs to be further explored. The differences

in drawbar pull can be attributed to the differences in the vehicles grouser pattern and due to the fact that the tracked vehicle could no produce as much torque due to a high level or internal resistance. The tracked vehicle has a much smaller grouser pattern which caused the tracked vehicle to have poor traction in sandy silt loam. However this small grouser pattern provided the tracked vehicle with a much larger surface contact area and produced a much larger value of traction on a rigid surface. The wheeled vehicle has a much more pronounced grouser pattern and therefore excelled on the sandy silt loam but performed poorly on the rigid surface.

This pronounced effect of the grouser pattern on overall tractive effort warrants further exploration. While it goes with convention that a larger grouser pattern will produce better traction results, it remains to be seen how significant of an impact this has on vehicles in the robotic range. This effect in the future should be explored on a larger scale with a larger candidate pool that has very large discrepancies in grouser patterns.

Pressure distribution in the contact patch. One of the goals of this comparative analysis was to compare the vehicles pressure distribution differences between the wheeled and the tracked configuration. The pressure distribution was measured using two different methods and both methods produced substandard results. The Tekscan I-scan 3150 pressure sensor was not able to accurately measure the pressure because the vehicle was not heavy enough to activate the pressure sensels. Following the Tekscan system the pressure distribution was measured use Fujifilm prescale pressure measurement film and the results were once again substandard. The vehicle was not able to produce enough pressure to elicit a response from the Prescale film.

The pressure distribution is a parameter of interest and an accurate measure of the pressure distribution for vehicles on the robotic scale should be pursued in future research. It remains to be seen if vehicles on the robotic scale follow common pressure-sinkage relations developed by Bekker and others. With an accurate measure of the pressure distribution and an accurate measure of the vehicles sinkage the results can be compared with predictions made by accepted pressure-sinkage relations. Through this

future research a direction comparison can be made and conclusions can be drawn regarding the applicability of Bekker's pressure-sinkage relation to vehicles on the robotic scale.

Vehicle slip effect on traction analysis. One final area of future research interested would be to develop a system to accurately measure the vehicles slip. During this case study an attempt was made to measure the slip using a novel LIDAR measurement system developed at Virginia Tech by Holton. After preliminary studies indicated that the data collected in highly affect by noise introduced by the vibration of the fixture built to mount the measurement system on the vehicle, it has been decided to eliminate this aspect from the study the system was not suitable for attachment for a vehicle on the robotic scale. In future work the slip measurement system could be refined and adapted for attachment on a robotic vehicle and the slip could be accurately measured. This research would be of great interest and would help further classify SUGV mobility performance.

Recommendations for future work. While this comparative analysis was as encompassing as possible and the comparisons are conclusive, in the future this analysis should be carried out at a more extensive scale. In this study only one vehicle was used and it was switched between a wheeled and tracked configuration. Further analysis should include a larger variety of robotic vehicle. This would add value to the analysis and be of more use to engineers in the SUGV industry as well as user groups.

7. References

1. United States. Joint Chiefs of, S., *Department of Defense dictionary of military and associated terms.* Department of Defense dictionary of military and associated terms, 1972.

2. Richmond, P.W., *Mobility Performance Algorithms for Small Unmanned Ground Vehicles*. 2009, DTIC Document.

3. Army, *Brigade Modernization Command History.* 2011.

4. Steeds, W., *Tracked vehicles.* Automobile Engineer, 1950. **40**(526).

5. Bekker, M.G., *Theory of land locomotion; the mechanics of vehicle mobility*. 1956, Ann Arbor: University of Michigan Press.

6. Worley, M.E., *Experimental study on the mobility of lightweight vehicles on sand*. 2007, Blacksburg, Va: University Libraries, Virginia Polytechnic Institute and State University.

7. Wong, J.Y., *Theory of ground vehicles*. 4th ed. 2008, Hoboken: John Wiley.

8. Unger, R.F., *WHEELED VS. TRACKED VEHICLES.* Military Engineer, 1987. **79**(516): p. 435-437.

9. Weiss, K.R., *Skid-steering*. 1971. p. 22.

10. Crosheck, J.E., *SKID STEERING OF CRAWLERS.* SAE Preprints, 1975(750552).

11. Wismer, R. and H. Luth, *Prediction of wheel and track performance.* Prediction of wheel and track performance, 1971.

12. Kar, M.K., *PREDICTION OF TRACK FORCES IN SKID-STEERING OF MILITARY TRACKED VEHICLES.* Journal of terramechanics, 1987. **24**(1): p. 75-86.

13. Kitano, M. and H. Jyozaki, *A theoretical analysis of steerability of tracked vehicles.* Journal of terramechanics, 1976. **13**(4): p. 241-258.

14. Ehlert, W., B. Hug, and I. Schmid, *Field measurements and analytical models as a basis of test stand simulation of the turning resistance of tracked vehicles.* Journal of terramechanics, 1992. **29**(1): p. 57-69.

15. Meirion-Griffith, G. and M. Spenko, *A modified pressure-sinkage model for small, rigid wheels on deformable terrains.* Journal of terramechanics, 2011. **48**(2): p. 149-155.

16. Kitano, M. and M. Kuma, *An analysis of horizontal plane motion of tracked vehicles.* Journal of terramechanics, 1977. **14**(4): p. 211-225.

17. Wong, J.Y. and C.F. Chiang, *A general theory for skid steering of tracked vehicles on firm ground.* Proceedings of the Institution of Mechanical Engineers -- Part D -- Journal of Automobile Engineering (Professional Engineering Publishing), 2001. **215**(d3): p. 343-355.

18. Al-Milli, S., *Track-terrain modelling and traversability prediction for tracked vehicles on soft terrain.* Journal of terramechanics, 2010. **47**(3): p. 151-160.

19. Yi, J., *Adaptive trajectory tracking control of skid-steered mobile robots.* Engineering of Complex Computer Systems, IEEE International Conference on, 2007: p. 2605-2610.

20. Mohammadpour, E., *Robust adaptive stabilization of skid steer wheeled mobile robots considering slipping effects.* Advanced robotics, 2011. **25**(1): p. 205-227.

21. Wang, Z.P., *Robust adaptive control of a wheeled mobile robot violating the pure nonholonomic constraint*. 2004. p. 987-992.

22. Murakami, H., K. Watanabe, and M. Kitano, *A mathematical model for spatial motion of tracked vehicles on soft ground.* Journal of terramechanics, 1992. **29**(1): p. 71-81.

23. Le, A.T., *Estimation of track-soil interactions for autonomous tracked vehicles.* Engineering of Complex Computer Systems, IEEE International Conference on, 1997. **2**: p. 1388-1393.

24. Shiller, Z., *Trajectory planning of tracked vehicles.* Robotics and Automation (ICRA), IEEE International Conference on, 1993. **3**: p. 796-801.

25. Song, Z., *Identification of soil parameters for unmanned ground vehicles track-terrain interaction dynamics*. 2004. p. 1651-1656.

26. Zibin, S., *Non-linear observer for slip estimation of skid-steering vehicles.* Engineering of Complex Computer Systems, IEEE International Conference on, 2006. **2006**: p. 1499-1504.

27. Iagnemma, K., *On-line terrain parameter estimation for planetary rovers.* Robotics and Automation (ICRA), IEEE International Conference on, 2002. **3**: p. 3142-3147.

28. Iagnemma, K., *Online terrain parameter estimation for wheeled mobile robots with application to planetary rovers.* IEEE transactions on robotics, 2004. **20**(5): p. 921-927.

29. Dar, T.M., *Estimating Traction Coefficients of Friction for Small-Scale Robotic Tracked Vehicles*. 2010. p. 157-164.

30. Dar, T.M., *Slip estimation for small-scale robotic tracked vehicles*. 2010. p. 6816-6821.

31. Ray, L.R., *Estimation of net traction for differential-steered wheeled robots.* Journal of terramechanics, 2009. **46**(3): p. 75-87.

32. Ojeda, L., *Terrain characterization and classification with a mobile robot.* Journal of Field Robotics, 2006. **23**(2): p. 103-122.

33. Bekker, M.G., *Introduction to terrain-vehicle systems*. 1969, Ann Arbor: University of Michigan Press.

34. Bekker, M.G., *Off-the-road locomotion; research and development in terramechanics*. 1960, Ann Arbor: University of Michigan Press.

35. Reece, A., *Principles of soil-vehicle mechanics.* Proc. Inst. Mech. Engrs (Automobile Division), 1965. **180**(2): p. 45-67.

36. Ishigami, G., et al., *Terramechanics-based model for steering maneuver of planetary exploration rovers on loose soil.* Journal of Field Robotics, 2007. **24**(3): p. 233-250.

37. Richter, L., M. Bernasconi, and P. Coste. *Analysis, design and test of wheels for a 4kg-class mobile device for the surface of mars*. 2002.

38. Society of Automotive Engineers. Vehicle Dynamics, C., *Vehicle dynamics terminology : report*. 1978, Warrendale, Pa.: SAE.

39. Wills, B.M.D., *The measurement of soil shear strength and deformation moduli and a comparison of the actual and theoretical performance of a family of rigid tracks.* Journal of terramechanics, 1964. **1**(2): p. 83-88.

40. *International society for terrain-vehicle systems standards.* Journal of terramechanics, 1977. **14**(3): p. 153-182.

41. Gerhart, G., *Off-road vehicle locomotion using Bekker's model.* Proceedings of SPIE, the international society for optical engineering, 2000. **4024**: p. 127-136.

42. Rohani, B., *CORRELATION OF CONE INDEX WITH SOIL PROPERTIES*. 1981. p. 128-144.

43. Ojeda, L., J. Borenstein, and G. Witus, *Terrain trafficability characterization with a mobile robot.* Unmanned Ground Vehicle Technology VII, 2005. **5804**: p. 235-243.

44. Lever, J.H., *Mobility of lightweight robots over snow.* Proceedings of SPIE, the international society for optical engineering, 2006. **6230**.

45. Lever, J.H., *Mobility of a lightweight tracked robot over deep snow.* Journal of terramechanics, 2006. **43**(4): p. 527-551.

46. Jones, W., *Snow-Trac*. 2008, Warren Jones.

47. Rula, A.A., *An analysis of ground mobility models (ANAMOB)*. 1971, DTIC Document.

48. Ansorge, K.H., *Robotics vehicle mobility study*. Proceedings of SPIE, the international society for optical engineering, 2000. **4024**: p. 159-169.

49. Godbole, R., R. Alcock, and D. Hettiaratchi, *THE PREDICTION OF TRACTIVE PERFORMANCE ON SOIL SURFACES.* Journal of terramechanics, 1993. **30**(6): p. 443-459.

50. Dwyer, M.J., D.R. Comely, and D.W. Evernden, *The field performance of some tractor tyres related to soil mechanical properties.* Journal of agricultural engineering research, 1974. **19**(1): p. 35-50.

51. ERDC, R.A.U.S.A., et al., *Case Study of the Evaluation and Verification of a PackBot Model in NRMM.* 2005.

52. Corporation, i., *PackBot.* 2012.

53. Worley, M.E., *The development of an assessment tool for the mobility of lightweight autonomous vehicles on coastal terrain.* Proceedings of SPIE, the international society for optical engineering, 2007. **6564**.

54. Automated Systems Association of, S.M.E., *Review of QFD and related deployment techniques.* Journal of manufacturing systems, 1998. **17**(3): p. 221.

55. Whitlow, R., *Basic soil mechanics*. 1995, Harlow, Essex, England; New York: Longman Scientific & Technical ; Wiley.

56. *Pololu TReX Jr User's Guide*. 2009 [cited 2011.

57. Pololu. *TReX Jr.* . 2012; Available from: http://www.pololu.com/catalog/product/767.

58. Monmasson, E., *Power electronic converters : PWM strategies and current control techniques*. 2011, London; Hoboken, NJ: ISTE ; Wiley.

59. Zureks, *Example PWM waveform*. 2007.

60. Sparkfun, *XBee Pro* 2012.

61. Inc., S.P., *FujiFilm Prescale*. 2012.

62. Holton, C. and M. Ahmadian, *Doppler sensor for the derivation of torsional slip, friction and related parameters*. 2010, Google Patents.

63. Arduino, *Arduino Uno.* 2012.

64. Industries, A., *Adafruit Data loggin shield for Arduino - v1.0*. 2012.

65. Specialties, M., *FC22 Low Profile Compression Load Cell*. 2012.

66. Sparkfun, *ACS712 Low Current Sensor.* 2012.

67. Sparkfun, *Dual Axis Gyro - LPY503AL - 30?/s* 2012.

68. Technologies, C., *RE08A Rotary Encoder User Manual*. 2012.

69. Sandu, C., M. Worley, and J. Morgan. *Experimental study on the mobility of lightweight vehicles on sand*. 2008.

70. Sandu, C., M.E. Worley, and J. Morgan, *Experimental study on the contact patch pressure and sinkage of a lightweight vehicle on sand.* Journal of terramechanics, 2010. **47**(5): p. 343-359.

A. Appendix

In the appendix a sample of the data collected that correspond to the plots in chapter 6 can be found. All the collected data will not be displayed due to the volume of data.

Table A-1: Wheeled vehicle sinkage data

Trial #	Sinkage Measurement (mm)									
1	5.48	7.48	5.48	6.48	4.48	4.98	5.28	5.48	4.48	4.38
2	4.38	5.38	4.98	4.48	3.98	3.48	4.28	4.48	4.38	4.98
3	3.68	3.38	4.68	4.78	5.28	4.28	4.38	4.18	4.68	4.38
4	4.38	4.48	4.58	4.98	4.28	4.38	5.48	5.28	3.78	4.78
5	5.38	6.38	4.28	4.78	5.48	5.28	6.38	5.28	5.28	5.98

Table A-2: Tracked vehicle sinkage data

Trial #	Sinkage Measurement (mm)									
1	3.48	1.48	2.88	2.78	1.98	2.28	2.58	2.98	2.38	2.48
2	1.58	2.38	2.48	2.68	2.38	2.58	1.88	2.68	2.38	1.58
3	1.38	2.58	2.38	1.58	1.48	2.48	1.78	2.58	2.58	2.38
4	2.58	2.48	2.38	1.58	1.48	2.48	1.88	2.18	1.48	2.38
5	2.48	2.28	2.18	2.48	1.98	2.38	2.48	1.48	2.48	1.98

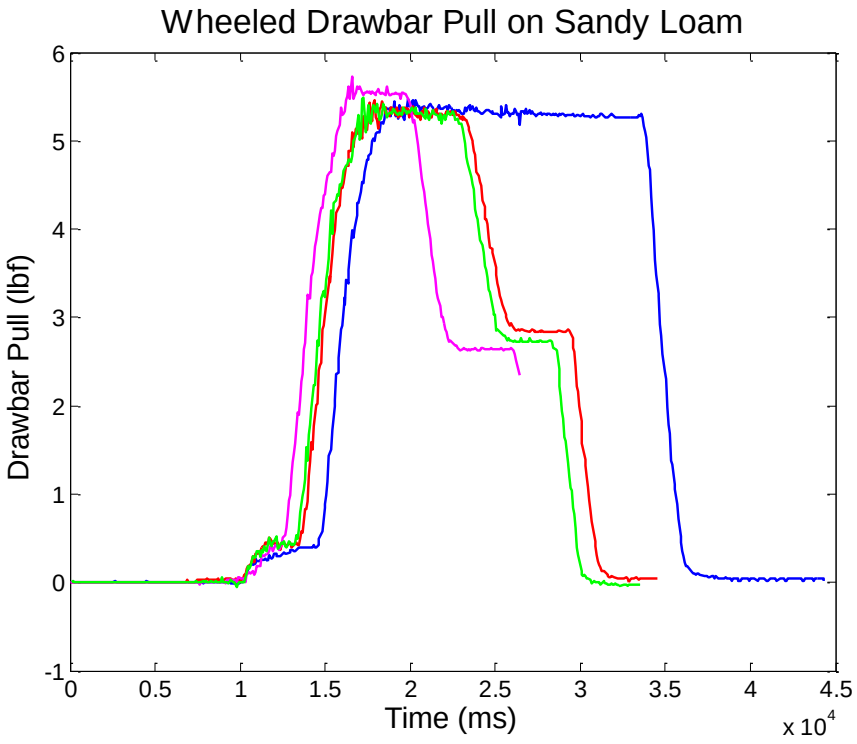

Figure A-1: Wheeled drawbar pull on sandy silt loam

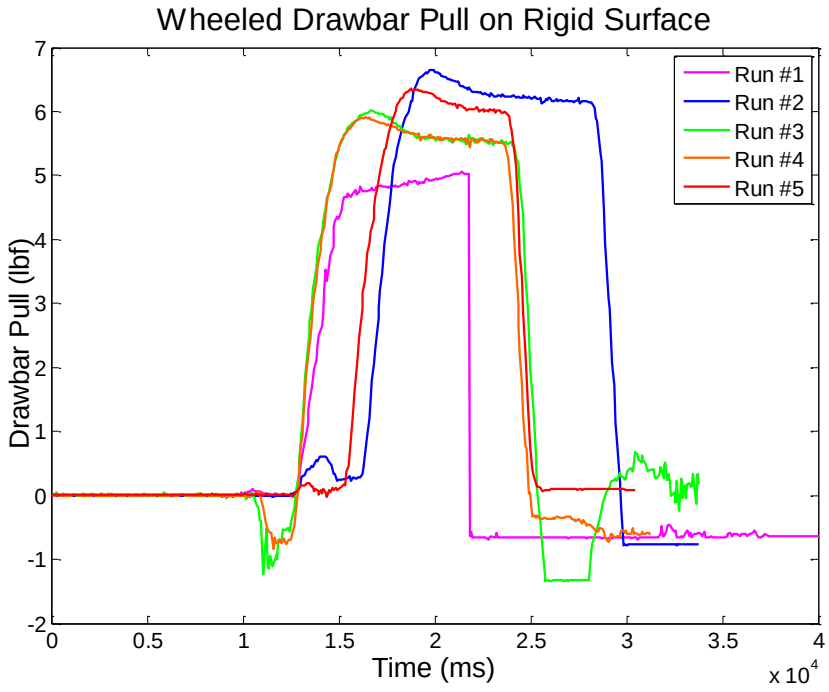

Figure A-2: Wheeled drawbar pull on rigid surface

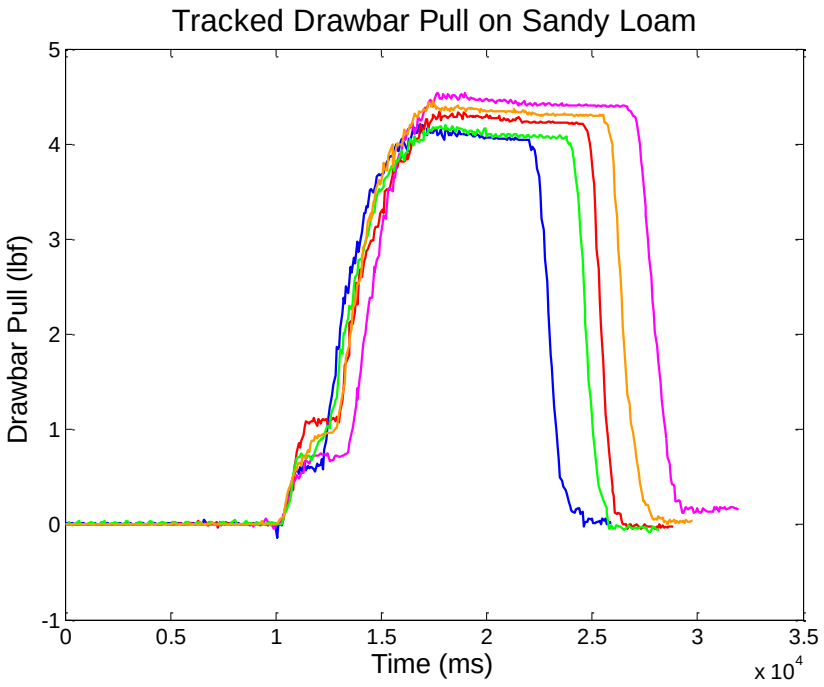

Figure A-3: Tracked drawbar pull on sandy silt loam

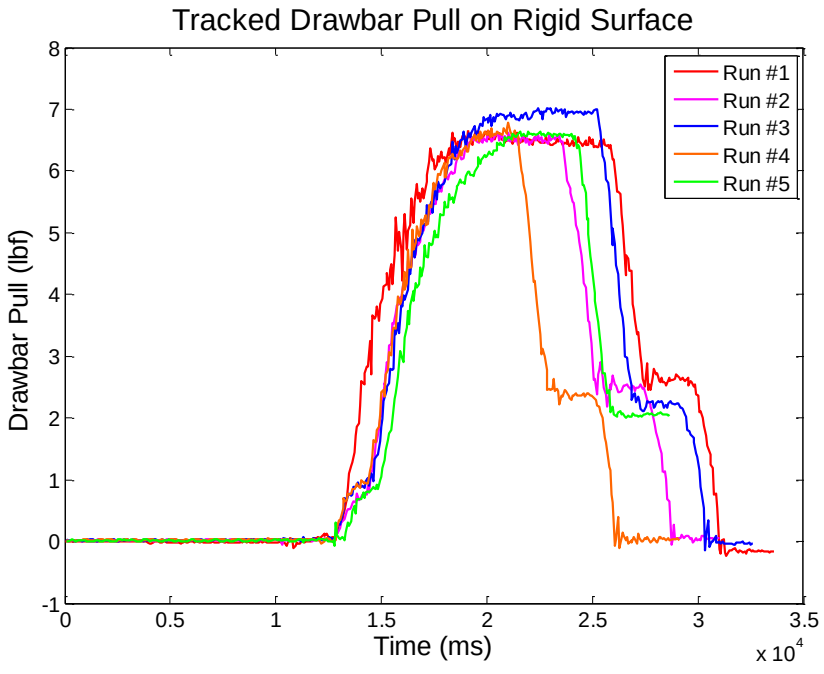

Figure A-4: Tracked drawbar pull on rigid surface